AN ON-TARGET PERFORMIC ACID OXIDATION METHOD SUITABLE FOR DISULFIDE BOND ELUCIDATION USING CAPILLARY ELECTROPHORESIS – MASS SPECTROMETRY

A Dissertation

by

BRAD JAY WILLIAMS

Submitted to the Office of Graduate Studies of
Texas A&M University
in partial fulfillment of the requirements for the degree of

DOCTOR OF PHILOSOPHY

May 2010

Major Subject: Chemistry

AN ON-TARGET PERFORMIC ACID OXIDATION METHOD SUITABLE FOR DISULFIDE BOND ELUCIDATION USING CAPILLARY ELECTROPHORESIS – MASS SPECTROMETRY

A Dissertation

by

BRAD JAY WILLIAMS

Submitted to the Office of Graduate Studies of
Texas A&M University
in partial fulfillment of the requirements for the degree of

DOCTOR OF PHILOSOPHY

Approved by:

Chair of Committee,	David H. Russell
Committee Members,	James C. Hu
	Emile A. Schweikert
	Gyula Vigh
Head of Department,	David H. Russell

May 2010

Major Subject: Chemistry

ABSTRACT

An On-Target Performic Acid Oxidation Method Suitable for Disulfide Bond Elucidation Using Capillary Electrophoresis - Mass Spectrometry. (May 2010)

Brad Jay Williams, B.S., Southeastern Oklahoma State University

Chair of Advisory Committee: Dr. David H. Russell

Disulfide bonds play important roles in establishing and stabilizing three-dimensional protein structure, and mass spectrometry (MS) has become the primary detection method to decipher their biological and pathological roles. Several experimental methods before or after MS detection have been developed to aid in disulfide bond assignment, such as tandem MS followed by database searching or modification of the disulfide bond via chemical reduction or oxidation. Despite these technological advancements, the detection and proper assignment of disulfide bonds have remained experimentally difficult. Therefore, we have developed an alternative method for disulfide bond elucidation using capillary electrophoresis – mass spectrometry (CE-MS) combined with an on-target performic acid oxidation method for matrix assisted laser desorption/ionization (MALDI) deposited samples.

An information rich CE-MS method that results in distinct charge-state trends observed in two-dimensional plots of $\log(\mu^{eff})$ versus log (MW) was developed to enhance the confidence of peptide and protein identifications. The charge-state trends provide information about the number of basic amino acid residues present within each

peptide. This information can be used to develop methods to screen for post-translationally modified peptides (*e.g.,* phosphorylation, disulfide bonds, etc.). In the case of disulfide bonds, the highly charged peptides (*i.e.,* +3, +4 or greater charge states) have a high probability of being disulfide-linked peptides, owing to charge contribution of both peptides forming the disulfide bridged peptide. However, intra-linked disulfide bridged peptides can also be present at lower charge states. Therefore, a chemically selective method to rapidly locate disulfide-linked peptides that have been separated by CE-MS must be developed.

An on-target performic acid oxidation method was developed to provide the chemical selectivity towards disulfide bonds, *i.e.,* converting the cystine bond to form two peptides modified with a cysteic acid (SO_3H) side chain. The on-target oxidation method offers (i) no post-oxidation sample cleanup, (ii) improved throughput over solution-phase oxidation methods, and (iii) easily adapted to CE separations coupled off-line with MALDI-MS. The evaluation of the on-target oxidation experimental parameters, the fragmentation behavior of cysteic acid-containing peptides and an alternative method for disulfide bond elucidation, using CE-MS combined with the on-target oxidation method, are discussed within.

DEDICATION

This dissertation is dedicated to both of my grandparents: Ina and T.J. Williams and the late Mae and Russell Oden for their encouragement to explore my interests in chemistry and computer technology. I wish they all could be here today to see me complete my goal.

ACKNOWLEDGEMENTS

I would like to thank my advisor, Prof. David H. Russell, for his guidance, support and patience with me while developing my writing skills throughout my graduate career. I especially appreciate the opportunity to further explore my interests with separation science and combine them with mass spectrometry.

I would like to thank committee members, Dr. Gyula Vigh, Dr. Emile Schweikert, and Dr. James C. Hu, for their guidance and support throughout the course of this research. I very much appreciate the many valuable discussions with Dr. Vigh on the CE-MS aspect of the project. I would like to thank my mentor, Dr. William K. Russell, for teaching me how to become an independent researcher and for being critical and patient when proofreading my manuscripts. Also, a special thanks to Dr. Hu for suggesting disulfide-containing proteins as a model system to investigate cross-linked peptides with CE-MS.

I would like to thank all of the past and present members of the Russell Research Group. Thanks also go to my friends and colleagues for making my time at Texas A&M University a great experience. I would like to thank Dr. Fernando Albertorio for being a true friend; he was always there to talk to when times were tough, even today. I also would like to thank my colleague, Dr. Stephanie M. Cologna, for proofreading several dissertation chapters and for always being a great friend who was always there to discuss research and other animal related issues she may have going on. I would also like to thank Dr. Bennie J. Bench for being a good roommate and friend throughout the years.

He was always encouraging me to finish up. In addition, thank you to my friend from the beginning, Dr. Elky Almaraz. She has been there to experience all of the graduate school's ups and downs with me. It was also nice to have a friend like Mr. Ryan Blase that shares a similar taste in music; somehow listening to great music keeps my mind going, especially the TDAGARIM album by Brand New.

I also want to extend my gratitude to the Department of Energy, Division of Chemical Sciences, Office of Basic Energy Sciences, BES DE-FG02-04ER15520 and the National Institutes of Health (RR0119587) for providing research funding for the instruments and materials used for these studies.

Finally, thanks to my family for their encouragement, understanding, and love during my graduate studies.

TABLE OF CONTENTS

CHAPTER Page

LIST OF FIGURES

Page

Page

Page

Page

Page

Page

LIST OF TABLES

Page

LIST OF SCHEMES

Page

CHAPTER I

INTRODUCTION

Improvements in the fields of separation science, mass spectrometry (MS) and bioinformatics have been required to gain insight into the proteome and cellular processes of various microorganisms. Traditional proteome level protein separations are carried out using two-dimensional polyacrylamide gel electrophoresis (2D-PAGE) utilizing isoelectric focusing as the first dimension separation followed by a size-based separation in the second dimension.[1-4] After appropriate protein staining the protein spots are excised and subjected to in-gel proteolytic digestion, which can be quite laborious and mid-to-low throughput. The in-gel digestions are then analyzed by either electrospray ionization (ESI) or matrix-assisted laser desorption/ionization (MALDI) – MS followed by database searching and peptide mass mapping for protein identification.[5-8] Even today, 2D-PAGE still remains a workhorse in the proteomics field owing to the high resolving power of the two-dimensional separation.

Several liquid-phase separation techniques (*e.g.,* high-performance liquid chromatography (HPLC) or capillary electrophoresis (CE)) have proven useful to increase dynamic range, reduce sample complexity, and increase the confidence level of

---

This dissertation follows the style and format of *Analytical Chemistry*.

peptide identification for "bottom-up" proteomics.[9-11] In the traditional bottom-up proteomics experiment, intact proteins are first subjected to proteolytic digestion using trypsin (cleaves C-terminally to lysine and arginine residues, except when followed by proline) followed by pre-fractionation prior to MS analysis and subsequent peptide mass mapping. As a brute force approach, multi-dimensional separation schemes using strong cation exchange chromatography (SCX) combined with reverse phase liquid chromatography (RPLC) and ESI-MS have been developed as an alternative to 2D-PAGE. For example, Yates and coworkers developed the multidimensional protein identification technology (MudPIT) in which they successfully identified *ca.* 1500 yeast proteins.[12] As opposed to increasing the number of separation dimensions, some research groups have increased the information content by incorporating LC retention time into their proteomic study to increase specificity, throughput, and proteome coverage.[13-18] The LC retention time combined with high mass measurement accuracy (*i.e.,* ~ 1 ppm) can be used to streamline LC-MS proteomic analyses to nearly eliminate the need for tandem MS to identify proteins.[13]

On the other hand, CE offers certain advantages over LC including increased separation efficiency and an alternative separation mechanism based on the peptide hydrodynamic size-to-charge ratio. Several successful proteomic studies have employed CE-MS for protein identification[9, 19] and biomarker discovery from urine polypeptides.[20-24] CE-MS also provides a migration time which is inherent of the peptide's size-to-charge ratio. For example, Wittke and coworkers[23] presented data on urine polypeptides using CE-MS in which 2D plots of m/z versus migration time yield visible trends,

although at the time an explanation of their origin was not given. Similar trends can also be seen in CE-MS data taken from similar studies of Kaiser, et al.[20, 21] and Theodorescu, et al.[22] The distinct trends observed in CE-MS plots of log(μ^{eff}) versus log (MW) were determined to be related to the peptide charge state which gives an indication of the number of basic amino acid residues present within the peptide.[19] This additional information adds analytical utility towards improving the confidence of protein identification and provides means for detecting charge state altering modifications (*e.g.,* phosphorylation, cysteine oxidation, etc.) within complex mixtures. Hence, the main goal of the work presented within is to utilize the information provided in the 2D CE-MS plots to simplify the detection of post-translationally modified peptides, such as phosphorylation, cysteine oxidation, and disulfide bonds.

Even though CE-MS provides high separation efficiency, low sample consumption, and the distinct charge state trends; there is a significant disadvantage in the loading capacity of CE compared to LC. Typical CE capillaries have a total capillary volume of 1-2 μL allowing injection volumes in the nanoliter range. As a rule of thumb injections for CE are ≤1% of the total capillary length.[25] This helps prevent concomitant band broadening associated with large injection volumes. As for LC, injection volumes are in the microliter range allowing more analyte to be injected. Hence, the main difference between LC and CE is the concentration limit of detection, *i.e.,* more concentrated samples are required for CE-MS. In an effort to enhance the loading capacity of CE, several sample stacking protocols (*e.g.,* field-amplified sample stacking,[26, 27] large volume sample stacking,[28, 29] isotachophoresis,[30, 31] etc.) have been

developed to mitigate this issue. The majority of the sample stacking protocols work on the basis of a high field strength created within the low conductivity sample zone. The low conductivity sample zone can be achieved by preparing the sample in pure water, mixed organic solvent with partial aqueous content (*e.g.,* acetonitrile, ethanol, methanol) or a low conductivity buffer such as triethanolamine or tris(hydroxymethyl)aminomethane.[32] Briefly, the sample stacking results from the low conductivity sample plug which causes a drastic increase in field strength and the positive ions rapidly stack as a narrow band at the sample plug / background electrolyte interface.[27, 33] Once the positive ions reach the electrophoresis buffer they continue to migrate according to their size-to-charge ratio. Typical sample enrichment factors range from 10-50 fold depending on the sample stacking technique and the sample composition.[34] Overall, these relatively simple CE sample stacking protocols can improve the sensitivity to compare to those achieved by LC methods.

The detection of post-translational modifications (*e.g.,* phosphorylation, cysteine oxidation, and disulfide bonds) has become important to understand protein and cellular functions. For example, cysteine oxidation away from the active site of a protein kinase can result in disulfide bond formation with a nearby cysteine residue, which changes the protein conformation and enzymatic activity.[35] Lately, several research groups have focused their attention towards studying the variable states of cysteine oxidation and their biological and pathological roles.[36-39] The most commonly known states of cysteine oxidation are the thiol (RSH) and disulfide bond (R-S-S-R), but several cysteine oxoforms including sulfenic (RSOH), sulfinic (RSO_2H), and sulfonic (RSO_3H) acid are

being observed in an increasing number of proteins.[40] Figure 1 contains the chemical structures of these cysteine oxidation states including the intermediates of disulfide bond oxidation. When disulfide bonds are exposed to a chemical oxidant (*e.g.,* performic acid or hydrogen peroxide) several oxygen atoms are incorporated into the different cysteine oxoforms until the final product becomes a sulfonic acid. Sulfenic acids are known to have short lifetimes before additional oxidation occurs to produce disulfide bonds or sulfinic/sulfonic acids. Technologies to capture sulfenic acids using dimedone (*i.e.*, 5,5-dimethyl-1,3-cyclohexadimone) chemistry followed by antibody recognition and MS have been reported.[36-38, 41, 42] Over thirty protein crystal structure have been reported to contain sulfenic acid modifications.[43] The detection of the final cysteine oxidation product, sulfonic acid is rather straightforward since the oxidation is irreversible and MS-based detection schemes have proven effective.[44, 45-48] However, the detection and assignment of disulfide bonds within proteins remains an analytical challenge.

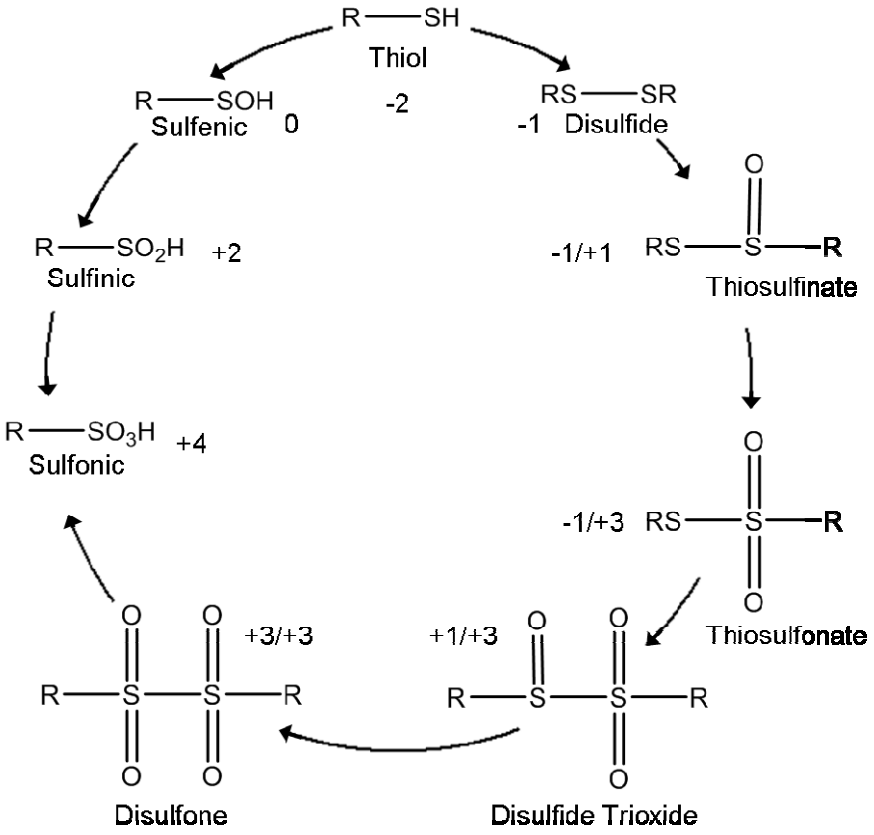

Figure 1. Various states of oxidation for post-translationally modified cysteine. The oxidation number of the sulfur atom in each cysteine oxoform is shown. This figure was adapted from Reddie and Carroll.[40]

Disulfide bonds are particularly important to stabilize and maintain native protein structures,[49, 50] and MS has played an increasingly important role in deciphering these processes,[51] especially protein folding/unfolding kinetics.[52-54] The basic experimental scheme for assigning disulfide bond involves: (i) proteolytic digestion of the non-reduced protein into disulfide-linked peptides with cleavage between all half-cystine residues, (ii) separation of the disulfide-linked peptides; (iii) locate and identify the disulfide-linked peptides in each fraction; (iv) cleave the disulfide-linked peptides at the

disulfide bond to leave the half-cystinyl products to be further characterized. [51] This basic strategy to identify disulfide bonds has been modified with the development of advanced separation science and MS methodologies, but overall the experimental scheme remains similar. For example, Morris and Pucci developed a method to compare the mass spectra for the non-reduced and reduced proteolytic digest of bovine insulin.[55] The different disulfide bond arrangements were proposed based on the observed half-cystinyl peptides. The comparison of non-reduced versus reduced proteolytic digests of disulfide-containing proteins has become the classical approach to determine disulfide bond patterns within proteins.

Prior to MS analysis, there are several experimental variables during proteolytic digestion of a disulfide-containing protein that are important to maintain the native disulfide bond pattern. For example, disulfide bonds can undergo nucleophilic cleavage under alkaline conditions (pH 8) and can readily react with a free thiol group to produce a scrambled/exchanged disulfide bond.[51] Since the majority of the proteases (*e.g.,* chymotrypsin, trypsin, endoproteinase AspN) used for MS-based proteomics are active at or near pH 8 this becomes an issue to maintain the native disulfide bond pattern. To overcome this issue, alternative proteases such as pepsin (C-terminal cleavage after Ala, Leu, Phe, Tyr, Trp) that are active at acidic conditions (pH 2-3) or digestion can be performed under mildly acidic (pH 6) conditions to minimize disulfide scrambling.[56] The temperature must be carefully controlled to minimize disulfide bond scrambling. For example, severe disulfide scrambling results (*ca.* 20 non-native disulfide-linked peptides) when thermal denaturation (90˚C) procedures are used to denature bovine

Ribonuclease A (RNase A) prior to proteolytic digestion. Another challenge during proteolytic digestion is the inaccessibility of the protease to cleave the protein in regions where the disulfide bonds are buried or not solvent exposed.[53, 54] Dual enzyme digestion schemes (*e.g.,* trypsin followed by chymotrypsin)[56] or alternative proteases (*e.g.,* pepsin, Endoproteinase AspN, Endoproteinase LysC, etc.) could help improve the digestion efficiency.

Several experimental approaches to assign disulfide bonds within proteins have been reported over the last thirty years.[51] Particularly, several different MS-based methods including: tandem MS,[57, 58] database search algorithms,[56, 59-61] chemical reduction, [55, 62, 63] chemical oxidation, [46, 47, 64] metal ion cleavage of disulfide bonds, [65, 66] and recently gas-phase scrambling of disulfide bonds during MALDI-MS.[67] Many recent experimental schemes to determine disulfide bonds involve fragmentation of intact disulfide-linked peptides followed by database searching using a newly developed search algorithm. For example, Xu and coworkers developed a tandem MS search

engine to simplify database searches of fragment ion spectra of intact disulfide-linked peptides.[56] As illustrated in Figure 2, the fragment ions of an interlinked disulfide bridged peptide can be quite complicated. The accepted peptide fragmentation nomenclature[68] has been modified for disulfide and/or cross-linked peptides,[57] *i.e.,* fragmentation on the α-chain would be denoted as αy_n or αb_n for cleavage of the peptide bond with charge retention at the C- or N-terminus, respectively. Further fragmentation nomenclature including side-chain loss fragment ions will be discussed in more detail in Chapter V. The majority of interlinked disulfide-containing peptides primarily fragment at the disulfide bond to produce the signature fragment ions for a disulfide bond (See Figure 2 inset). A limited number of sequence-informative fragment ions can result from each α- and β-chain peptide forming the disulfide linkage depending of their amino acid composition.[57] Therefore, every single disulfide-linked peptide cannot be assigned via tandem MS alone, additional chemical modifications or other methodologies could be needed to further assist in the disulfide bond assignment.

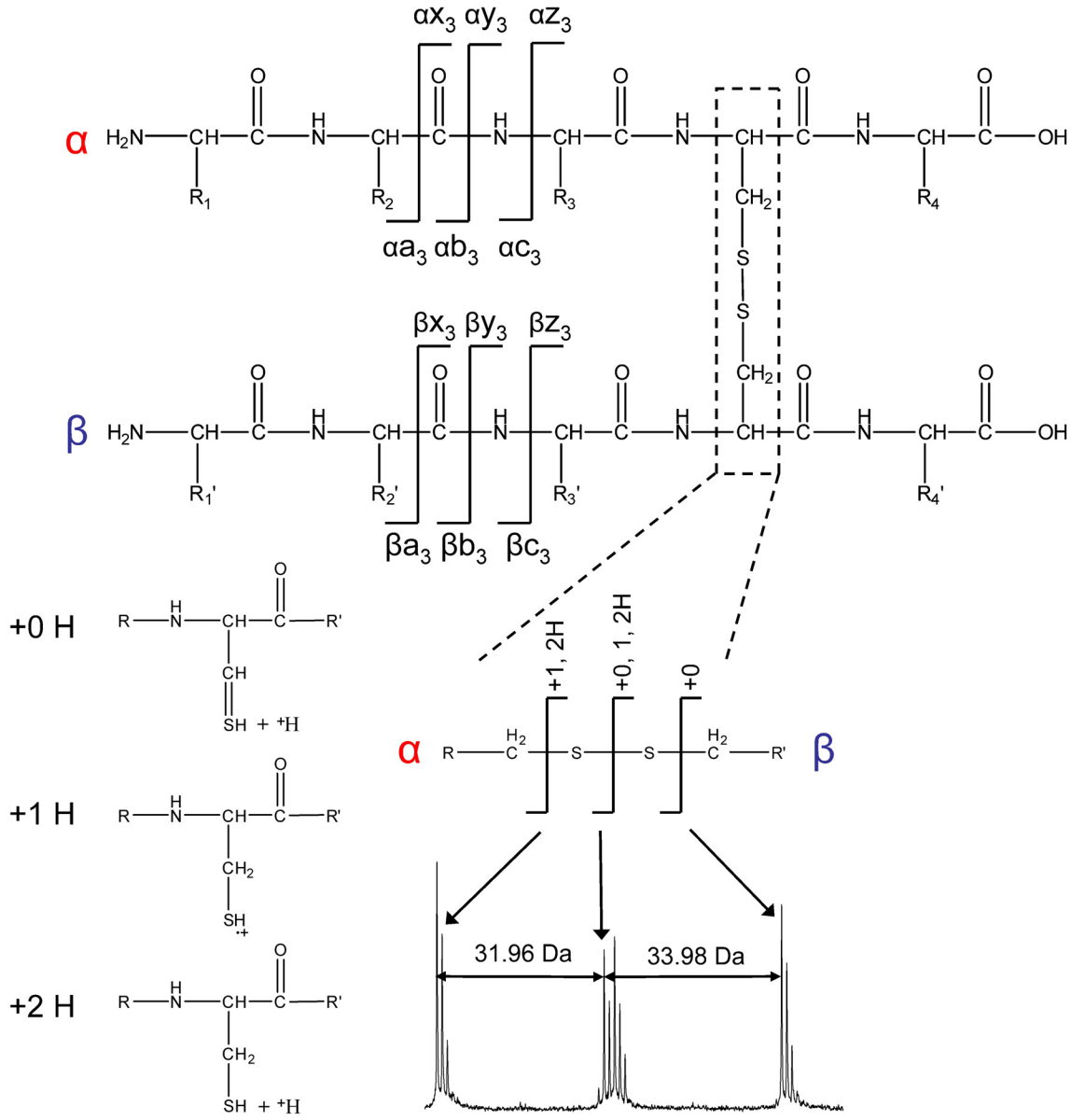

Figure 2. Fragmentation nomenclature for an inter-linked disulfide bridged peptide with generic side chains. Inset figure: the signature disulfide bond fragment ions resulting from gas-phase cleavage of the disulfide bond are also shown. The fragment ions resulting from cleavage of the -S-S- bond between the two sulfur atoms are shown (bottom left).[57]

Through chemical reduction or oxidation the disulfide bond can be chemically cleaved to produce two peptides with either the free thiol (RSH) form or the cysteic acid (RSO_3H) form. As a modification of the traditional Morris and Pucci [55] approach using chemical reduction to assign disulfide bonds, a reductive MALDI matrix, 1,5-diaminonapthalene (1,5-DAN) has been used to reduce the disulfide bond during the MALDI process.[62, 63] For example, Quinton and coworkers used 1,5-DAN as the MALDI matrix to characterize disulfide-linked peptides using LC coupled off-line with MALDI-MS/MS.[63] The reductive MALDI matrix reduces disulfide bonds during the MALDI event; however, 1,5-DAN yields a high relative abundance of matrix clusters up to 1000 m/z, which prevents the analysis of low molecular weight disulfide and/or cysteine-containing peptides. Disulfide bonds can also be cleaved during the MALDI process without the use of a reductive MALDI matrix. For example, Schnaible *et al.* developed a screening method for disulfide bonds based on LC pre-fractionation combined with post-source decay of the disulfide bond during the MALDI process to produce two peptide chains that form the inter-linked disulfide bond.[58] The disulfide bonds from bovine serum albumin and bovine RNase A can be elucidated by back-calculating the intact disulfide-linked peptide masses. Using this approach, the free cysteine-containing peptides become difficult to distinguish from those that are formed from gas-phase cleavage of the disulfide bond as a result of post-source decay. Therefore, an approach such as chemical oxidation that can simultaneously cleave and chemically modify the sulfur atoms involved in the disulfide bond would be beneficial.

Compared to chemical reduction of the disulfide bond, chemical oxidation offers the following benefits: (i) a 48 Da mass shift occurs per cysteine residue, (ii) cysteic acid (SO_3H) enhances negative ion formation, and (iii) the chemical oxidant simultaneously cleaves the disulfide bond and chemically modifies each peptide involved in the disulfide bridge. Chemical oxidation can be achieved using either performic acid [46, 47, 64, 69]} or hydrogen peroxide.[37, 70] Performic acid under controlled conditions selectively oxidizes cystine, cysteine, and methionine amino acid residues. In the case of disulfide bonds, the sulfur – sulfur bond is broken to form two peptides, each modified with a cysteic acid (See Figure 1). As for methionine, up to two oxygen atoms can be incorporated to produce the sulfone form (RSO_2CH_3). Sun and Smith reported the first approach using performic acid oxidation combined with MS for disulfide bond determination.[46] Solution-phase oxidation was used to successfully oxidize standard peptides and proteolytic digests of bovine insulin and RNase A. Using this approach they were able to elucidate two disulfide bonds of bovine insulin. Despite their success, the experimental protocol for solution-phase performic acid oxidation is quite laborious and low-to-mid throughput.

Traditional solution-phase oxidation methods are performed on lyophilized peptide/protein samples using reaction times ranging from 2-4 hrs [47, 71, 72] and several steps are required after oxidation to remove the performic acid reagent prior to MS analysis. Solution-phase oxidation methods with decreased reaction times (10-30 min) have been reported for the oxidation of cysteine/methionine containing peptides; however, the additional clean-up steps after oxidation make this method less desirable.[46]

In an effort to decrease reaction time and the steps prior to MS analysis, on-target oxidation methods using solution-phase performic acid have also been successfully applied to MALDI spots containing peptides and/or proteolytic digests.[71] For example, we showed that directly adding the performic acid solution to a pre-spotted MALDI deposit containing a bovine apo-transferrin tryptic digest yields oxidized tryptic peptides; however, the signal-to-noise (S/N) ratios of the oxidized peptide negative ions decreased by 5-fold because of ion suppression effects. The overall amino acid sequence coverage also decreased by half compared to the solution-phase oxidized sample. Thus, an on-target performic acid oxidation method that can mitigate these adverse effects would be highly beneficial. The ideal on-target oxidation method would offer the following characteristics over solution-phase oxidation methods: (i) simple experimental procedure with no post-oxidation sample cleanup; (ii) decreased ion suppression effects following oxidation; (iii) improved throughput over solution-phase methods; and (iv) maintain positive and negative ion mass spectral quality following on-target oxidation. Additionally, an on-target oxidation method that can simultaneously oxidize entire CE or LC-MALDI separations which would certainly be beneficial to develop screening methods to locate disulfide bonds within complex mixtures.

Herein we describe an alternative method for disulfide bond elucidation using on-target oxidation combined with CE-MS. The 2D CE-MS plots of $\log(\mu^{eff})$ versus log (MW) provide additional information (charge state or number of basic amino acid residues) which improves the confidence of peptide and protein identifications. Owing to the high charge state (*i.e.,* +3, +4 or greater) of an intact disulfide-linked peptide, these

2D CE-MS plots can be used to develop a screening method for disulfide-linked peptides. The entire CE-MS separation can be subjected to on-target oxidation which provides chemical selectivity towards oxidizing the intact disulfide-linked peptides. Presented within is the (i) development of CE-MS methods resulting in distinct charge state trends, (ii) introduction of a high-throughput on-target oxidation method, (iii) evaluation of the on-target oxidation experimental parameters, (iv) investigation of the effect of the cysteic acid position on the negative ion fragmentation of oxidized cysteine-containing peptides, and (v) the combination of the on-target oxidation method with CE-MS separations as an alternative method for disulfide bond elucidation.

CHAPTER II

UTILITY OF CE-MS DATA IN PROTEIN IDENTIFICATION*

Introduction

The task of identifying and quantifying the proteome is daunting and has required continued improvements in separation science, mass spectrometry (MS), and bioinformatics. A great deal of progress has been made in studies of protein expression by using 2D gel electrophoresis to separate/isolate individual proteins, which are then identified by MS methods such as peptide mass mapping and peptide sequencing.[1-4] The low throughput nature of these experiments led to the development of bottom-up MS and top-down MS techniques, as well as multidimensional separations (LC-MS and LC-MS/MS) strategies for the identification of proteins within complex mixtures,[12, 73, 74] and the characterization of protein complexes and microorganisms.[75-77] The combination of liquid-phase separation techniques, *i.e.,* high-performance liquid chromatography (LC), with MS increase dynamic range, reduce sample complexity, and increase confidence level of peptide identification.[9-11] Two-dimensional (2D) LC-MS methods are also frequently used.[12, 78] Although 2D separation increases the depth the proteome can be analyzed, there is a concomitant increase in the analysis time. In an effort to enhance proteomic analysis to include the complete proteome, several groups have added even

---

* Reproduced with permission from Williams, B.J.; Russell, W.K.; Russell, D.H. Utility of CE-MS Data in Protein Identification. *Anal. Chem.* **2007**, 79, 3850-3855. Copyright 2007 American Chemical Society. (APPENDIX A)

more separation dimensions, whereas other groups have attempted to increase the information content of the current analysis by incorporating LC retention time into proteomic studies to increase specificity, throughput, and proteome coverage.[13-18]

The majority of LC-MS proteomic studies are based on electrospray ionization mass spectrometry (ESI-MS);[79, 80] however, coupling separations with matrix-assisted laser desorption/ionization mass spectrometry (MALDI-MS) offers numerous advantages and is becoming more commonplace.[81-85] MALDI yields almost exclusively singly-charged ions resulting in less spectral congestion, and an increase in sensitivity, due to all ion current being in one ion species. MALDI also has a relatively higher tolerance of salts, and the ability to archive samples for later study.

An advantage of capillary electrophoresis (CE) over HPLC based separations is the increased separation efficiency. There are several studies which have utilized CE-MS to analyze complex mixtures of peptides with great success.[20-24, 86] CE-MS also provides a migration time for each peptide and perhaps additional information. Wittke and coworkers[23] presented data on urine peptides analyzed using CE-MS. Plots of m/z versus migration time yielded visible trends in the data, although an explanation of their origin was not given. Similar trends are also seen in CE-MS data taken from the studies of Kaiser, et al.[20, 21] and Theodorescu, et al.[22] The goal of our work is to utilize the information provided in these 2D plots of m/z versus CE migration time to determine specific applications where CE-MALDI-MS can be employed as a tool to aid in peptide/protein identification.

This report describes a CE-MALDI-MS method that results in distinct trends observed in plots of m/z versus CE migration time from proteolytic digests. To explore the origin of these trends, we use two sets of lysine-containing peptides to validate the charge state of α-casein proteolytic peptides along each trend. In addition, a peptide electromigration model for peptides is used to validate this charge state trend observation to ensure our CE-MALDI-MS data behave according to theory.[87] Potential applications where these charge-specific trends exhibit analytical utility for more confident peptide identifications and to aid in post-translational modification (PTM) detection are discussed.

Experimental

Chemicals and Sample Digestion Procedures

Bradykinin (2-9) (PPGFSPFR), adrenocorticotropic hormone (ACTH) (18-39) (RPVKVYPNGAENESAEAFPLEF), bovine α-casein, α-cyano-4-hydroxycinnamic acid (CHCA), dihydrogen ammonium phosphate (AP), and ammonium bicarbonate (ABC) were purchased from Sigma (St. Louis, MO). Ac-$(AAKAA)_n$Y-NH_2 (n = 3-7) and Ac-Y$(AEAAKA)_n$F-NH_2 (n = 2-5) peptides were purchased from Genscript Corporation (Piscataway, NJ). Mass spectrometry grade trypsin was purchased from Promega (Madison, WI). HPLC grade methanol (MeOH) and isopropanol (IPA) were purchased from EMD Chemicals Inc. (Gibbstown, NJ). All experiments were performed with 18-MΩ water (ddH_20) purified using a water purification unit (Barnstead International, Dubuque, IA). CHCA was recrystallized prior to use. All other chemicals were used as

received. A modified procedure from Park and Russell[88] was used to perform proteolytic digestion. Briefly, α-casein was prepared at 1 mg mL^{-1} concentration in 50-mM aqueous ABC. A 100-μL aliquot of the protein solution was thermally denatured by incubating at 90˚C for 15 min and subsequently quenched in a -20˚C freezer. The protein samples were digested overnight at 37˚C using trypsin (20 μg mL^{-1}) prepared in 50-mM acetic acid. The *Escherichia coli* (*E. coli*) lysate sample was first separated using LC into 16 fractions and subsequent fractions were digested with trypsin. A single digested fraction was used for CE-MALDI-MS analysis shown here.

MALDI Matrix Preparation for CE-MALDI-MS

A layer of 5-mg mL^{-1} CHCA was applied prior to the CE separations using an x-y-z translation stage (ProBot™, LC Packings, Sunnyvale, CA). CHCA was dissolved in 12:7:1 MeOH:ddH_20:IPA with 10-mM AP and doped with 50-fmol μL^{-1} bradykinin fragment 2-9 and 150-fmol μL^{-1} ACTH fragment 18-39 as internal calibrants. AP was added according to a modified matrix preparation procedure by Smirnov and coworkers.[89] The matrix solution was infused through a fused-silica capillary at 1.0 μL min^{-1} with a 5 second spotting interval to prepare a 30 row by 30 column array (900 total spots). MALDI plates were used for CE fraction collection using the sheath liquid mentioned in the CE-MALDI section as an overlayer.[90, 91]

Sample Preparation for CE-MALDI-MS

Ac-$(AAKAA)_n$Y-NH_2 (n = 3-7) and Ac-Y$(AEAAKA)_n$F-NH_2 (n = 2-5) peptides were prepared at 5 mg mL^{-1} in ddH_20 and diluted 10-fold in 250-mM formic acid (FA) 5-mM AP for CE-MALDI-MS analysis. These charge-state marker peptides were spiked into the α-casein digest (1 mg mL^{-1}) at a concentration of 0.5 mg mL^{-1}. The *E. coli* lysate fraction digest was prepared using a sample stacking protocol, field-amplified sample stacking (FASS),[33] to improve the loading capacity of CE. Briefly, a 15 μL aliquot of the digested *E. coli* lysate fraction was lyophilized and resuspended in 5 μL of a 66% MeOH solution containing 85-mM FA and 1.7-mM AP then vortexed for 30 seconds.

CE-MALDI

CE separations were carried out on a 70-cm (50 μm i.d., 360 μm o.d.) fused-silica capillary (Polymicro Technologies, Phoenix, AZ) with 200-nm UV detection at 50 cm on a homebuilt apparatus equipped with pressurized rinsing and timed injections. The cathodic capillary tip was uniformly tapered using a rotary polishing tool (Dremel, Racine, WI) and interfaced to the ProBot as previously described by Johnson and coworkers.[83] Sheath liquid composed of 50% MeOH, 125 mM FA, and 2.5 mM AP was applied at the cathodic end of the capillary at 500 nL min^{-1}. The background electrolyte consisted of 250-mM FA and 5-mM AP at pH 2.20. Pressurized injections were performed at 1.0 psi and 2.0 psi for 6 and 30 seconds, respectively. These injections correspond to 10 nL and 100 nL as estimated by CE Expert™ software (Beckman Coulter, Fullerton, CA). The experiments with the charge-state marker peptides and α-casein were performed using 10-nL injections with a 10-second spotting interval

between fractions. The *E. coli* lysate fraction CE-MALDI-MS experiments were performed using 100-nL injections and a 5-second spotting interval. CE separations were performed at a potential of +25 kV, using a 30-kV high-voltage power supply (Gamma High-Voltage Research, Ormond Beach, FL). UV electropherograms were collected using a homebuilt virtual instrument interface in the LabView 7.1 (National Instruments, Austin, TX) environment.

MALDI-MS and MALDI-MS/MS

All MALDI-MS experiments were performed using a 4700 Proteomics Analyzer MALDI-TOF/TOF (Applied Biosystems, Foster City, CA). The MS data for the CE-MALDI plates were acquired using the reflectron detector in positive mode (700-4500 Da, 1900 Da focus mass) using 800 laser shots (40 shots per sub-spectrum) with internal calibration. Tandem MS data were acquired using the following precursor threshold criteria: S/N 40, 5 precursors/fraction, 150 ppm fraction-to-fraction precursor mass tolerance, chromatographic peak width 2 fractions, and 3600 laser shots (36 shots/sub-spectrum). Collision induced dissociation tandem MS spectra were acquired using 10-20% greater laser power than the MS spectra acquisition using air at the medium pressure setting as the collision gas with 1 kV of collision energy. All MS and MS/MS data were searched against the Swiss-Prot protein sequence database using the GPS Explorer (Applied Biosystems) software. The database search parameters used for Mascot[92] (Matrix Science, London, UK) were the following: precursor mass tolerance:

50 ppm, taxonomy: mammalia, enzyme: trypsin, missed cleavages: 2, and variable modifications: oxidation (M) and phosphorylation (ST).

Results and Discussion

Figure 3 contains a plot of a proteolytic digest of an *E. coli* lysate, which illustrates the trends typically observed in plots of m/z versus CE migration time for our work and others.[20-24, 86] There are roughly 400 unique peptides that appear to separate into at least four distinct trends. The slope of each trend relative to each other decreases at longer migration times. The observation of these trends in our CE-MALDI-MS data lead us to explore the relationship between the physicochemical properties of peptides, their migration times, and find if this information can be exploited to aid in the analysis of peptides.

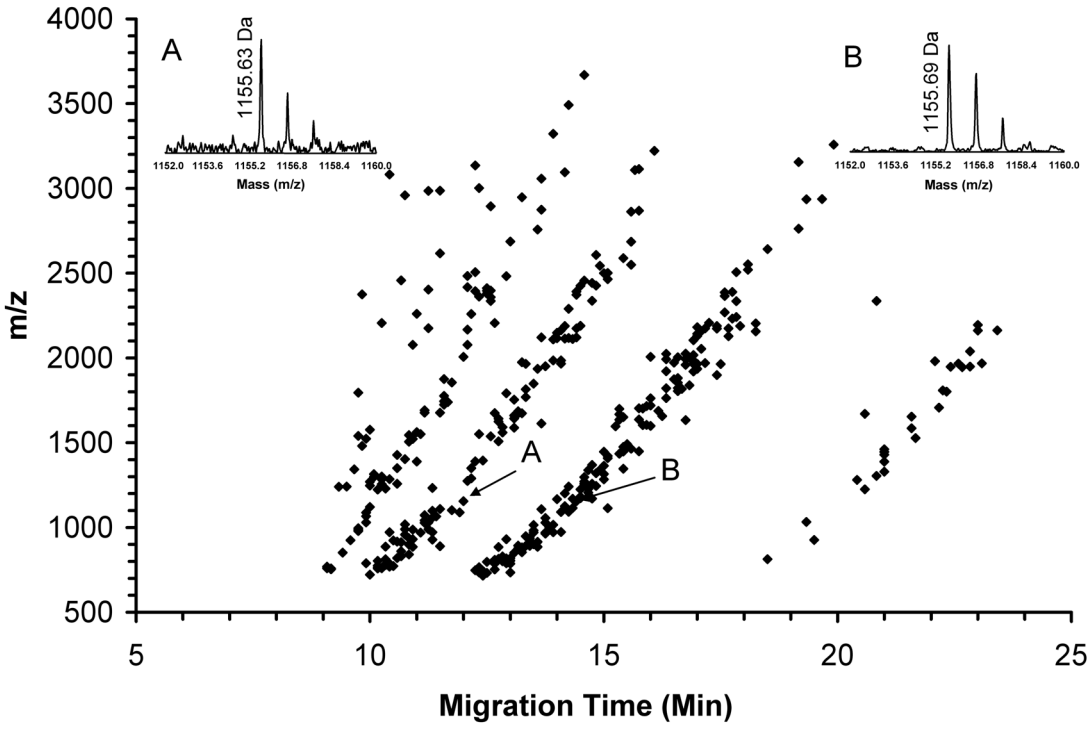

Figure 3. Plot of m/z versus CE migration time for an *E. coli* lysate fraction digest illustrating the observed trends in CE-MALDI-MS data. The peptides denoted as A and B correspond to ADLNVPV*K*DG*K* (m/z 1155.626) and ASLPTIELAL*K* (m/z 1155.698), respectively. The inset figures correspond to the MALDI-MS data for these two *E. coli* derived peptides.

Several models have been developed that relate the electrophoretic mobility to the charge and peptide size.[87, 93-98] For example, the Offord model states that the effective electrophoretic mobility (μ^{eff}) of a peptide is proportional to the charge-to-size ratio of the hydrated ion ($q/MW^{2/3}$), where q is the charge and $MW^{2/3}$ is an expression of the hydrodynamic size (Equation 1).[87]

$$\mu^{eff} \propto \frac{q}{MW^{2/3}} \qquad (1)$$

Further derivation of Equation 1 reveals that the CE migration time (t_m) is directly proportional to the size-to-charge ratio ($MW^{2/3}/q$) (Equation 2).

$$t_m \propto \frac{MW^{2/3}}{q} \qquad (2)$$

Based on Equation 2, the peptide charge can be deduced from CE migration times and measured mass-to-charge (m/z) values. The coefficient on the MW term in Equation 2 can be experimentally derived from a plot of log (μ^{eff}) versus log (MW) to yield Equation 3:

$$\log(u^{eff}) = -s\log(MW) + \log(kq) \qquad (3)$$

Where the *s*-term is the MW coefficient and *k* is a constant. The experimentally derived expression can be exploited to predict migration times of peptides, given the peptide molecular weight and charge. Kim and coworkers have also reported the use of an experimentally derived, semi-empirical model to correlate the μ^{eff} with a slightly different expression ($q/MW^{0.56}$) for peptides resulting from proteolytic digestion of standard proteins.[97] The relationship between the electromigration and physicochemical properties of peptides in CE separations can be illustrated by data obtained from two homologous series of lysine-containing peptide standards (Figure 4a). The corresponding UV electropherogram for this CE data is shown in Figure 4B to illustrate separation efficiency and short run times. These peptides, $(AAKAA)_nY$ and $(AEAAKA)_nF$, are both acetylated at the N-terminus and amidated at the C-terminus. Effectively, these peptides function as in-solution charge state markers, the charge states of which correspond to the number of lysine residues within each peptide. For example,

the Ac-$(AAKAA)_4Y$-NH_2 peptide would exist in the +4 charge state at pH 2.2. The charge state of peptides are determined using a charge-state calculator,[99] which takes into account the acidic residues (Asp, Glu), the basic residues (Arg, His, Lys), the termini, and any charge altering modifications (N-terminal amidation, phosphorylation, etc.). Since our experiment is performed at pH 2.2, the acidic residues do not influence the charge state of the peptide in solution. The $[M + H]^+$ ions for these standard peptides plotted against the measured CE migration time at the 70 cm elution point are shown in Figure 4a. In both the $(AAKAA)_nY$ and $(AEAAKA)_nF$ series of peptides the higher molecular weight, highly charged species elute first, with the lowest charged peptides eluting at the longest time. It is clear that peptides with similar mass but differing in charge state are easily separated, *e.g.,* Ac-$(AAKAA)_3Y$-NH_2 with m/z = 1459.84 elutes ca. 4 minutes before Ac-$Y(AEAAKA)_2F$-NH_2 (m/z = 1452.75). There also appears to be a correlation between peptides of the same charge-state, *i.e.,* the standard peptides of identical charge state model the trends observed in Figure 3.

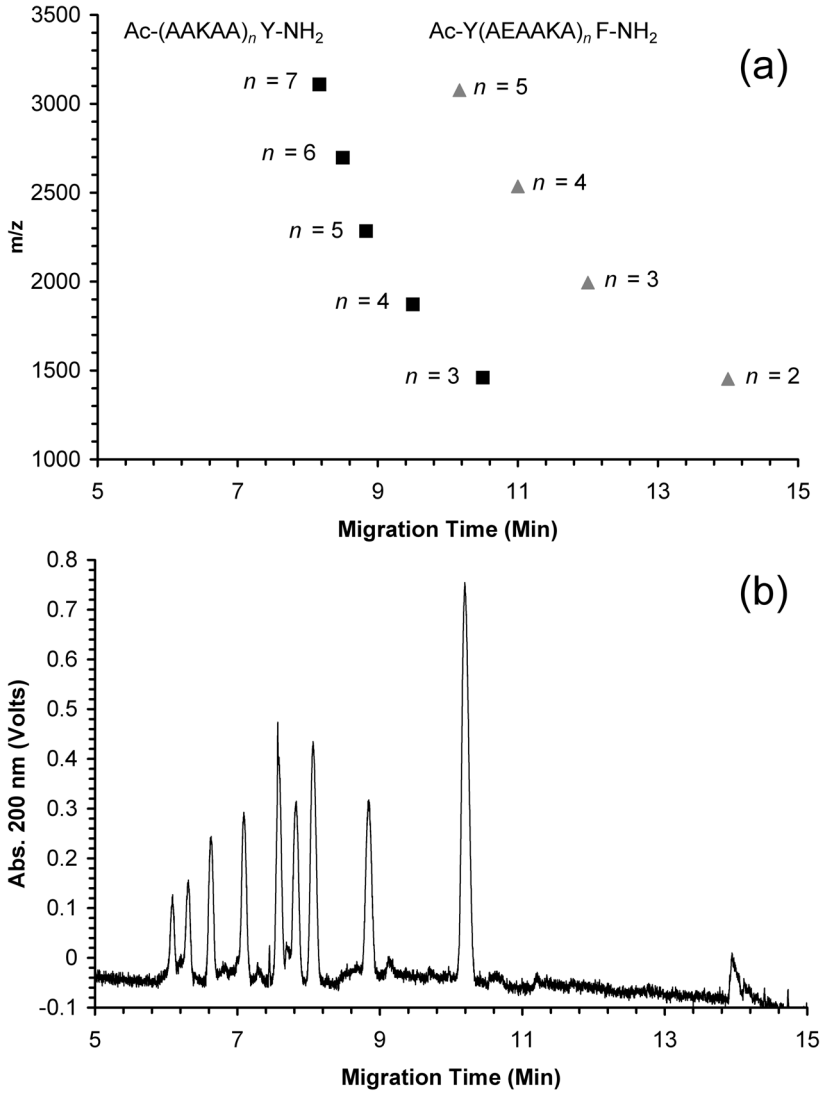

Figure 4. a.) Plot of m/z versus CE migration time for Ac-(AAKAA)$_n$Y-NH$_2$ (n = 3-7, solid squares) and Ac-Y(AEAAKA)$_n$F-NH$_2$ (n = 2-5, solid triangles) standard peptides. b.) Corresponding UV electropherogram for the charge-state marker peptides, with migration times measured at the 50-cm detection point.

Charge-based trends are most easily observed in Figure 5a, where peptides resulting from a digest of α-casein were spiked with the charge-state marker standard peptides and analyzed by CE-MALDI-MS. Figure 5a is plotted as the log (μ^{eff}) versus

log (m/z) to allow the experimental determination of MW coefficient (*s*-term) in Equation 3. Plotting the CE-MS data in this manner is important as μ^{eff} will correct for any inconsistencies in the experimental setup (*e.g.,* potential, capillary length, capillary coating, etc.) between laboratories and experiments. Therefore, plotting CE-MS data this way becomes more useful in developing databases, since migration time can vary per experiment. The average coefficient of MW for all charge-based trends was 0.52 (R^2 value of 0.94), which is similar to the value of 0.56 obtained using an iterative analysis of experimental data by Kim and coworkers.[97] This small inconsistency may be due to the relatively low number of peptides in our analysis and the scatter in the data. The scatter should improve by using a coated capillary for the analysis, which is currently being investigated. The MW coefficient for each charge-based trend can be used to predict the migration time of an unknown peptide, given the potential peptide sequence and charge. Candidate peptides that fall along the proper charge-state trend are confirmed, whereas, those peptides that fall along the wrong trend are either post-translationally modified or false positive identifications.

(a)

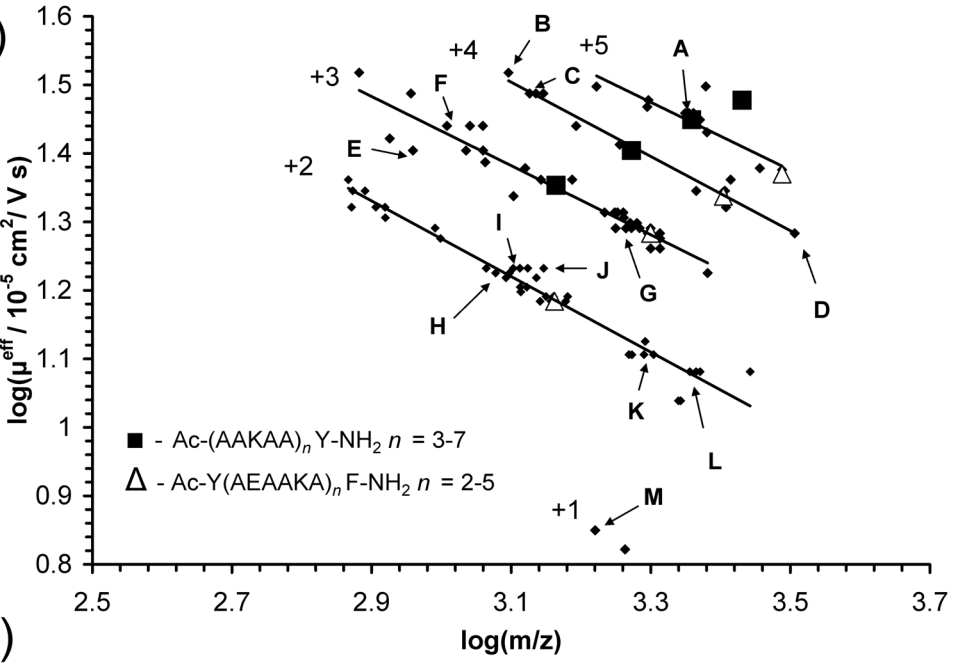

(b)

label	peptide sequence	$[M+H]^+_{obs}$	mass error (ppm)	q (a)	t_m (min)	μ^{eff} x 10^{-5} (c) (cm^2 V^{-1} sec^{-1})	acidic	basic
A	HPIKHQGLPQEVLNENLLR (94)	2235.2432	3.4	5	9.33	28.75	1	4
B	TKLTEEEKNR (b)	1247.6609	1.5	4	8.33	32.96	3	3
C	HIQKEDVPSER (47)	1337.6831	-1.8	4	8.83	30.74	3	3
D	EGIHAQQKEPMIGVNQELAYFYPELFR (41)	3207.5610	-10.0	4	12.83	19.20	3	3
E	EGIHAQQK (13)	910.4655	-9.5	3	10.33	25.36	1	2
F	LTEEEKNR (b)	1018.5139	-2.4	3	9.66	27.56	3	2
G	HQGLPQEVLNENLLR (103)	1759.9490	2.3	3	12.17	20.59	2	2
H	NAVPITPTLNR (15)	1195.6798	0.4	2	14.17	16.80	0	1
I	YLGYLEQLLR (61)	1267.7096	4.0	2	14.00	17.07	1	1
J	ALNEINQFYQK (51)	1367.7021	4.9	2	14.33	16.54	1	1
K	YKVPQLEIVPN(pS)AEER (33)	1951.9551	1.4	2	17.17	12.77	3	2
L	EPMIGVNQELAYFYPELFR (14)	2316.1300	-2.9	2	17.83	12.06	3	1
M	VPQLEIVPN(pS)AEER (b)	1660.8021	4.8	1	24.50	7.07	3	1

(a) Calculated charge state at pH 2.20
(b) Confirmed by peptide mass fingerprint (PMF) database search
(c) $\mu^{eff} = \mu^{obs} - \mu^{eo}$

Figure 5. a.) Plot of log (μ^{eff}) versus log (m/z) for the α-casein proteolytic digest (closed diamonds) with the Ac-$(AAKAA)_n$Y-NH_2 (n = 3-7, empty squares) and Ac-Y$(AEAAKA)_n$F-NH_2 (n = 2-5, empty triangles) peptides added at 0.5 mg mL^{-1} each. b.) Table of α-casein peptides identified from each trend with their observed m/z values, mass error (ppm), calculated in-solution charge state (q), migration time (t_m), effective electrophoretic mobility (μ^{eff}) and number of acidic/basic residues. Parenthetical numbers adjacent to each peptide sequence correspond to the Mascot MS/MS ion score.

The sequence of the α-casein derived peptides, and their corresponding charge states, were confirmed using accurate mass measurement and tandem MS. Figure 5b contains the observed m/z for each peptide, mass error (ppm), calculated charge state (q), effective electrophoretic mobility (μ^{eff}), migration time (t_m), and the number of acidic/basic residues for selected α-casein peptides that reside on each charge-state marked trend. For example, we would expect the peptide ***H***PI***KH***QGLPQEVLNENLL***R*** (m/z 2235.24), denoted as A, to fall on the +5 trendline as it has four charge carrying residues plus the N-terminus charge. This is in agreement with the experimental data (Figure 5A). Peptides denoted as B, G, and J in Figure 5b fall along the +4, +3, and +2 charge-state trends, respectively, as we would predict based upon the number of basic amino acids. An example mass spectrum is shown in Figure 6a for peptide G in Figure 5a illustrating high mass spectral resolution (R_s ~ 16,500) and decreased mass spectral convolution. Figure 6b shows the tandem MS data for peptide G, demonstrating a sequence informative ion series of *b* and *y*-type fragment ions.

The vast majority of peptides are found on the +2 and +3 trend, indicating that the majority of peptides have zero or one missed cleavage. Since the peptides are all tryptic, all peptides should carry at least a +2 charge (Lys or Arg plus the N-terminus), except for a C-terminal peptide fragment and any peptide modified by a negatively-charged group (*e.g.,* phosphate or sulfonate) at the pH these experiments were performed (pH = 2.2). Note that some peptides fall below the +2 trendline (See Figure 3a). For example, the peptide denoted as M should appear along the +2 trend, however this peptide is observed on the +1 peptide trendline. Upon examination of the tandem MS data, it was found that this peptide (VPQLEIVPN(pS)AEE***R***) contains a phosphorylation site, altering the peptide charge to the +1 state. Effectively, using CE-MS to analyze proteolytic digests reduces the number of required analyses of phosphorylated peptides to those that lie on the +1 trend. However, it is possible for phosphorylated peptides to fall on other trendlines. Such is the case for Y***K***VPQLEIVPN(pS)AEE***R*** (m/z 1951.955), denoted as K, which contains a missed cleavage and falls on the +2 trendline. Kim and coworkers also observed that peptides containing certain PTMs deviate from this linear correlation of μ^{eff} with $q/MW^{0.56}$, owing to an incorrect calculation of the charge state for those peptides.[97]

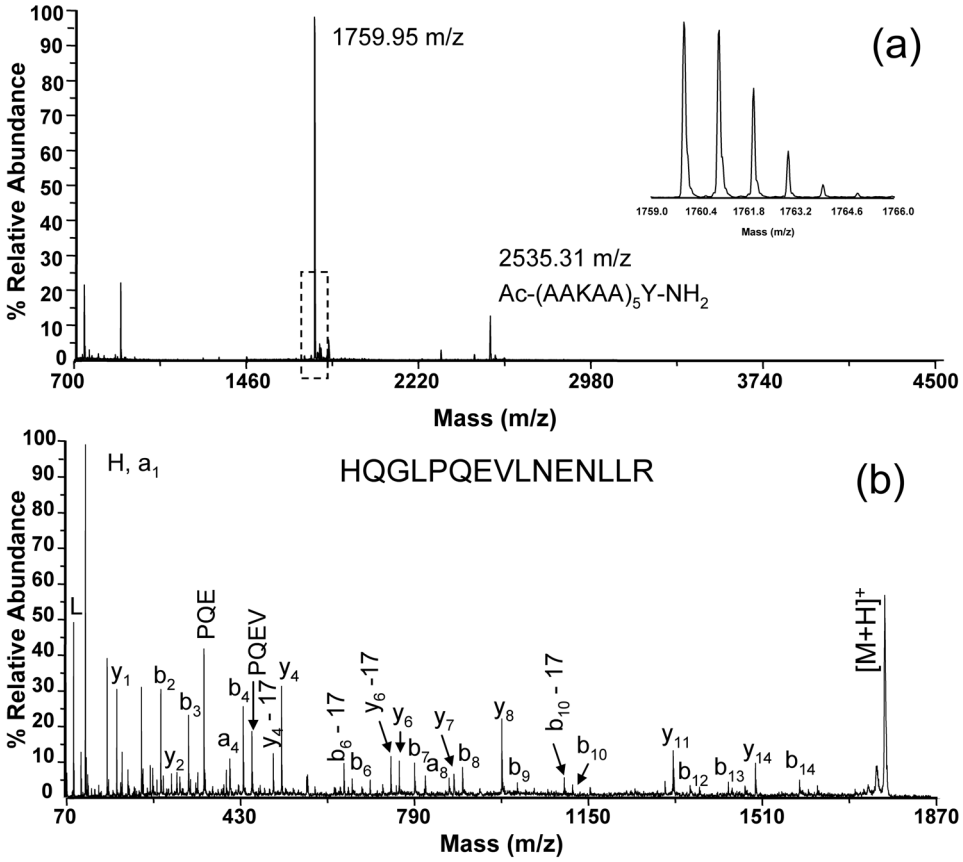

Figure 6. a.) Mass spectrum of a CE fraction (12.17 min) from the separation of α-casein proteolytic digest spiked with the charge-state marker peptides. Inset figure: expanded view of the peptide at 1759.94 m/z to illustrate the mass spectral resolution of ~ 16,500 measured at FWHM. b.) Tandem mass spectrum of the ion signal at 1759.94 m/z corresponds to HQGLPQEVLNENLLR from CASA1_BOVIN with a Mascot MS/MS ion score of 103.

Utility of Charge-State Specific Trends for Protein Identification

The CE-MS charge-based trends observed provide complementary information to proteomic analysis similar to AMT tags from LC-MS analysis.[13, 14, 16] However, the CE-MS data provides much more information than LC-MS. LC-MS data plotted as mass versus retention time typically yields a scatter plot, while CE-MS results in data with well defined charge-based trends.[16, 20, 86, 100] These trends are dependent upon the number of basic residues present, in effect providing compositional information for each peptide; this additional information adds confidence in assigning the peptide sequence. As mentioned from the α-casein data, tryptic phosphopeptides with no missed cleavages tend to reside along the +1 trend and are easily selectable from the plot. In a complex proteomic mixture, the search for tryptic phosphopeptides can be simplified to a list of candidate phosphopeptides. These selected candidates that reside on the +1 trend can then be submitted to tandem MS analysis using an inclusion mass list for the peptides of interest, cutting the analysis time for that PTM by more than one order of magnitude. This would also be true for other negatively charged PTMs. A major benefit of coupling separations off-line with MALDI-MS is the ability to re-interrogate the CE separation as needed.

These charge-based trends also show specific utility towards protein identification in the case of limited tandem MS data. Proteolytic α-casein peptides denoted as (E, H, and L) in Figure 5b all have relatively low MS/MS ion scores. This insufficient tandem MS data may be due to a low abundance of these peptides or poor fragmentation chemistry. Additional physicochemical properties on these peptides can

be obtained upon examining the location of these peptides on the CE-MS charge-based trends (Figure 5a). The number of basic residues present in peptides (E, H, and L) is in agreement with the charge-based trend each peptide resides. Effectively, these charge-based trends provide further confidence to assign the peptide identification. In addition, this CE-MS method can confirm questionable peptides with limited MS/MS data, hence a new way rule out false positives. For example, a peptide appears on the +3 trendline with a mass of 1871.9882 Da, this could be the αS2-casein peptide ***K***TVDMESTEVFT***KK***T***K*** with 5 ppm mass error. However, this peptide exists at the +5 charge state. Given MS data alone, this peptide could be incorrectly identified based on mass accuracy. The added dimension from CE-MS allows for the removal of this false positive identification. The correct assignment for mass 1871.9882 m/z is the peptide Y***K***VPQLEIVPNSAEE***R*** (1 ppm mass error), which migrates along the +3 charge-state trend as predicted. Overall, these charge-based trends add utility toward peptides with phosphorylations, similar mass, or insufficient tandem MS data.

Peptides of similar mass, but different basic residue composition are easily identified. For example, two peptides ADLNVPV***K***DG***K*** (m/z 1155.626) and ASLPTIELAL***K*** (m/z 1155.698) derived from an *E. coli* lysate digest differ in mass by 51 ppm. These two peptides are separated by 144 seconds in the CE dimension. The separation in time is due to the difference in the number of basic residues, which can be determined in short by examining the charge-specific trend upon which each peptide resides, ADLNVPV***K***DG***K*** (denoted as A in Figure 3) falls on the +3 trendline and ASLPTIELAL***K*** (denoted as B) falls on the +2 trendline as predicted. In effect providing

some compositional information for each peptide, this additional information adds confidence in assigning peptide sequence.

Conclusion

Trends observed in plots of m/z versus CE migration time for CE-MALDI-MS data were used in concert with two series of charge-state marker peptides to aid in charge state assignment. These 2D plots of CE-MALDI-MS data are simple and clear, providing compositional information on each peptide based on the peptides location on the plot. From the analysis of a proteolytic digest of α-casein, phosphopeptides were easily identifiable from deviations in the trends observed (which are predominantly non-phosphorylated peptides). Additionally, peptides with insufficient tandem MS data gain confidence in their identification owing to the added basic reside information. The overall simplicity of the 2D plots of the CE-MALDI-MS data we present offers advantages over LC-MS due to the reproducibility, clarity, and the information provided from the charge-state specific trends. The coupling of CE with mass spectrometry is a powerful tool for proteomics which not only provides high-resolution, high efficiency separations, but the analysis also yields compositional information, charge state, and a streamlined process for analyzing charged PTMs. In addition, we plan to utilize bioinformatics technologies to create an automated process for analyzing CE-MS data of complex proteomic systems.

CHAPTER III

HIGH-THROUGHPUT METHOD FOR ON-TARGET PERFORMIC ACID OXIDATION OF MALDI DEPOSITED SAMPLES*

Introduction

Disulfide bonds play important roles in stabilizing and maintaining native protein structure,[49, 50] and mass spectrometry (MS) plays an increasingly important role in deciphering these processes,[51] especially protein folding/unfolding kinetics.[52-54] Disulfide bond locations within proteins can be determined using a variety of MS-based methods including: tandem MS,[57, 58] database search algorithms,[56, 59-61] chemical reduction,[55, 62, 63] chemical oxidation,[46, 47, 64] and metal ion cleavage of disulfide-bonds.[65, 66] Xu and coworkers developed a tandem MS search engine to simplify database searches for disulfide-linked peptides fragment ion spectra,[56] but such spectra can be complicated by direct cleavage of the disulfide bond between inter-linked disulfide bridged peptides, which results in a limited number of sequence-informative fragment ions from each peptide α and β-chain peptide forming the disulfide linkage.[57] Disulfide-linked peptides can also be identified through chemical reduction of the disulfide bond.

---

* Reproduced with permission from Williams, B.J.; Russell, W.K.; Russell, D.H. High-throughput on-target performic acid oxidation of MALDI deposited samples. *J. Mass Spectrom.* **2010**, 45, 157-166. Copyright 2009 John Wiley & Sons Limited. (APPENDIX B)

For example, a reductive MALDI matrix, 1,5-diaminonapthalene (1,5-DAN),[62] was used by Quinton and coworkers to characterize disulfide-bridged peptides using liquid chromatography (LC) coupled off-line with MALDI-MS/MS.[63] This reductive MALDI matrix successfully reduces disulfide bonds during the MALDI process; however, 1,5-DAN also yields a high relative abundance of matrix clusters up to 1000 m/z, which complicates the analysis of low molecular weight disulfide and/or cysteine-containing peptides.

Chemical oxidation offers the following benefits over performing chemical reduction of the disulfide bond: (i) a 48 Da mass shift occurs per cysteine residue, (ii) cysteic acid (SO_3H) enhances negative ion formation, and (iii) the performic acid simultaneously cleaves the disulfide bond and chemically modifies each peptide involved in the disulfide bridge. For example, performic acid oxidation has been used to study disulfide-containing proteins prior to proteolytic digestion and strong cation exchange (SCX) chromatography.[47] The oxidized cysteine-containing peptides undergo an elution shift owing to a decrease in peptide solution-phase charge state, because low charge-state peptides are weakly retained on the SCX column. The resulting enriched oxidized cysteine-containing peptides are then subjected to off-line MALDI-MS/MS followed by peptide identification via database searching or *de novo* sequencing. This methodology utilizes a combination of oxidation, mass spectrometry, and database searching for analyzing the cleaved disulfide-bonds of bovine serum albumin. Because performic acid cleaves the disulfide bonds prior to digestion, the native disulfide bond pattern is lost; therefore, it is important to maintain intact disulfide-linked peptides

throughout proteolytic digestion in order to characterize the disulfide bond connectivity within proteins.

Although performic acid oxidation is widely used, there are several challenges associated with solution-phase oxidation methods. For example, typical solution-phase oxidation methods are performed on lyophilized peptide/protein samples using reaction times ranging from 2-4 hrs[47, 71, 72] and several steps are required following oxidation to remove the performic acid reagent prior to MS analysis.[47, 71] Some solution-phase oxidation methods have decreased reaction times to 10-30 min for oxidation of cysteine/methionine containing peptides; however, the additional clean-up steps following oxidation make this method less desirable.[46] On-target oxidation methods using solution-phase performic acid have also been successfully applied to MALDI spots containing peptides and/or proteolytic digests.[71] For example, we showed that directly adding the performic acid solution to a pre-spotted MALDI deposit containing a bovine apo-transferrin tryptic digest yields oxidized tryptic peptides; however, the S/N ratios of the oxidized peptide negative ions decreased by 5-fold because of ion suppression effects. The overall amino acid sequence coverage also decreased by half compared to the solution-phase oxidized sample. Thus, an on-target performic acid oxidation method that can mitigate these adverse effects would be highly beneficial. The ideal on-target oxidation method would offer the following characteristics over solution-phase oxidation methods: (i) simple experimental procedure with no post-oxidation sample cleanup; (ii) decreased ion suppression effects following oxidation; (iii) improved throughput over

solution-phase methods; and (iv) maintain positive and negative ion mass spectral quality following on-target oxidation.

This report describes an on-target performic acid oxidation method using performic acid vapor to oxidize disulfide-containing peptides/proteins deposited for MALDI-MS analysis. Brown and Hartley have reported a similar approach using performic acid vapor to oxidize disulfide-linked peptides on electrophoresis paper.[101] The novel aspect of our method is found within the ability to successfully oxidize multiple MALDI spots simultaneously using performic acid vapor contained within a reaction chamber without sample cleanup. Reaction times for the on-target performic acid oxidation method (10-60 min) are also shorter than traditional solution-phase oxidation methods (2-4 hrs). We apply this on-target performic acid oxidation method to a model disulfide-linked peptide, intact bovine insulin, and a proteolytic digest of bovine ribonuclease A. In addition, we discuss the advantages of this method over solution-phase oxidation methods and demonstrate the ability to elucidate disulfide-linked peptides from ribonuclease A.

Experimental

Chemicals

All chemicals were purchased from Sigma-Aldrich (St. Louis, MO) unless otherwise noted. Sequencing grade modified trypsin was obtained from Promega (Madison, WI). Oxytocin (C<u>YIQN</u>CPLG-NH_2) was purchased from American Peptide Company (Sunnyvale, CA). Hydrogen peroxide (35% w/w) and formic acid (99% w/w)

were obtained from Acros Organics (Morris Plains, NJ). HPLC grade acetone, acetonitrile (CH_3CN), and methanol (CH_3OH) were purchased from EMD Chemicals Inc. (Gibbstown, NJ). All experiments were performed with 18-MΩ water (ddH_2O) purified using a water purification unit (Barnstead International, Dubuque, IA).

Sample Preparation for MALDI-MS

A 15 μM stock solution of native oxytocin was prepared in 10 mM formic acid. Oxytocin was reduced by adding 2 μL of 50 mM tris(2-carboxyethyl)phosphine and incubating at 60˚C for 60 min. The synthetic mixture of native and reduced oxytocin (1:1 molar ratio of native: reduced oxytocin) was reacted with 2-iodoacetamide by increasing the solution pH from 3.0 to 7.1 with 40 μL of 25 mM ammonium bicarbonate (NH_4HCO_3) and incubated in the dark for 45 min at room temperature. The excess 2-iodoacetamide and NH_4HCO_3 was removed using a 10 μL C_{18} resin pipette tip (Millipore, Billerica, MA) and eluted with a 60:40 CH_3CN: ddH_2O solution containing 0.1% formic acid. A 1 μL aliquot of the eluate was spotted as the overlayer (analyte deposited on pre-spotted MALDI matrix) to α-cyano-4-hydroxycinnamic acid (CHCA) matrix. CHCA was prepared at 5 mg mL^{-1} in a 2:3 ddH_2O: CH_3OH solution containing 10 mM dihydrogen ammonium phosphate ($NH_4H_2PO_4$) and 1 μL was pre-spotted using the underlayer method.[90]

Stock solutions of α-melanocyte stimulating hormone (Ac-SYSMEHFRWGKPV-NH_2) and α1-mating factor (WHWLQL) were prepared at 10 μM in 10 mM formic acid. The resulting solutions were then mixed 1:1 (v/v) with CH_3OH

and 1 μL (5 pmol) was spotted onto the MALDI target as an overlayer to CHCA matrix. These MALDI deposits were initially oxidized using the on-target oxidation methods described below (-20˚C for 60 min). Additional oxidation was performed on the same MALDI deposits using room temperature (+24˚C) oxidation for an additional 60 minutes.

A stock solution (1 mg mL^{-1}) of bovine insulin was diluted to 10 μM in 10 mM formic acid. The insulin solution was then mixed 1:1 (v/v) with CH_3OH and 1 μL (5 pmol) was spotted onto the MALDI target as an overlayer to pre-spotted MALDI matrix. The on-target oxidation experiments using intact insulin were performed with three different MALDI matrices: CHCA, 2,4-dihydroxyacetophenone (2,4-DHAP), and 2,4-DHAP combined with CHCA as dual MALDI matrices. For the experiments with CHCA and 2,4-DHAP (10 mg mL^{-1} in 2:3 ddH_2O: CH_3OH with 10 mM $NH_4H_2PO_4$), the pre-spotted MALDI deposit was re-dissolved with an overlayer of insulin (1 μL of 5 μM insulin in 1:1 (v/v) CH_3OH: 10 mM formic acid). For the dual MALDI matrices experiment, 2,4-DHAP was spotted as an underlayer followed by an overlayer of insulin then subjected to on-target oxidation. Following oxidation, the 2,4-DHAP + insulin sample deposit was re-dissolved with overlayer of CHCA prior to MS analysis. The intact insulin experiments with the varied MALDI matrices were oxidized using the on-target performic acid oxidation methods described below with the exception of performing oxidation at room temperature (+23˚C) for 60 minutes.

Ribonuclease A Proteolytic Digestion

Dual protease digestion (trypsin followed by chymotrypsin) of bovine ribonuclease A (RNase A) was performed using methods described by Xu and coworkers with minor modifications.[56] Briefly, RNase A was dissolved at 1 mg mL^{-1} in a 25 mM ammonium acetate buffer adjusted to pH 6.0 with 10 mM formic acid. RNase A was initially digested with trypsin (1:50 (w/w) enzyme: protein ratio) for 4 hrs at 37˚C followed by chymotrypsin addition (1:50 (w/w) enzyme: protein ratio) and incubated for an additional 4 hrs. The RNase A proteolytic digest was alkylated following proteolytic digestion with 5 µL of 100 mM 2-iodoacetamide and incubating in the dark for 45 min at room temperature. Following alkylation, the sample was subjected to cleanup using a 10 µL C_{18} resin pipette tip. The RNase A proteolytic digest was eluted with a 60:40 CH_3CN: ddH_2O solution containing 0.1% formic acid and 1 µL of the eluate was spotted as the overlayer to CHCA matrix.

On-Target and Solution-Phase Performic Acid Oxidation

Performic acid was prepared using hydrogen peroxide (35% w/w) and formic acid (99% w/w) mixed at a 1:9 ratio, respectively, and allowed to age at room temperature for 2 hr.[71] On-target performic acid oxidation using performic acid vapor was performed by placing 40 µL of a 1:1 (v/v) mixture of acetone: performic acid directly on the MALDI target in an area that does not contain sample (distance from the performic acid reagent to the MALDI sample deposit is not critical). The MALDI target was then covered in a plastic petri dish and placed in a -20˚C freezer for 10-60 min.

Following on-target performic acid oxidation the MALDI plate was allowed to reach ambient temperature then subjected to MALDI analysis without sample cleanup. Solution-phase performic acid oxidation was performed using a 1:19 ratio of hydrogen peroxide: formic acid as previously described.[69] The performic acid solution was used to resuspend vacuum dried peptide samples or RNase A proteolytic digests then allowed to react at 0°C for 4 hr. Following oxidation, samples were diluted with 500 μL of ddH_2O and vacuum dried. Samples were then resuspended in ddH_2O and mixed 1:1 (v/v) with CH_3OH prior to spotting on the MALDI target as an overlayer.

MALDI-MS and MALDI-MS/MS

All MALDI-MS experiments were performed using a model 4700 Proteomics Analyzer MALDI-TOF/TOF (Applied Biosystems, Framingham, MA). The MALDI-MS data were acquired using the reflectron detector in both positive and negative ion modes using 1200 laser shots with external calibrants: bradykinin (2-9) (PPGFSPFR) and adrenocorticotropic hormone (ACTH) (18-39) (RPVKVYPNGAENESAEAFPLEF). Two different instrument parameters were used for MS experiments with peptides/proteolytic digests (500-4500 Da, 2100 Da focus mass) and intact bovine insulin (700-6000 Da, 3500 Da focus mass). The non-oxidized forms of RNase A proteolytic peptides, ^{118}YPNCAY^{123} and ^{73}VHESLADVQAVCSQK^{87} were used to internally calibrate the negative ion mass spectrum of the RNase A proteolytic digest. Collision-induced dissociation (CID) tandem MS spectra were acquired using 20% greater laser power than the MS spectra acquisition with atmosphere (medium pressure)

as the collision gas with 1 kV of collision energy. The average coefficient of variation (CV) was calculated to be ±6% for triplicate analysis of an RNase A proteolytic digest subjected to on-target oxidation. Normalized ion signals were determined using a ratio of the single peptide ion count to the total ion count for five oxidized RNase A peptides. The normalized ion signals were then used to calculate the CV.

Results and Discussion

The main motivation of this work is to develop a method to simultaneously scan complex mixtures for disulfide-linked peptides and be able to distinguish between free cysteine and bridged disulfide-containing peptides. Our strategy is to use thiol alkylation chemistry followed by on-target performic acid oxidation. Scheme 1 illustrates the resulting performic acid oxidation products for both (a) inter-linked and (b) intra-linked disulfide-containing peptides. For example, an inter-linked disulfide bridged peptide will form oxidized products for both α and β-chain peptides (Scheme 1a). The performic acid cleaves the disulfide bond to convert each cysteine thiol to cysteic acid (SO_3H), whereas an intra-linked disulfide containing peptide will form a single peptide containing two cysteic acid residues (Scheme 1b). Note that a peptide containing two free thiol side chains will yield the same product as Scheme 1b. Incorporating an alkylation reagent such as 2-iodoacetamide into the overall reaction scheme provides differentiation between peptides with two free cysteine residues or an intra-linked disulfide bond. The carbamidomethyl (CAM) group protects the free cysteine residues from oxidation, while the intra-linked disulfide bridged peptide will be fully oxidized (Scheme 1c).

Scheme 1. **Performic acid oxidation products of (a) inter-linked and (b) intra-linked disulfide-linked peptides, and (c) a mixture of an intra-linked disulfide-linked peptide and the 2-iodoacetamide alkylated form.**

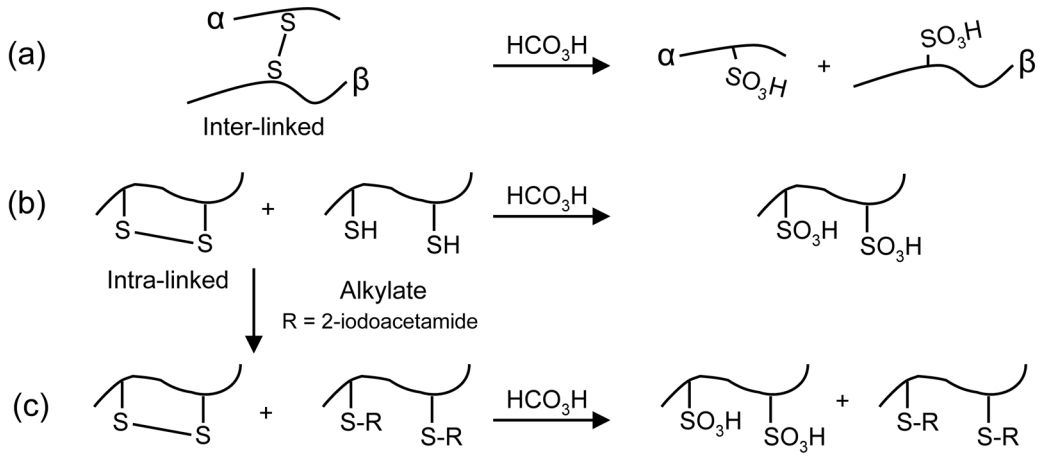

On-Target Oxidation of Oxytocin

The disulfide-containing peptide oxytocin (C<u>YIQN</u>CPLG-NH_2) is used to illustrate the reaction shown in Scheme 1c, and a synthetic mixture of native and chemically reduced oxytocin is used to demonstrate the mixture described in Scheme 1b. The synthetic mixture of native and reduced oxytocin was reacted with 2-iodoacetamide, and Figure 7 contains (a) positive and (b) negative ion MALDI-MS spectra for this sample taken after on-target performic acid oxidation of the native and CAM-modified oxytocin mixture. Ion signals for native oxytocin (m/z 1007.48 for $[M + H]^+$) and signals for alkylation products (m/z 1066.53 for $[M + H + CAM]^+$ and m/z 1123.55 for $[M + H + 2CAM]^+$) are observed in the positive ion mass spectrum after oxidation (Figure 7a). These assignments were confirmed by tandem MS (Figure 8b and Figure 8c). The intact disulfide bond of native oxytocin is cleaved and converted to cysteic acid, as evidenced

by the $[M - H + O_6]^-$ ion (m/z 1103.37) in the negative ion mass spectrum (Figure 7b). The negative ion tandem mass spectrum for fully oxidized oxytocin can be found in Figure 8a. Following oxidation $[M + H]^+$ ions of native oxytocin are still observed in the positive ion mass spectrum (Figure 7a), which suggests incomplete oxidation of native oxytocin. Experiments are currently underway to address issues related to incomplete oxidation, and preliminary data for these on-target oxidation optimization studies are discussed below. Despite incomplete conversion to the fully CAM-modified oxytocin, ion signals for $[M + H + CAM + O_3]^+$ or $[M - H + CAM + O_3]^-$ are not observed in the positive or negative ion mass spectra. Therefore, the single CAM-modified oxytocin does not complicate the differentiation between a peptide that contains two free cysteine residues from one that contains an intra-linked disulfide bond. Nonetheless, the 2-iodoacetamide alkylation chemistry incorporated into Scheme 1c allows a multiple free cysteine-containing peptide to be differentiated from an intra-linked disulfide bridged peptide such as oxytocin.

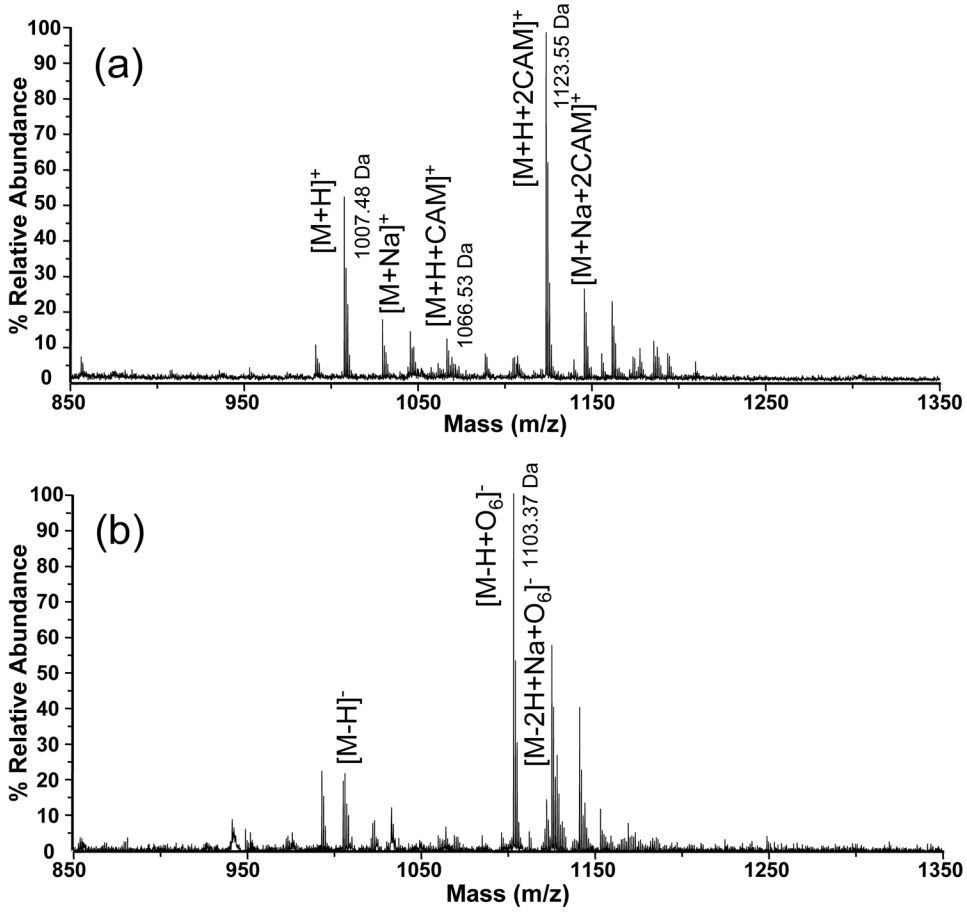

Figure 7. (a) Positive ion and (b) negative ion mass spectrum of native and CAM-modified oxytocin after 10 minutes of on-target performic oxidation performed at -20˚C.

Effect of On-Target Oxidation on His, Met, Trp, and Tyr Containing Peptides

The effect of on-target oxidation on peptides that contain other oxidizable amino acids, such as histidine, methionine, tryptophan, and tyrosine was investigated using α-melanocyte stimulating hormone (Ac-SYSMEHFRWGKPV-NH_2) and α1-mating factor (WHWLQL). Figure 9a contains a positive ion mass spectrum for α-melanocyte stimulating hormone taken before oxidation. Note that several oxidized peptide ion signals ($[M + H + O]^+$, $[M + H + O_2]^+$, etc.) are present in this spectrum. These oxidized

ion signals are a result of oxidation owing to air exposure over time. Following on-target oxidation (1 hr at -20˚C) (Figure 9b), the intensities of the oxidized peptide ion signals do not increase relative to the $[M + H]^+$ ion, thus it appears that on-target oxidation does not significantly oxidize other amino acids under cold oxidation conditions. The same MALDI sample deposit was subjected to an additional hour of oxidation at + 24˚C and the abundance of the oxidized ion signals do not increase relative to the $[M + H]^+$ ion signal for α-melanocyte stimulating hormone, thus it appears that oxidation is not occurring (Figure 9c). As a control experiment, native oxytocin (C<u>YIQN</u>CPLG-NH_2) was spotted on a separate sample deposit and oxidized simultaneously on the same MALDI target, and the MALDI mass spectrum from this sample contains a strong signal for the $[M - H + O_6]^-$ ion (m/z 1103.44) (Figure 9d) indicating the oxidation reaction was successful. Similar experiments for α1-mating factor also resulted in minimal increase in the relative abundance of the oxidized peptide ion signals as a result of oxidation (See Figure 10), thus we conclude that the on-target oxidation is not complicated by reactions with H, M, W, or Y amino acid containing peptides.

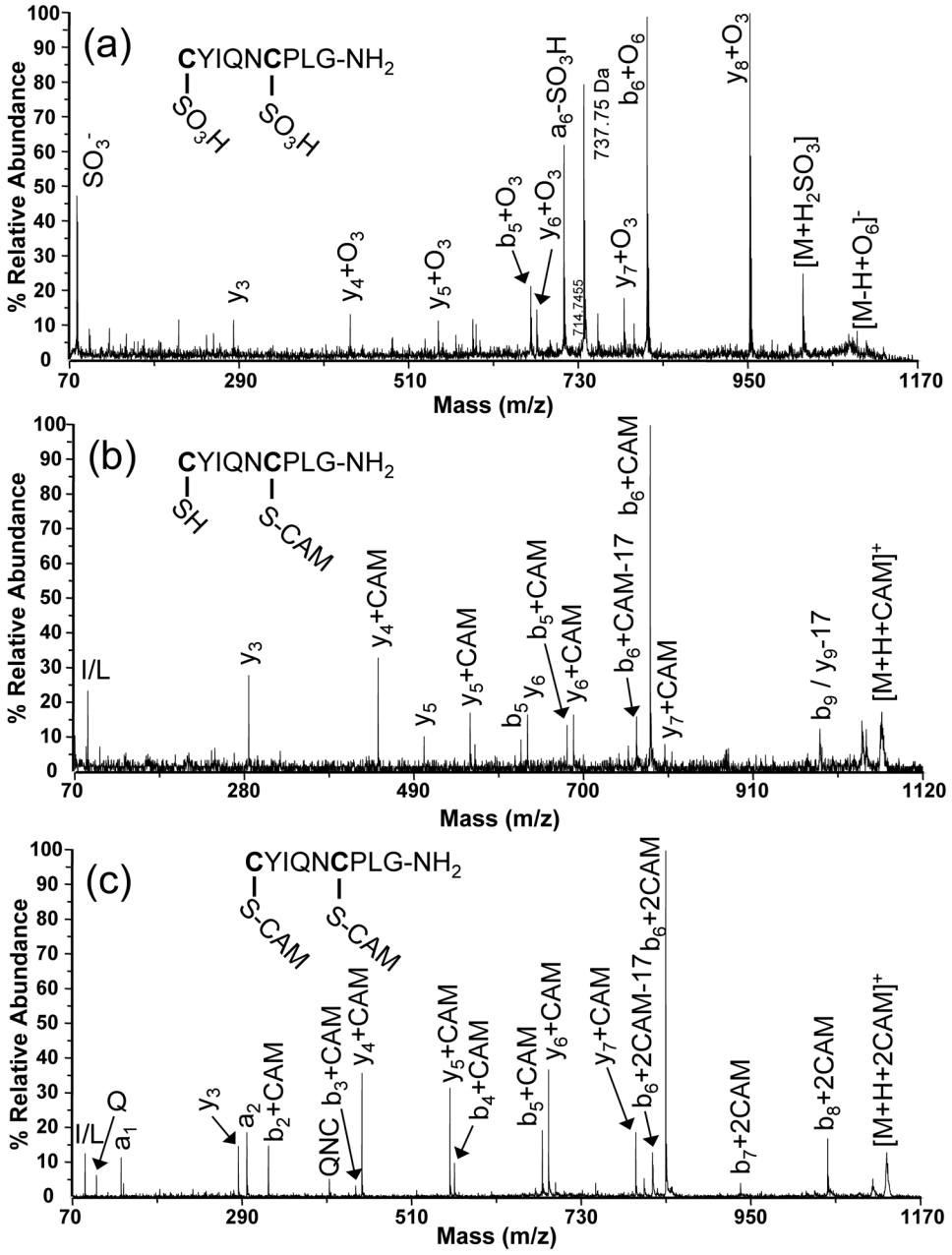

Figure 8. (a) Negative ion tandem mass spectrum for fully oxidized oxytocin $[M - H + O_6]^-$ ($C_{ox}YIQNC_{ox}PLG\text{-}NH_2$). Positive ion tandem mass spectra for the carbamidomethyl (CAM) modified oxytocin ion signals (b) $[M + H + CAM]^+$ and (c) $[M + H + 2CAM]^+$.

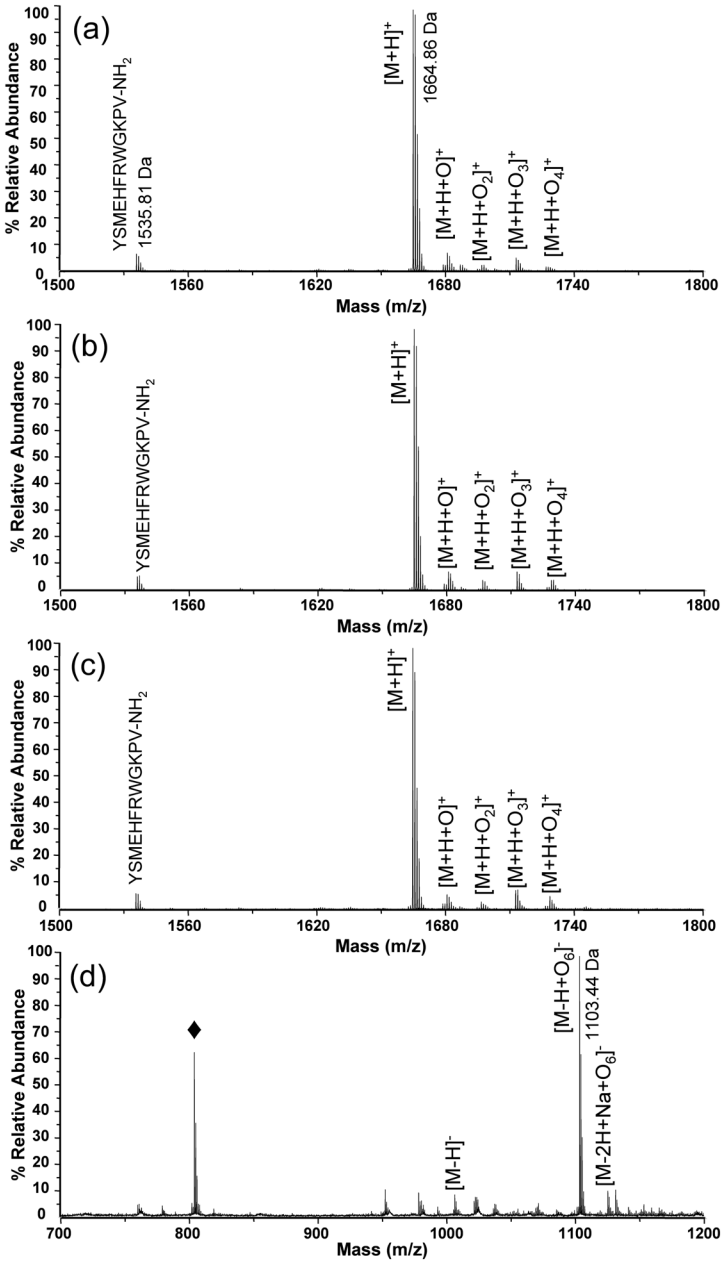

Figure 9. Typical positive ion mass spectra for α-melanocyte stimulating hormone (Ac-SYSMEHFRWGKPV-NH_2) (a) before and (b) after an hour of on-target performic acid oxidation at -20˚C. Panel (c) represents an additional hour of on-target oxidation performed on the same sample deposit at +24˚C. Panel (d) contains a negative ion mass spectrum of a control experiment performed using native oxytocin (CYIQNCPLG-NH_2) oxidized in parallel with α-melanocyte stimulating hormone on the same MALDI target. Ion signals denoted with closed diamonds (♦) represent contaminate ions arising from the CHCA matrix.

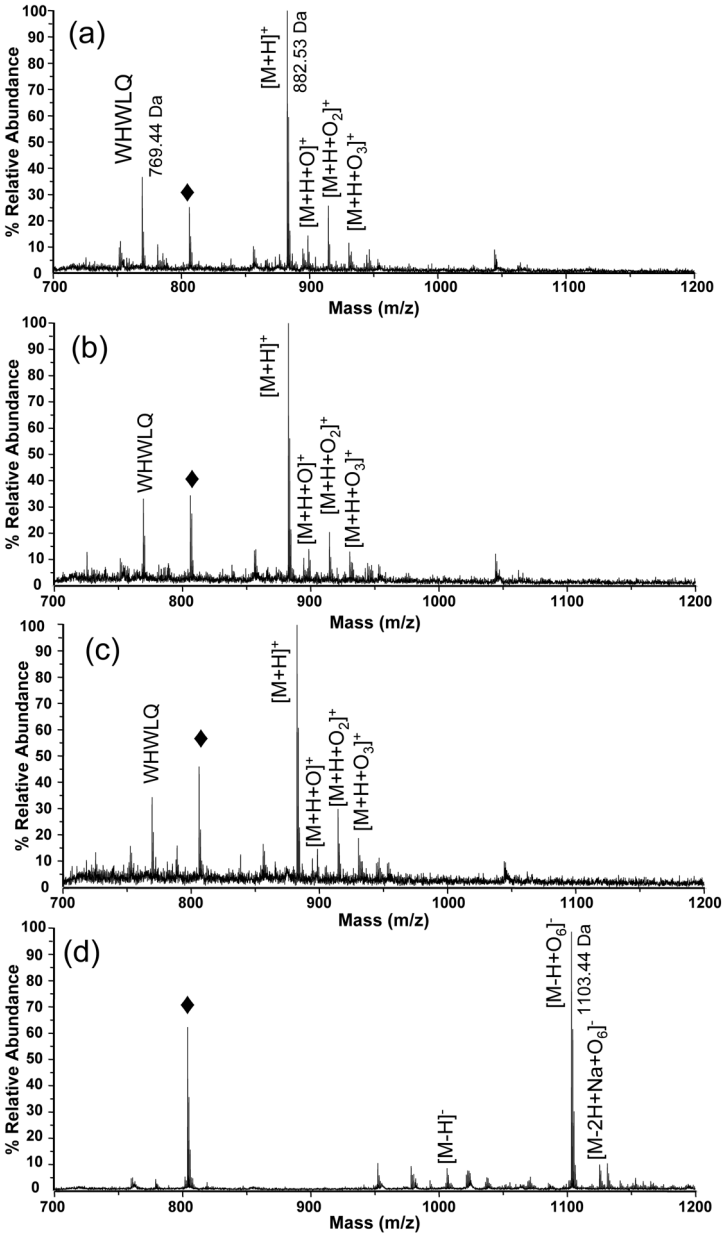

Figure 10. Typical positive ion mass spectra for α1-mating factor (WHWLQL) (a) before and after (b) an hour of on-target performic acid oxidation at -20˚C. Panel (c) represents an additional hour of on-target oxidation performed on the same sample deposit at +24˚C. Panel (d) contains a negative ion mass spectrum of a control experiment performed using native oxytocin (*C*YIQN*C*PLG-NH_2) oxidized in parallel with α1-mating factor on the same MALDI target. Ion signals denoted with closed diamonds (♦) represent contaminate ions arising from the CHCA matrix.

On-Target Oxidation of Intact and Reduced Insulin

Bovine insulin is an excellent model system to illustrate on-target performic acid oxidation of disulfide-containing proteins because it contains three disulfide bonds, two inter-chain disulfide bonds, which link the α and β-chains and one intra-chain disulfide bond within the α-chain (see below). Performic acid should cleave both the intra and inter-linked disulfide bonds to fully oxidize both α and β-chains.

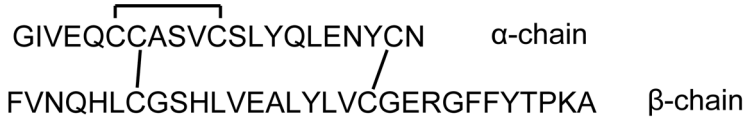

Figure 11 contains the negative ion mass spectra of oxidized intact insulin obtained using several different sample preparation methods. The spectrum contained in Figure 11a contains a strong ion signal for the fully oxidized β-chain $[\beta - H + O_6]^-$ at m/z 3492.83, but under these conditions ion signals for the fully oxidized insulin α-chain are not observed in either positive or negative ion spectra. On the other hand, ion signals at m/z 2463.08 are most likely partially oxidized α-chain, $[\alpha - H + O_9 - 17]^-_{calc}$ = 2463.89 Da (-333 ppm mass error) or $[\alpha - H + O_8]^-_{calc}$ = 2463.94 Da (-353 ppm mass error), but we were unable to confirm these assignments by using tandem MS owing to the low abundance of the signals. Note that oxidation of chemically reduced insulin yields abundant ion signals for both α- and β-chains, *i.e.,* the fully oxidized insulin α-chain $[\alpha - H + O_{12}]^-$ ion at m/z 2528.67 and β-chain $[\beta - H + O_6]^-$ ion at m/z 3492.34 are observed in the negative ion mass spectrum (Figure 11b).

Figure 11c contains the negative ion mass spectra for oxidized intact insulin from 2,4-DHAP, and Figure 11d contains similar spectra obtained from 2,4-DHAP prepared

using an overlayer of CHCA. When on-target oxidation is performed on deposits of 2,4-DHAP, the fully oxidized insulin α-chain $[\alpha - H + O_{12}]^-$ and β-chain $[\beta - H + O_6]^-$ ions are observed in the negative ion mass spectrum (Figure 11b). Note that the negative ion yields for both α- and β-chain oxidized forms are enhanced using 2,4-DHAP/CHCA sample preparation. The signal-to-noise ratio of the oxidized insulin α-chain increases 1.5-fold for the dual MALDI matrix method relative to using 2,4-DHAP as a MALDI matrix alone.

It appears that efficient oxidation of intact insulin to form oxidized α and β-chains is related to greater accessibility of the performic acid vapor to oxidize the insulin molecules within the 2,4-DHAP crystals. The presence of non-oxidized intact insulin ions following oxidation could indicate that insulin molecules are trapped within CHCA crystals, probably as inclusion complexes,[102] whereas with 2,4-DHAP, the insulin molecules are located on the 2,4-DHAP crystal surface and become more susceptible to oxidation (Figure 11c). Further investigation of different MALDI matrices used for the on-target performic acid oxidation method may provide additional insight to explain why some cysteine and/or disulfide-containing peptides are more readily oxidized.[103]

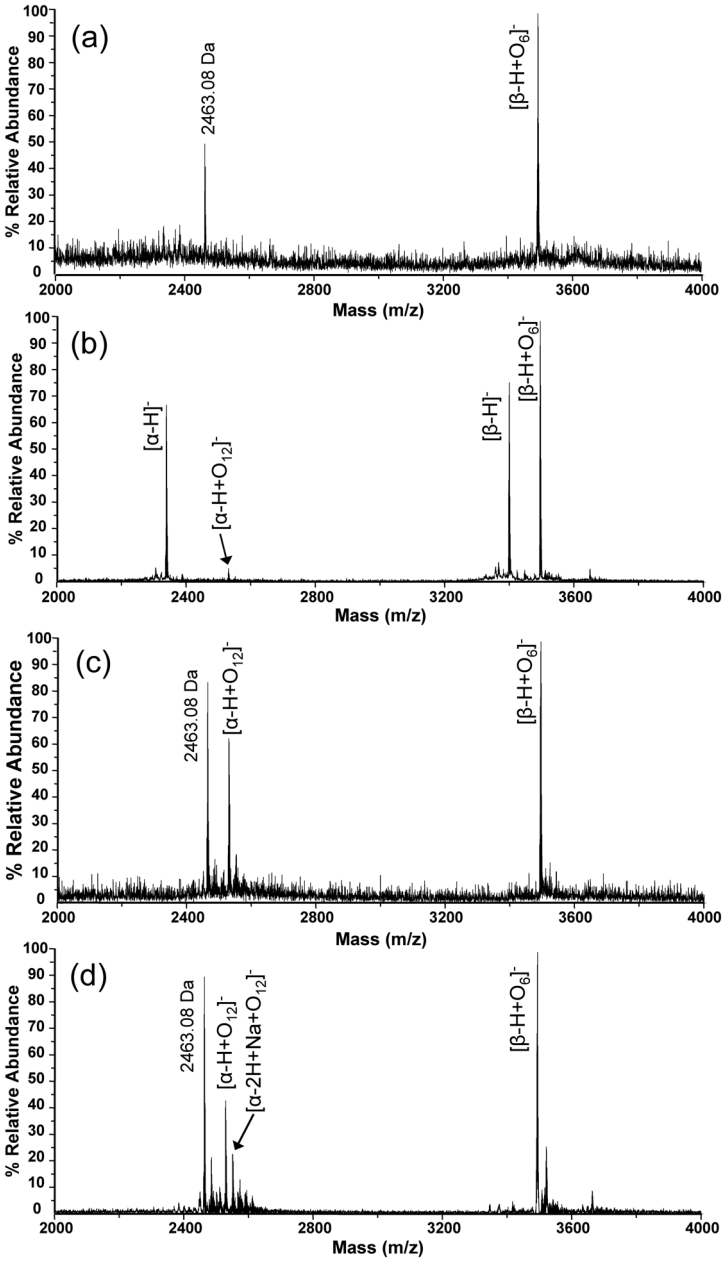

Figure 11. Negative ion mass spectra after on-target oxidation of (a) intact insulin and (b) chemically reduced insulin using CHCA as the MALDI matrix during oxidation. Panel (c) 2,4-DHAP was used as the MALDI matrix during on-target oxidation of intact insulin. Panel (d) 2,4-DHAP was used during oxidation followed by an overlayer addition of CHCA which we found improve the yield of negative ions.

On-Target Oxidation of RNase A Proteolytic Digest

RNase A is an excellent model protein to study disulfide bonds in proteins because it contains eight cysteine residues, each present as disulfide bonds.[46, 56, 69] RNase A contains four native disulfide bonds, three disulfide bonds are inter-linked and the other disulfide bond is intra-linked. Our experimental design involves performing proteolytic digestion under mildly acidic conditions (pH 6) to minimize disulfide scrambling[56] combined with 2-iodoacetamide alkylation chemistry to protect the free-cysteine residues (i.e., disulfide-linked peptides that may become reduced during digestion) from oxidation. Following proteolytic digestion, the intact disulfide-containing peptides are then subjected to on-target performic acid oxidation where the disulfide bond(s) are cleaved to form two peptides each containing a cysteic acid side chain (See Scheme 1a). Each oxidized peptide chain is then subjected to tandem MS, where the amino acid sequences of the two peptide chains forming the disulfide-bond can be determined.

Figure 12 contains negative ion mass spectra for the RNase A trypsin/chymotrypsin digest + 2-iodoacetamide acquired (a) before oxidation, (b) after on-target and (c) solution-phase oxidation. For this example, the on-target oxidation was performed for 1 hr at -20˚C and the solution-phase oxidation was performed for 4 hrs at 0˚C. Fourteen new peptide ion signals resulting from performic acid oxidation are observed and those confirmed by tandem MS are labeled A-J (Figure 12b), while the four additional ion signals too low in abundance to characterize by tandem MS are labeled with asterisks (*). The tandem MS confirmed amino acid sequences of the oxidized RNase A peptides are summarized in Table 1. Several cysteine-containing peptides $^{52}C_{ox}NQ\boldsymbol{MM}K^{57}$, $^{93}NGQTNC_{ox}Y^{99}$, and $^{88}NVAC_{ox}K^{92}$ only appear after oxidation, which is most likely a result of oxidative cleavage of the intact disulfide-linked peptides. Proteolytic peptides containing methionine residues (*e.g.,* $^{52}C_{ox}NQ\boldsymbol{MM}K^{57}$ and $^{52}C_{ox}NQ\boldsymbol{MM}^{56}$) were also oxidized owing to the incorporation of two additional oxygen atoms per methionine residue (denoted in ***bold italics***). Ten total oxidized peptides accounting for all eight RNase A cysteine residues involved in disulfide bonds were detected using on-target oxidation, whereas a total of eight (six of these peptides are involved in disulfide bridging) oxidized RNase A peptides were detected using solution-phase oxidation. Comparing the mass spectral quality of the on-target (Figure 12b) and solution-phase oxidation (Figure 12c) method clearly illustrates an advantage of the on-target oxidation method. At first glance the on-target oxidation method (Figure 12b) appears to contain additional chemical noise above m/z 1000; however, the majority of these ion signals correspond to $[M - H]^-$ ions for intact

disulfide-linked peptides that are present after oxidation. As for the solution-phase oxidation method (Figure 12c), these ion signals from m/z 1000-2000 are not observed because these intact disulfide-linked peptides have undergone oxidative cleavage to produce small oxidized cysteine-containing peptides. In terms of signal-to-noise improvement, the S/N ratios for the labeled ion signals increase an average 2.5-fold for the on-target oxidation method relative to the solution-phase oxidation method. A drastic S/N enhancement occurs for peptide I (^{131}HIIVAC$_{ox}$EGNPY^{141}) where the ratio of the S/N values for the on-target oxidation method improves *ca.* 6-fold over the solution-phase oxidation method. The decrease in relative abundance for the solution-phase oxidation method could be attributed to ion suppression effects or sample loss associated with post-oxidation vacuum drying prior to MS analysis. Overall, the RNase A negative ion MS data suggests that the on-target oxidation method is suitable for proteolytic protein digests.

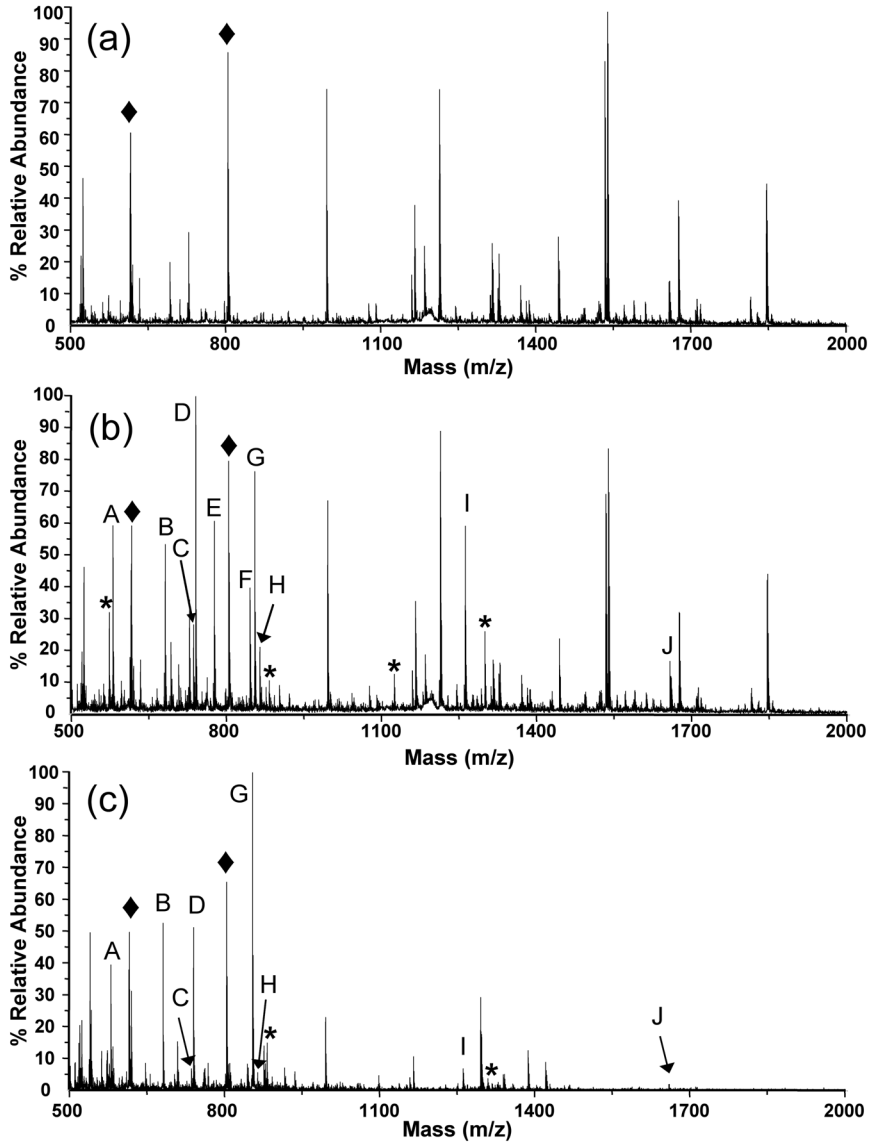

Figure 12. Negative ion mass spectra for an RNase A trypsin/chymotrypsin + 2-iodoacetamide digest a) before and b) after on-target performic acid oxidation and c) solution-phase oxidation. The peptides denoted with asterisks (*) correspond to new peptide ion signals resulting from performic acid oxidation not confirmed by tandem MS. The peptide ion signals denoted with closed diamonds (♦) indicate chemical contaminates arising from the CHCA matrix.

Table 1. Summary of Negative Ion MALDI-MS Data Resulting from On-Target Performic Acid Oxidation of RNase A Tryptic/Chymotryptic Peptides

Label	Peptide Sequence	$[M-H]^-_{obs}$	$[M-H]^-_{calc}$	Mass Error
				ppm
A	^{88}NVAC$_{ox}$K^{92}	580.2236	580.2398	-28
B	^{82}AVC$_{ox}$SQK^{87}	681.2732	681.2875	-21
C	^{52}C$_{ox}$NQ***MM***^{56}	736.1478	736.1585	-15
D	^{106}SITDC$_{ox}$R^{111}	740.2736	740.2883	-20
E	^{118}YPNC$_{ox}$AY^{123}	776.2419	776.2559	-18
F	^{93}NGQTNC$_{ox}$Y^{99}	845.2562	845.2733	-20
G	^{66}C$_{ox}$KPVNTF^{72}	854.3588	854.3709	-14
H	^{52}C$_{ox}$NQ***MM***K^{57}	864.2386	864.2535	-17
I	^{131}HIIVAC$_{ox}$EGNPY^{141}	1261.5394	1261.5521	-10
J	^{73}VHESLADVQAVC$_{ox}$SQK^{87}	1659.7649	1659.7646	0

(a)

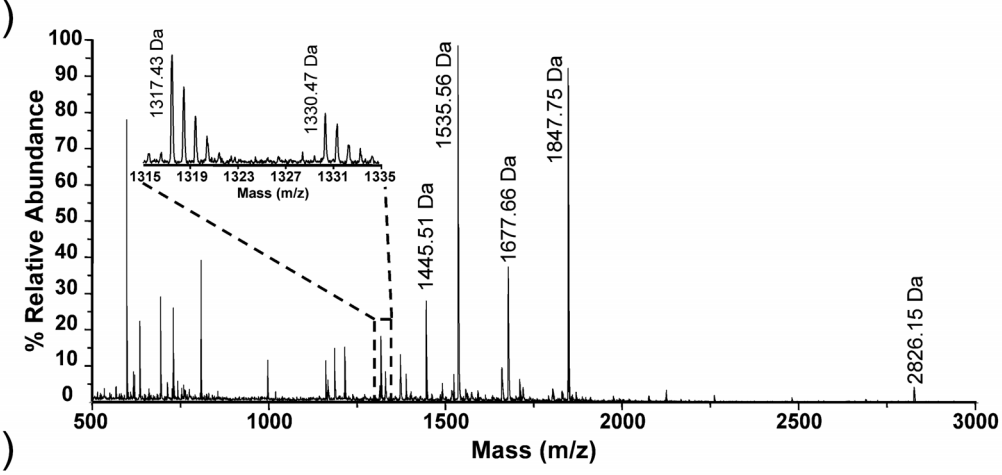

(b)

Cysteine Location			91	84	52	110	121	98	66	52	136	84
	Peptide Sequence											
		$[M+H]^+_{calc}$	534.25	635.30	626.20	694.30	730.28	799.29	808.39	754.30	1215.58	1613.78
91	^{88}NVAC*K^{92}	534.25						**1330.52**				
84	^{82}AVCSQK^{87}	635.30									**1847.86**	
52	^{52}CNQMM^{56}	626.20				**1317.48**						
110	^{106}SITDCR^{111}	694.30			**1317.48**					**1445.58**		
121	^{118}YPNCAY^{123}	730.28							**1535.64**			
98	^{93}NGQTNCY^{99}	799.29	**1330.52**									
66	^{66}CKPVNTF^{72}	808.39					**1535.64**					
52	^{52}CNQMMK^{57}	754.30				**1445.58**						
136	^{131}HIIVACEGNPY^{141}	1215.58		**1847.86**								**2826.33**
84	^{73}VHESLADVQAVCSQK^{87}	1613.78									**2826.33**	

Native RNase A disulfide bonds: (Cys^{52} - Cys^{110}), (Cys^{66} - Cys^{121}), (Cys^{84} - Cys^{136}), (Cys^{91} - Cys^{98})

Figure 13. (a) Positive ion mass spectrum of the RNase A trypsin/chymotrypsin digest + 2-iododacetamide following on-target oxidation. Inset figure: expanded view of mass range 1315-1335 m/z. (b) Table correlating the observed oxidized cysteine-containing peptides with their resulting candidate inter-linked disulfide bridged peptides.

Several disulfide-linked peptides can be elucidated from the observed oxidized cysteine-containing peptides summarized in Table 1. The correlation of the non-oxidized peptide masses and the calculated disulfide-linked peptide masses is shown in Figure 13b. The peptides are arranged according to increasing mass to form an array of calculated disulfide-linked peptide masses. All the different disulfide-linked peptide bridging possibilities are calculated from the list of peptide m/z values accounting for the mass difference of an inter-linked disulfide bond. The calculated disulfide-linked peptide masses that match an ion signal present in the positive ion mass spectrum of the oxidized RNase A trypsin/chymotrypsin digest (Figure 13a) are indicated with a box around the number. For example, an ion signal at m/z 1535.56 is present in the positive ion mass spectrum which corresponds to the disulfide-linked peptide (^{118}YPNCAY^{123} / ^{66}CKPVNTF^{72}) which is a native disulfide linkage between Cys^{66} and Cys^{121}. This assignment was further confirmed by tandem MS by observing several *b*-type fragment ions and the signature fragment ions for an inter-linked disulfide bond. The ion signal at m/z 1677.66 is most likely the disulfide-linked peptide (^{84}CSQK^{87} / ^{131}HIIVACEGPNY^{141}) with an $[M + H]^{+}_{calc}$ = 1677.77 Da (-67 ppm mass error) and a 170.09 Da mass difference (Ala-Val residue mass = 170.11 Da) from the m/z 1847.75 ion signal. All four native disulfide bonds from RNase A can be elucidated from the oxidized cysteine-containing peptides resulting from the on-target oxidation of the RNase A proteolytic digest. At this point we are not claiming a method for complete disulfide-bond elucidation from a single MALDI deposit; there are several other possible RNase A disulfide-linked peptides that can be produced from different proteolytic

digestion products that were not identified. Therefore, we plan to further expand on the disulfide bond elucidation capability using this on-target oxidation method in combination with CE-MALDI-MS to deconvolute the negative ion mass spectra prior to oxidation.

Conclusion

On-target oxidation using performic acid vapor was achieved for MALDI deposited samples containing model disulfide-linked peptides, intact insulin, and a proteolytic digest of RNase A. Cysteine, cystine, and methionine amino acid side chains are readily oxidized after on-target oxidation. On the other hand, other oxidizable amino acids such as histidine, tryptophan, and tyrosine are not significantly oxidized as a result of on-target oxidation. The oxytocin experiments demonstrate the compatibility of the on-target oxidation method with alkylation chemistry to distinguish between a peptide containing two free-cysteine residues from a peptide with a single intra-linked disulfide bond. The intact insulin experiments illustrate the ability to oxidize small disulfide-containing proteins and suggest that the MALDI matrix plays a role in the oxidation process by the matrix crystals affecting the ability of the performic acid vapor to reach the analyte. All four native RNase A disulfide bonds were successfully elucidated from the negative ion MALDI-MS data from the on-target performic acid oxidation of an RNase A proteolytic digest.

The on-target oxidation method is advantageous over solution-phase oxidation methods because of the decreased sample handling and reaction time. Another major

benefit of the on-target oxidation method is the ability to perform simultaneous oxidation of several MALDI sample deposits. In addition, the positive and negative ion mass spectral quality is not sacrificed following oxidation. The on-target performic acid oxidation method provides a very powerful technique to distinguish between free-cysteine containing peptides and those peptides that contain disulfide bonds. Additionally, this method will make a drastic impact for disulfide-linked peptide characterization from complex mixtures, owing to the ability to rapidly screen an entire MALDI target for sample deposits that contain enhanced negative ion signals, *i.e.,* these are MALDI spots that may contain candidate disulfide-linked peptides. Hence, the motivation to combine the on-target oxidation method with off-line separations (*e.g.,* capillary electrophoresis or liquid chromatography) coupled with MALDI-MS[19, 85] to analyze disulfide-linked peptides from complex proteomic mixtures.

CHAPTER IV

EVALUATION OF EXPERIMENTAL VARIABLES FOR THE ON-TARGET OXIDATION OF CYSTEINE-CONTAINING PEPTIDES AND PROTEINS

Introduction

Cysteine oxidation in proteins can occur during a time of oxidative stress and more importantly these oxidized cysteine residues may play important biological and pathological roles.[36-39] For example, in kinase enzymes, cysteine oxidation away from the active site causes the oxidized cysteine to form a disulfide bond with a nearby cysteine residue, thus changing the protein conformation and therefore enzymatic activity.[35] The thiol side chain of cysteine can exist in several oxidized forms including: disulfide bonds (R-S-S-R), sulfenic (RSOH), sulfinic (RSO_2H), or sulfonic (RSO_3H) acids. An estimated 5% of cellular protein cysteine residues occur in the sulfinic or sulfonic acid form.[104] Sulfenic acids are known to have short lifetimes before they undergo disulfide bond formation or further oxidation to sulfinic or sulfonic acids. Technologies to capture sulfenic acids using dimedone (*i.e.*, 5,5-dimethyl-1,3-cyclohexadimone) chemistry followed by antibody recognition and mass spectrometry (MS) analysis have been reported.[36-38, 41, 42] The detection of the final cysteine oxidation product, sulfonic acid is rather straightforward to detect since the oxidation is irreversible and MS-based detection schemes have proven to be effective.[44, 45-48]For example, we recently published an on-target performic acid oxidation method which can readily form cysteic acid-containing peptides using performic acid vapor to oxidize

MALDI deposited samples.[48] The intact disulfide bonds are broken via oxidative cleavage to produce two new peptides each containing a cysteic acid. From the resulting oxidized cysteine-containing peptides observed in the negative ion mass spectra we are able to elucidate intact disulfide-linked peptides from bovine Ribonuclease A. However, the various experimental parameters (*e.g.,* temperature, exposure time, and MALDI matrix) associated with the on-target oxidation method were not extensively evaluated to improve the oxidized peptide yield.

The motivation to investigate the on-target oxidation experimental parameters was inspired by initial difficulty completely oxidizing intact insulin to form oxidized α- and β-chains.[48] The insulin β-chain readily oxidizes on the surface (co-crystallized with MALDI matrix) of the MALDI target when exposed to performic acid vapor. However, the insulin α-chain required an alternative MALDI matrix during on-target oxidation in order to be successfully oxidized. Analyte-matrix inclusion complexes [102] with α-cyano-4-hydroycinnamic acid are suspected to inhibit α-chain oxidation. Another hypothesis could be related to the increased analyte size causing the matrix crystals to grow less oriented; therefore, the voids in the crystal lattice become large in number and smaller in size.[105] Additionally, some MALDI matrices are known (*e.g.,* 2,6-dihydroxybenzoic acid) to exclude the protein molecule from the crystal lattice,[106, 107] which could prevent performic acid vapor exposure. Therefore, we chose to evaluate several commonly used MALDI matrices to effectively change the type of analyte-matrix crystal lattice.

Herein we investigate the effect of various experimental variables associated with the on-target oxidation experiment. The effect of oxidation temperature, performic

acid exposure time, and varying the MALDI matrix during oxidation are investigated. Standard cysteine-containing peptides (*e.g.,* Cys-kemptide, Arg^8-Vasopressin, and Cys^8-renin) and intact bovine insulin were used for these on-target oxidation studies with varied experimental conditions. In addition, this on-target oxidation method was adapted towards on-target oxidation of disulfide-containing proteins (*e.g.,* bovine pancreatic trypsin inhibitor) followed by on-target proteolytic digestion to enhance the digestion efficiency.

Experimental

Chemicals

All chemicals were purchased from Sigma-Aldrich (St. Louis, MO) unless otherwise noted. Hydrogen peroxide (35% w/w) and formic acid (99% w/w) were purchased from Acros Organics (Morris Plains, NJ). HPLC grade acetone and methanol (CH_3OH) were purchased from EMD Chemicals Inc. (Gibbstown, NJ). All experiments were performed with 18-MΩ water (ddH_2O) purified using a water purification unit (Barnstead International, Dubuque, IA).

Sample Preparation for MALDI-MS

A stock solution of cys-kemptide (CLRRASLG) was prepared at 10 μM in 10 mM formic acid. To remove disulfide-linked contaminant, the Cys-kemptide stock solution was reduced with tris(2-carboxyethyl)phosphine (50 mM prepared in ddH_2O) by incubating at 60˚C for 60 min. The peptide solution was mixed 1:1 with CH_3OH and

1 μL was spotted as an overlayer to MALDI matrix. Each MALDI matrix (2,4-dihydroxyacetophenone, 2,5-dihydroxybenozic acid, 4-hydroxy-α-phenylcinnamic acid, 4-hydroxy-α-cyanocinnamic acid, and 3,5-dimethyl-4-hydroxycinnamic acid) were prepared at 5 mg mL^{-1} in a 2:3 ddH_2O: CH_3OH solution containing 10 mM $NH_4H_2PO_4$ and 1 μL was pre-spotted as the underlayer.[90] This cysteine-containing peptide was later oxidized using the on-target oxidation procedures described below.

On-Target Performic Acid Oxidation

On-target oxidation was performed as described previously.[48] Briefly, 40 μL of a 1:1 mixture of acetone: performic acid was placed directly on the MALDI target in a region that does not contain sample. The MALDI target was then covered in a plastic petri dish and was allowed to react at three different temperatures (-20˚C, +25˚C, and +50˚C) with reaction times ranging from 10-60 min. Following on-target performic acid oxidation the MALDI plate is then subjected to MALDI analysis without sample cleanup. The on-target oxidation experiments with intact insulin were performed using room temperature oxidation (+23˚C) for 60 minutes. The cys-kemptide on-target oxidation experiments were performed at +23˚C for 15 minutes.

On-Target Proteolytic Digestion

On-target proteolytic digestion was performed similar to as previously described.[108] Briefly, following on-target oxidation of the intact protein in the presence of 2,4-DHAP trypsin was added at a 1:20 (w/w) enzyme: protein ratio. A 1 μL aliquot of

the trypsin solution (5 mM NH_4HCO_3 buffer with 50% CH_3OH) was added to the MALDI deposit and placed in a humidity chamber at 37˚C for 60 minutes. Following on-target proteolytic digestion, an additional deposit of CHCA was added to each MALDI sample prior to MS analysis.

MALDI-MS and MALDI-MS/MS

All MALDI-MS experiments were performed using a model 4700 Proteomics Analyzer MALDI-TOF/TOF (Applied Biosystems, Framingham, MA). The MALDI-MS data were acquired using the reflectron detector in both positive and negative ion modes using 1200 laser shots with external calibration using bradykinin (2-9) (PPGFSPFR) and ACTH (18-39) (RPVKVYPNGAENESAEAFPLEF). Positive and negative ion collision-induced dissociation (CID) tandem MS spectra were acquired using 10-20% greater laser power than the MS spectra acquisition with atmosphere (medium pressure) as the collision gas with 1 kV of collision energy.

Results and Discussion

The major goal of these on-target oxidation experimental variable studies is to improve the overall oxidation efficiency through varying the conditions of the on-target oxidation experiment. Specifically, we investigate the effect of altering the (i) oxidation temperature, (ii) performic acid exposure time, and (iii) the MALDI matrix during oxidation. We also demonstrate the feasibility of performing on-target oxidation of intact disulfide-containing proteins followed by on-target proteolytic digestion. The native

disulfide bond pattern would be lost using this approach; however, a protein that has inaccessible (*e.g.,* bovine pancreatic trypsin inhibitor) proteolytic cleavage sites will now be easily digested on the MALDI target.

Effect of Oxidation Temperature

Initial on-target oxidation experiments were performed using cold oxidation temperatures (-20˚C) to prevent undesired oxidation of histidine, tryptophan, and tyrosine amino acid residues. Three standard peptides: Arg^8-vasopressin (C<u>YFQN</u>CPRG-NH_2), α-melanocyte stimulating hormone (Ac-SYSMEHFRWGKPV-NH_2) , and Cys^8-renin (DRVYIHPCHLLYYS) were used to further investigate the effect of oxidation temperature. This experiment is designed to oxidize the cysteine-containing peptides with minimal oxidation products of α-melanocyte stimulating hormone (α-MSH) as the temperature increases.

Figure 14 contains the negative ion mass spectra (a) before and after on-target oxidation of these standard peptides performed at (b) -20˚C, (c) +25˚C, and (d) +50˚C. Notice that some oxidation products from α-MSH ($[B - H + O]^-$) and Cys^8-renin ($[C - H + O_3]^-$) are observed prior to oxidation. Arg^8-vasopressin readily oxidizes within the peptide mixture to produce $[A - H + O_6]^-$ ions at m/z 1180.40 with an improved negative ion yield because of the two cysteic acid groups drastically increase the peptide acidity.

Three oxygen atoms are also incorporated into Cys^8-renin to produce the $[C - H + O_3]^-$ ion at m/z 1824.82. Figure 14d illustrates that several α-MSH oxidation products are present when the oxidation is performed at elevated temperatures. For example, the relative abundance of the $[B - H + O_6]^-$ ion increases as the oxidation temperature increases. Relative to the oxidation performed at or below +25˚C there is additional chemical noise present in Figure 14d. Oxidation at elevated temperatures (+50˚C) can be problematic because of the undesired chemical noise and oxidation products. Containing the performic acid vapor at elevated temperatures and pressures can be difficult without the proper reaction vessel to prevent the vapor from escaping the chamber. In the +50˚C oxidation experiment, the oxidation time was *ca.* 10-20 min owing to the performic acid vapor escaping the reaction chamber. At this point, oxidation at +25˚C seems suitable to oxidize these standard peptides with minimal oxidation side products for α-MSH. The increased oxidation temperature may become important to successfully oxidize difficult-to-oxidize disulfide-containing peptides and/or proteins (*e.g.,* intact bovine insulin).

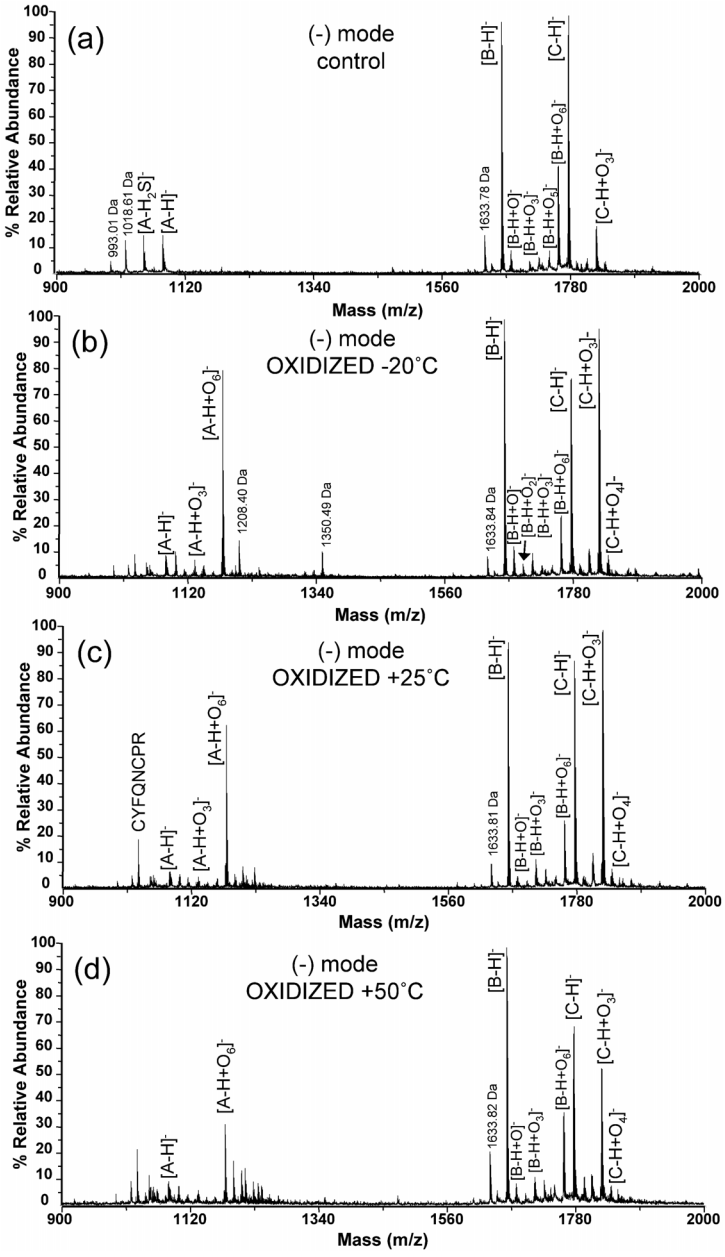

Figure 14. Effect of on-target oxidation temperature on the resulting oxidation products from a mixture of standard peptides. The standard peptides labeled are as follows: (A) Arg^8-Vasopressin (CYFQNCPRG-NH_2), (B) α-melanocyte stimulating hormone (Ac-SYSMEHFRWGKPV-NH_2), and (C) Cys^8-renin (DRVYIHPCHLLYYS). Negative ion mass spectra are shown (a) before and after on-target oxidation at (b) -20˚C, (c) +25˚C, and (d) +50˚C using CHCA as the MALDI matrix during oxidation.

Performic Acid Exposure Time

Initial on-target oxidation experiments were performed using an hour of oxidation because traditional solution-phase oxidation methods use similar oxidation times.[46] An on-target oxidation time course from 0-60 min was carried out using Arg^8-vasopressin (CYFQNCPRG-NH_2), α-melanocyte stimulating hormone (Ac-SYSMEHFRWGKPV-NH_2), and Cys^8-renin (DRVYIHPCHLLYYS) denoted as A, B, and C, respectively.

Figure 15 contains the negative ion mass spectra (a) before and after on-target oxidation performed for (b) 5 min and (c) 15 min at room temperature (+25˚C) using CHCA as the MALDI matrix during oxidation. Note that oxidized Cys^8-renin $[C - H + O_3]^-$ is present prior to oxidation (Figure 15a). Following oxidation the relative abundance of the oxidized Cys^8-renin $[C - H + O_3]^-$ ion at m/z 1824.98 increases drastically after 5 min of oxidation (Figure 15b). Oxidized Arg^8-vasopressin $[A - H + O_6]^-$ is also readily observed at m/z 1180.50 in the negative ion mass spectrum after 5 min of oxidation. After 15 min of oxidation (Figure 15c), the relative abundance of both Arg^8-vasopressin and Cys^8-renin increase compared to oxidation for only 5 min. Overall, it appears the improved ion signal for the oxidized products from 0-15 min indicates the oxidation time can improve the oxidized peptide ion yield. However, as the oxidation time increases from 15-60 min the oxidized peptide ion yield appears not to improve in terms of the relative abundance increasing over time. Another possible explanation is the peptide molecules on the surface of the MALDI matrix crystal are becoming readily oxidized while those peptide molecules co-crystallized within the matrix are inaccessible

to the performic acid vapor. Therefore, we must investigate the effect of the MALDI matrix (crystal lattice) on the resulting oxidized peptide ion yield.

Alternative MALDI Matrices for On-Target Oxidation

Initial difficulty completely oxidizing insulin α-chain motivated further investigation of alternative MALDI matrices used for on-target oxidation. Nine different MALDI matrices and a dual matrix with 2,4-DHAP combined with CHCA were used to investigate the effect of the MALDI matrix on the oxidized peptide ion yield (Table 2). The oxidized insulin α- and β-chains are monitored in terms of being observed (+) and not observed (-) in the positive and negative ion mass spectra. Take notice that only 2,4-DHAP and CHCA have oxidized peptide ion signals present. Figure 16 contains negative ion mass spectra of intact insulin after on-target oxidation using (a) CHCA, (b) 2,4-DHAP, and (c) 2,4-DHAP used during oxidation followed by an overlayer of CHCA. Note that ion signals corresponding to fully oxidized insulin α-chain are not present when using CHCA during oxidation. However, when 2,4-DHAP is used throughout oxidation the fully oxidized insulin α-chain (m/z 2528.61 for $[\alpha - H + O_{12}]^-$) is observed in the negative ion mass spectrum at S/N 66 (Figure 16b). Enhanced negative ion yields are observed for oxidized insulin α-chain when CHCA is added as an overlayer to 2,4-DHAP. For example, the $[\alpha - H + O_{12}]^-$ ion signal improves *ca.* 2.8-fold when using the dual matrix approach compared to using 2,4-DHAP alone.

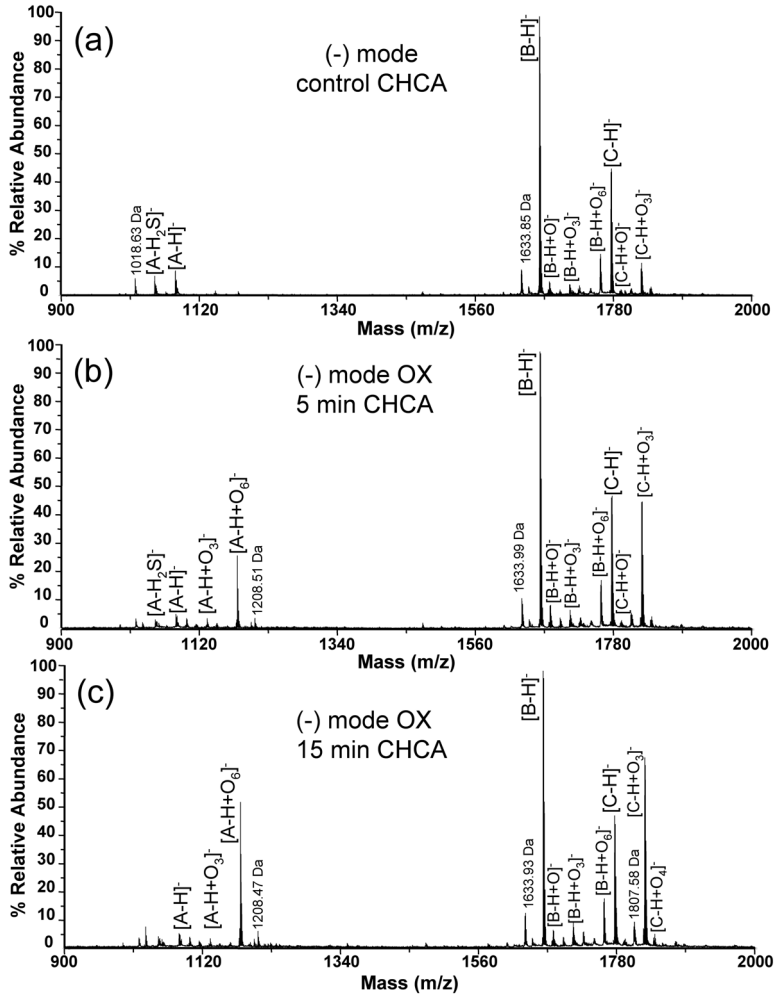

Figure 15. Selected negative ion mass spectra from the oxidation time course designed to evaluate the effect of performic acid vapor exposure time on the oxidation of a standard peptide mixture. On-target oxidation performed for (a) 0 minutes, (b) 5 minutes, and (c) 15 minutes are shown. The standard peptides are denoted in the mass spectra as follows: (A) Arg^8-Vasopressin (C<u>YFQN</u>CPRG-NH_2), (B) α-melanocyte stimulating hormone (Ac-SYSMEHFRWGKPV-NH_2), and (C) Cys^8-renin (DRVYIHPCHLLYYS). Oxidation for these experiments was performed at +25˚C using CHCA as the MALDI matrix during oxidation.

For comparative purposes, each MALDI sample deposit shown in Table 2 received an overlayer of CHCA following oxidation. The dual MALDI matrix may improve the negative ion yield of the oxidized peptides on the MALDI sample deposit. Several MALDI matrices now have detectable ion signals present for the insulin α- and β-chains. Only two methods, 2,4-DHAP and ferulic acid combined with CHCA as dual MALDI matrices, have detectable ion signals for the fully oxidized insulin α-chain [α – H + O_{12}]$^-$ at m/z 2528.64. Abundant signal for fully oxidized insulin β-chain [β – H + O_6]$^-$ ion at m/z 3492.88 is observed in each method with the exception of sinapic acid in which lacks oxidized peptide ion signals. The remainder of the matrices (*e.g.,* 3,5-DMHCA, 4-HPCA, and 2,6-DHAP) have an enhanced negative ion signal for partially oxidized insulin α-chain (m/z 2463.13). It appears that partially oxidized insulin α-chain is the predominant oxidation product when starting with intact insulin. A portion of the insulin α-chain amino acid sequence was confirmed by tandem MS; however, the lack of sequence informative fragment ions below m/z 800 prevents complete sequence determination (data not shown). Overall, it appears that only 2,4-DHAP successfully oxidizes both the insulin α- and β-chains. These select MALDI matrices were then used to oxidize Cys-kemptide (CLRRASLG) to further understand the improved oxidation with an alternative matrix.

Table 2. Summary of On-Target Performic Acid Oxidation of Intact of Insulin using Varied MALDI Matrices

MALDI Matrix	Matrix Abbrev.	(+) mode OX	(+) mode OX	(-) mode OX	(-) mode OX
		$[\alpha + H + O_{12}]^+$	$[\beta + H + O_6]^+$	$[\alpha - H + O_{12}]^-$	$[\beta - H + O_6]^-$
2,4-dihydroxyacetophenone	2,4-DHAP	-	+ (s)	+ (w)	+ (w)
2,6-dihydroxyacetophenone	2,6-DHAP	-	-	-	-
2,5-dihydroxybenzoic acid	2,5-DHB	-	-	-	-
2,4,6-trihydroxyacetophenone	2,4,6-THAP	-	-	-	-
3,5-dimethoxy-4-hydroxycinnamic acid	Sinapic acid	-	-	-	-
3-methoxy-4-hydroxycinnamic acid	Ferulic acid	-	-	-	-
4-hydroxy-α-phenyl-cinnamic acid	4-HPCA	-	-	-	-
3,5-dimethyl-4-hydroxycinnamic acid	3,5-DMHCA	-	-	-	-
α-cyano-4-hydroxycinnamic acid	α-CHCA	-	+ (w)	-	+ (s)
2,4-DHAP (OX) + α-CHCA		-	+ (s)	+ (s)	+ (s)

(s) - indicates strong ion signals ≥ 100 S/N

(w) - indicates weak ion signals ≤ 100 S/N

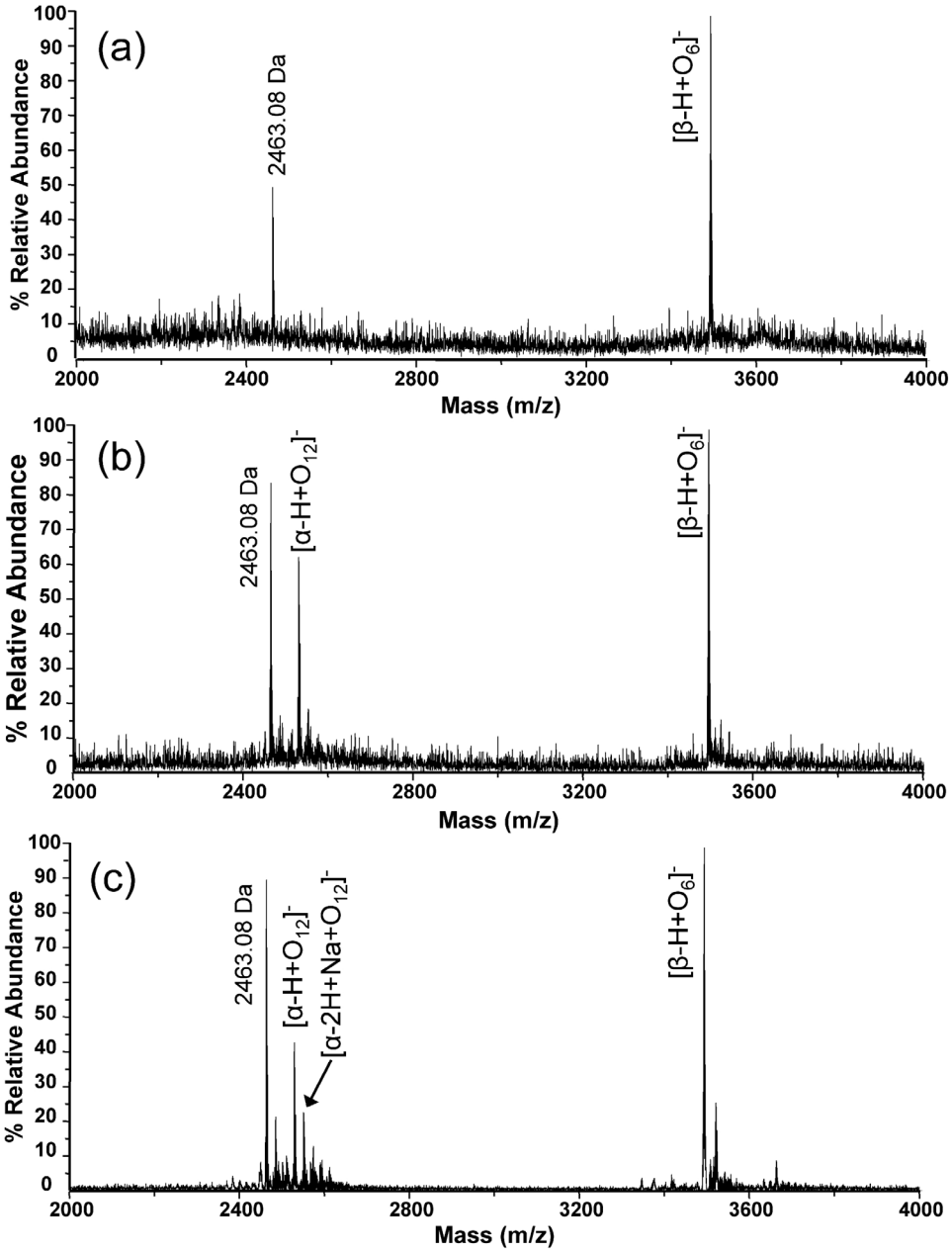

Figure 16. Typical negative ion mass spectra resulting from on-target oxidation of intact bovine insulin using (a) α-cyano-4-hydroxycinnamic acid, (b) 2,4-dihydroxyacetophenone and (c) 2,4-DHAP used during oxidation followed by an overlayer of CHCA. The on-target oxidation was performed at room temperature (+23˚C) for 60 minutes prior to mass spectrometry analysis.

Initial experiments designed to evaluate several MALDI matrices for on-target oxidation were performed with oxytocin (CYIQNCPLG-NH_2) as the model oxidizable analyte. The majority of the MALDI matrices used for on-target oxidation were successful in forming fully oxidized oxytocin $[M - H + O_6]^-$ ions in the negative ion mass spectra (See Table 3). The initial MALDI matrix list of ten was narrowed down to five matrices to further evaluate the effect of the matrix on the resulting ion yield of oxidized product. Specifically, on-target oxidation with (a) 2,4-dihydroxyacetophenone (2,4-DHAP), (b) 2,5-dihydroxybenzoic acid (2,5-DHB), (c) 4-hydroxy-α-phenylcinnamic acid (4-HPCA), (d) α-cyano-4-hydroxycinnamic acid (CHCA), and (e) 3,5-dimethyl-4-hydroxycinnamic acid (3,5-DMHCA) are shown (See Scheme 2).

An evaluation of the oxidized peptide ion yield for each MALDI matrix (a-e) is presented in Figure 17a for Cys-kemptide. The average signal-to-noise ratios for native cys-kemptide $[M - H]^-$ ions and fully oxidized cys-kemptide $[M - H + O_3]^-$ ions are compared for oxidized peptides formed via on-target oxidation performed in triplicate (average of nine MALDI spots was used for statistical evaluation). Note that oxidized Cys-kemptide $[M - H + O_3]^-$ ions are observed for each MALDI matrix

Table 3. Summary of On-Target Oxidation of Oxytocin (C<u>YIQN</u>CPLG-NH_2) using various MALDI Matrices

MALDI Matrix	Matrix Abbrev.	(+) mode OX	(+) mode OX	(-) mode OX
		$[M + H]^+$	$[M + H + O_6]^+$	$[M - H + O_6]^-$
2,4-dihydroxyacetophenone	2,4-DHAP	-	+ (w)	+ (w)
2,6-dihydroxyacetophenone	2,6-DHAP	-	+ (w)	+ (s)
2,5-dihydroxybenzoic acid	2,5-DHB	+ (s)	+ (w)	+ (s)
2,4,6-trihydroxyacetophenone	2,4,6-THAP	-	+ (w)	+ (w)
3,5-dimethoxy-4-hydroxycinnamic acid	Sinapic Acid	+ (w)	-	+ (w)
3-methoxy-4-hydroxycinnamic acid	Ferulic Acid	+ (s)	+ (w)	+ (w)
4-hydroxy-α-phenyl-cinnamic acid	4-HPCA	+ (s)	+ (s)	+ (s)
3,5-dimethyl-4-hydroxycinnamic acid	3,5-DMHCA	+ (w)	+ (s)	+ (s)
3-hydroxy-picolinic acid	3-HPA	-	-	-
α-cyano-4-hydroxycinnamic acid	α-CHCA	+ (s)	-	+ (s)
2,4-DHAP (OX) + α-CHCA		+ (w)	-	+ (s)

(s) - indicates strong ion signals ≥ 250 S/N

(w) - indicates weak ion signals ≤ 250 S/N

Scheme 2. Images (60X magnification) of typical MALDI sample deposits of (a) 2,4-dihydroxyacetophenone, (b) 2,5-dihydroxybenzoic acid, (c) 4-hydroxy-α-phenylcinnamic acid, (d) α-cyano-4-hydroxycinnamic acid, and (e) 3,5-dimethyl-4-hydroxycinnamic acid co-deposited with analyte. Their corresponding chemical structure is found below each MALDI spot image.

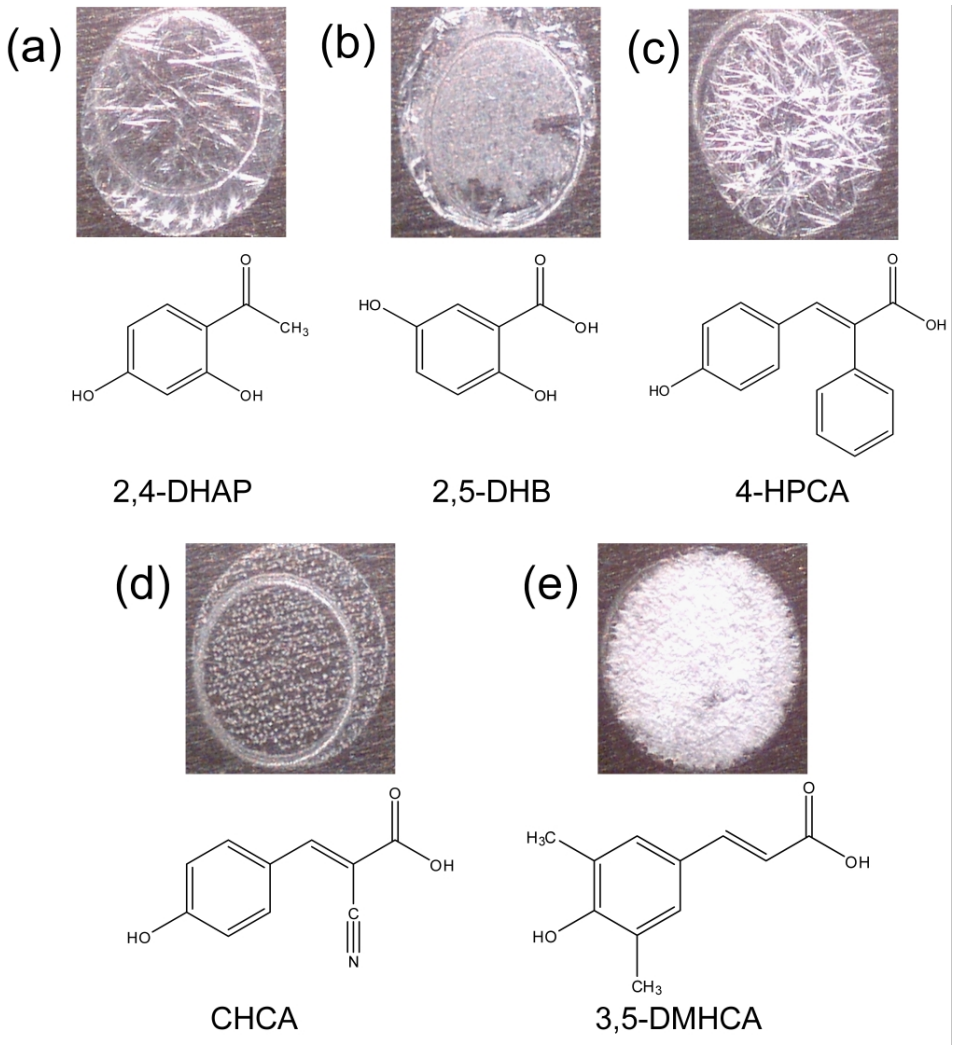

with the exception of 2,5-DHB. However, a low abundance of oxidized Cys-kemptide is observed for 2,5-DHB in the positive ion mass spectrum (data not shown). We suspect that 2,5-DHB either suffers from ion suppression effects from the performic acid vapor

or becomes oxidized to the hydroquinone form then functions poorly as a MALDI matrix, similar as previously reported.[109] Additionally, the hydroquinone form of 2,5-DHB appears to be reacting with the free thiol of Cys-kemptide during the MALDI process, similar as reported by Qiao and coworkers.[110] Therefore, 2,5-DHB is not suitable for on-target oxidation of free cysteine-containing peptides. A high relative abundance of oxidized Cys-kemptide $[M - H + O_3]^-$ ions are observed when using 4-HPCA and CHCA during oxidation. Note that a similar abundance of native Cys-kemptide $[M - H]^-$ ions are remaining after oxidation for both 4-HPCA and CHCA. It also appears that cysteic acid-containing peptides are more readily ionized when using 2,4-DHAP and 3,5-DMHCA. Additionally, non-oxidized peptide ion signals for Cys-kemptide $[M - H]^-$ ions remain after on-target oxidation for each MALDI matrix except 2,4-DHAP and 3,5-DMHCA. However, the decreased oxidized ion yield for these matrices suggests that non-oxidized peptide molecules are not being successfully ionized owing to poor ionization efficiency of the MALDI matrix to produce negative ions. To further probe the non-oxidized peptide molecules on these sample deposits we added an overlayer of CHCA to enhance the negative ion yield of the $[M - H]^-$ ion.

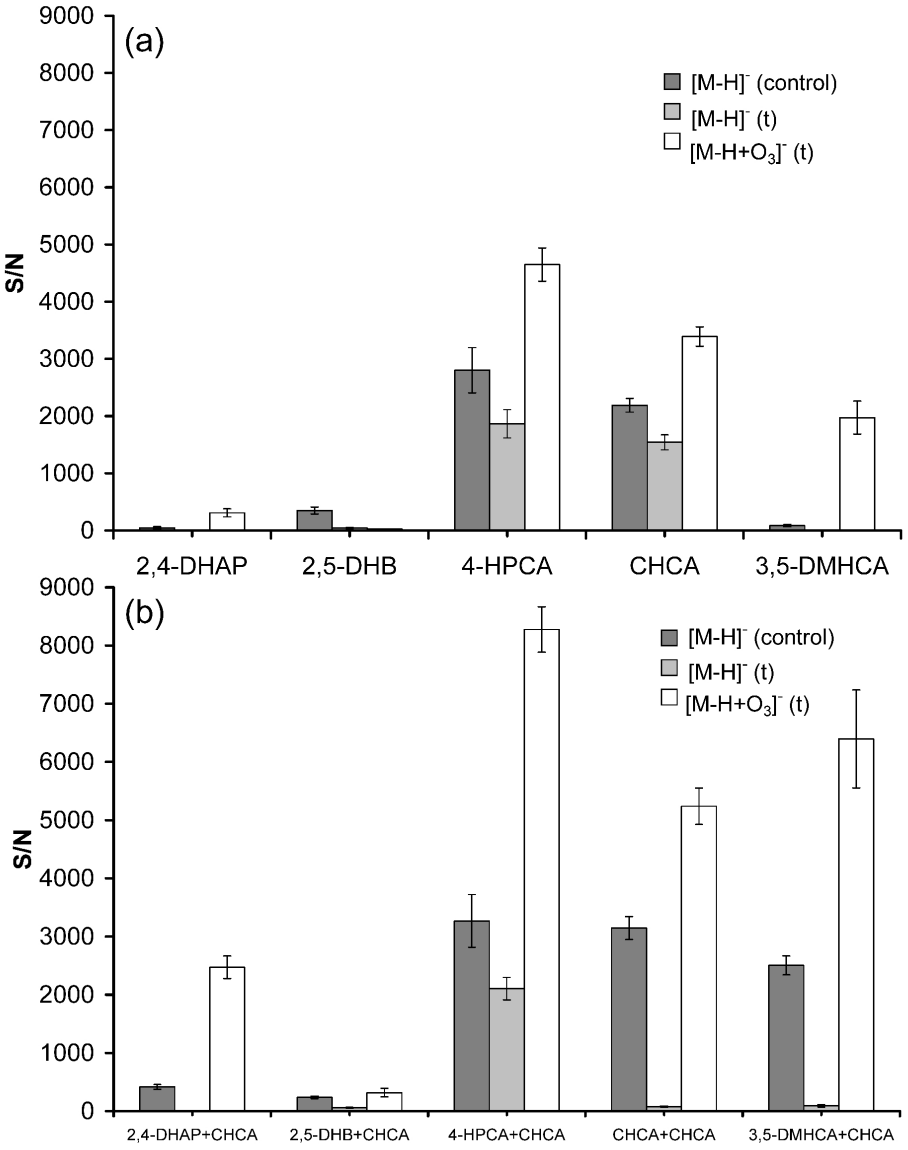

Figure 17. Graphical depiction of the signal-to-noise comparison for each MALDI matrix used for on-target oxidation of Cys-kemptide (CLRRASLG) (a) Summary of negative ion mass spectrometry data using varied MALDI matrices (a-e) for on-target oxidation of Cys-kemptide. Panel (b) represents the negative ion mass spectral data for Cys-kemptide oxidized in the presence of varied MALDI matrices with an overlayer of CHCA added prior to mass spectrometry analysis.

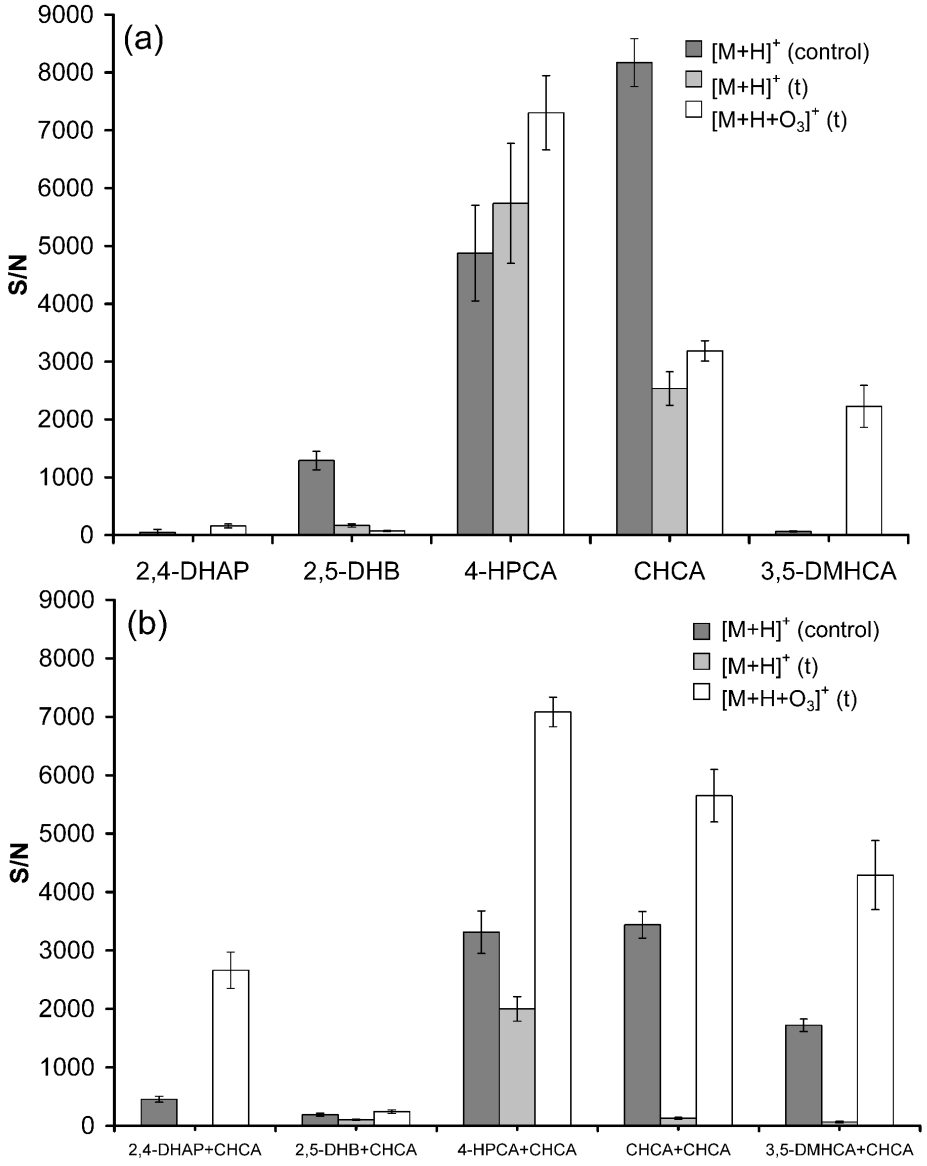

Figure 18. Graphical depiction of the signal-to-noise comparison for each MALDI matrix used for on-target oxidation of Cys-kemptide (CLRRASLG) (a) Summary of positive ion mass spectrometry data using varied MALDI matrices (a-e) for on-target oxidation of Cys-kemptide. Panel (b) represents the positive ion mass spectral data for Cys-kemptide oxidized in the presence of varied MALDI matrices with an overlayer of CHCA added prior to mass spectrometry analysis.

Figure 17b contains the graphical evaluation of each MALDI matrix (a-e) combined with CHCA applied after on-target oxidation of Cys-kemptide. These MALDI spots were oxidized in parallel with the data presented in Figure 17a with the exception of the dual MALDI matrix prior to mass spectrometry analysis. The abundance of the $[M - H + O_3]^-$ ion drastically increases for each MALDI matrix with the exception of 2,5-DHB. Oxidized Cys-kemptide formed in the presence of 4-HPCA has the most abundant oxidized ion signal when compared to the other matrices. However, native Cys-kemptide $[M - H]^-$ are observed after oxidation which suggests the oxidation is incomplete. Note that native Cys-kemptide $[M - H]^-$ ions are not observed in Figure 17a or 17b for 2,4-DHAP which suggests that the oxidation has gone to completion. Additionally, native Cys-kemptide $[M + H]^+$ ions are not observed in the positive ion mass spectrum for either 2,4-DHAP or the 2,4-DHAP + CHCA dual MALDI matrix (See Figure 18). Interestingly, the abundance of native Cys-kemptide is low for both CHCA and 3,5-DMHCA. The native Cys-kemptide abundance is *ca.* 2500 S/N when CHCA is used without CHCA re-deposition (Figure 17a). We suspect that additional oxidation chemistry is occurring with the residual performic acid on the CHCA matrix crystalline surface to result in enhancement of oxidized product yield. To probe this hypothesis, we oxidized a deposit of CHCA without analyte then added second deposit containing a mixture of CHCA combined with Cys-kemptide and a very low abundance of oxidized peptide is observed in the negative ion mass spectrum (data not shown). This control experiment suggests that additional oxidation does not occur when a CHCA overlayer is applied to an oxidized sample deposit. It is also important to note that oxidation does

occur when the analyte is deposited directly on the stainless steel MALDI target without matrix. Additionally, on-target oxidation occurs when Cys-kemptide is co-crystallized with MALDI inactive crystalline solids such as fructose and 4-phenylbutyric acid (4-PBA). However, the abundance of the oxidized Cys-kemptide $[M - H + O_3]^-$ ion is the greatest when using CHCA during oxidation as opposed to fructose and 4-PBA used during oxidation (See Figure 19).

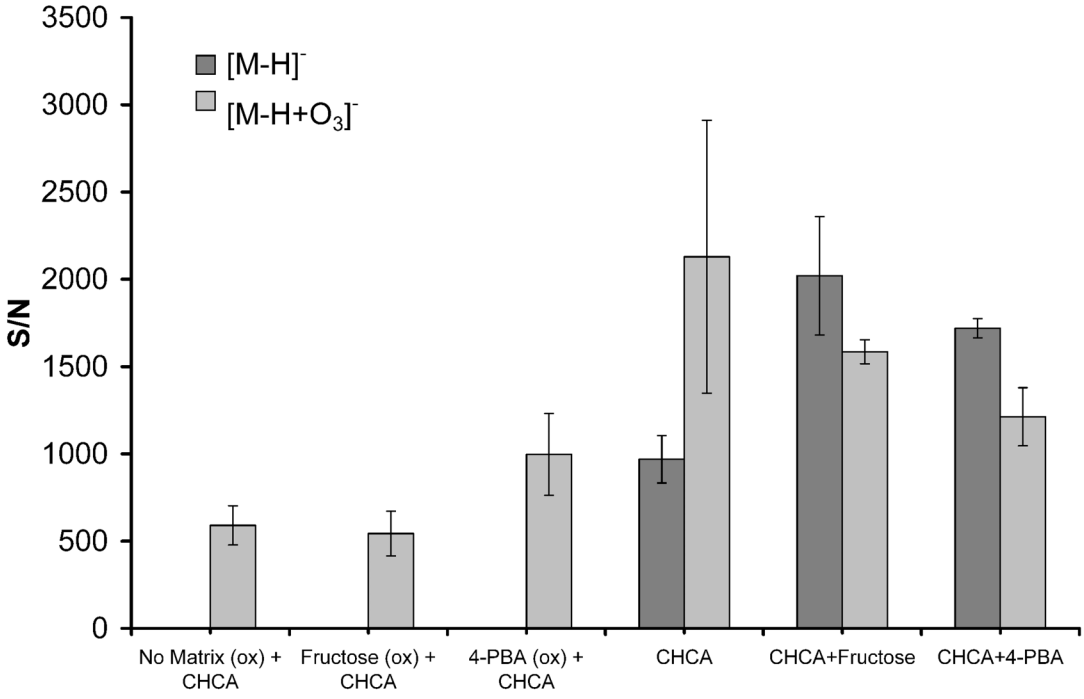

Figure 19. Comparison of the resulting oxidized peptide ion yield using various crystalline solids used for on-target oxidation of Cys-kemptide (error bars represent an average of three oxidized MALDI spots). For each crystalline solid, the analyte was deposited as an overlayer to pre-spotted fructose, 4-phenylbuytric acid, and CHCA. This particular on-target oxidation was performed at 25˚C for 15 min.

On-Target Oxidation and Subsequent Proteolytic Digestion of Intact Proteins

In a previous manuscript we demonstrated the ability to elucidate disulfide linked peptides from Ribonuclease A (RNase A) proteolytic digest using the combined positive and negative ion mass spectra following on-target oxidation.[48] Disulfide bonds within proteins (*e.g.,* bovine pancreatic trypsin inhibitor) are known to prevent complete proteolytic digestion owing to inaccessible proteolytic cleavage sites which results in inefficient protein digestion. Several research groups have successfully employed on-target proteolytic digestion techniques to various tissue sections for imaging mass spectrometry experiments.[108, 111] On-target oxidation of an intact protein would cleave the native disulfide bond pattern leaving the protein accessible to proteolytic digestion. Herein, we demonstrate an alternative protein digestion scheme using two on-target methods to oxidize/digest bovine pancreatic trypsin inhibitor (BPTI) and bovine RNase A.

Scheme 3. Experimental scheme for on-target oxidation of intact disulfide-containing proteins followed by subsequent on-target proteolytic digestion and MALDI-MS analysis.

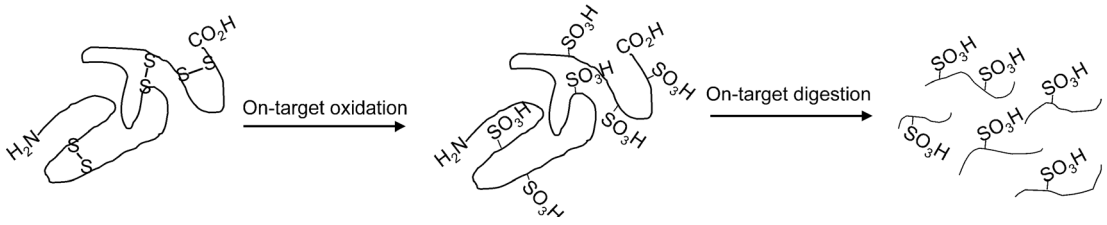

The experimental scheme for the on-target oxidation and subsequent proteolytic digestion of an intact disulfide-containing protein is shown in Scheme 3. First, the intact protein is co-crystallized with the MALDI matrix then oxidized using the on-target oxidation method. Second, the oxidized protein is digested using a protease (*e.g.,* trypsin) in the presence of MALDI matrix then subjected to MS analysis. BPTI is an excellent model disulfide-containing protein to illustrate the ability to both oxidize and digest proteins on the MALDI target. BPTI contains three disulfide bonds and several trypsin cleavage sites as shown in Scheme 4.

Scheme 4. Amino acid sequence of bovine pancreatic trypsin inhibitor shown with its native disulfide-bonds (Cys^{5}- Cys^{55}, Cys^{14}- Cys^{38}, Cys^{30}- Cys^{51}). The trypsin cleavage sites are denoted in *bold italics*.

Figure 20a contains the negative ion mass spectrum of BPTI oxidized and digested with trypsin on the MALDI target. Note that both the oxidation (10 min) and proteolytic digestion (60 min) were performed in the presence of 2,4-DHAP MALDI matrix. CHCA was added after oxidation and digestion to enhance the negative ion yields. Several oxidized peptides labeled (A-I) are observed in the negative ion mass spectrum after oxidation and digestion (Figure 20b). The amino acid sequence coverage for this small protein is 100% with all six cysteine residues involved in disulfide bridging detected in their oxidized form. For example, the oxidized BPTI peptide $^{27}AGLC_{ox}QTFVYGGC_{ox}R^{39}$ (m/z 1468.62) is observed with two cysteic acid groups

because it lacks trypsin cleavage sites in this region of the protein. In the control experiment without oxidation, proteolytic peptides are not observed in the negative ion mass spectrum (data not shown). Hence, the oxidation breaks each disulfide bond converting each cysteine residue to cysteic acid which improves the accessibility of the protease to cleave after proteolytic cleavage sites. This on-target oxidation followed by on-target proteolytic digestion has also been applied to bovine Ribonuclease A which contains one intra- and three inter-linked disulfide bonds. RNase A oxidized peptides are readily observed after only 5 min of oxidation followed by proteolytic digestion (See Figure 21a). The oxidized RNase A peptides account for 70% of the amino acid sequence with four oxidized cysteine residues. The missing portion of the RNase A sequence is suspected to be either inaccessible to the performic acid vapor or the protease to successfully cleave this protein section. Overall, this on-target oxidation and subsequent proteolytic digestion protocol could be applied to tissue sections which are profiled using imaging mass spectrometry. The on-target oxidation will rapidly improve the protease accessibility to successfully digest difficult-to-digest proteins within tissue sections.

(a)

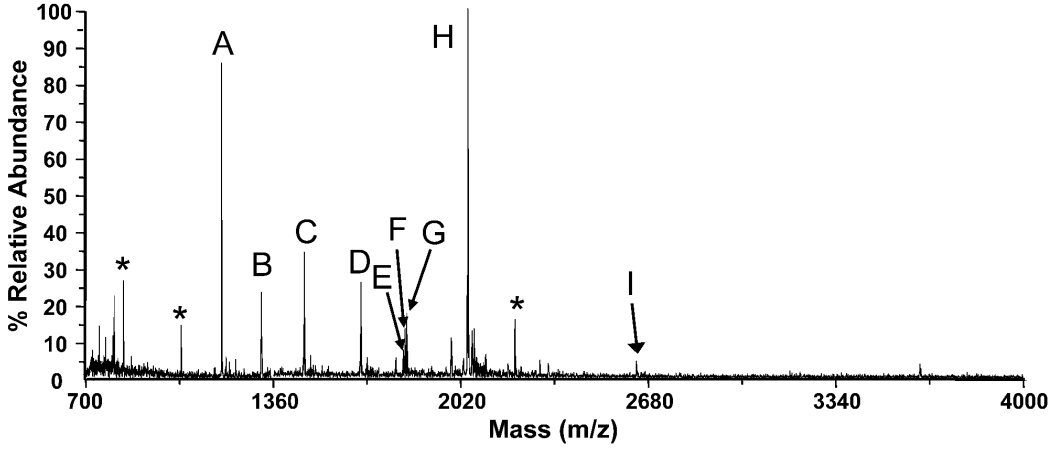

(b)

Label	Peptide Sequence	$[M-H+O_x]^-_{obs}$	$[M-H+O_x]^-_{calc}$	Mass Error
				ppm
A	^{18}IIRYFYNAK^{26}	1185.678	1185.642	31
B	^{47}SAEDC$_{ox}$***M***RTC$_{ox}$GGA^{58}	1326.402	1326.388	10
C	^{27}AGLC$_{ox}$QTFVYGGC$_{ox}$R^{39}	1468.619	1468.583	24
D	^{27}AGLC$_{ox}$QTFVYGGC$_{ox}$RAK^{41}	1667.753	1667.716	22
E	^{1}RPDFC$_{ox}$LEPPYTGPC$_{ox}$K^{15}	1816.803	1816.752	28
F	^{27}AGLC$_{ox}$QTFVYGGC$_{ox}$RAKR^{44}	1823.861	1823.817	24
G	^{43}NNFKSAEDC$_{ox}$***M***RTC$_{ox}$GGA^{58}	1829.656	1829.637	10
H	^{1}RPDFC$_{ox}$LEPPYTGPC$_{ox}$KAR^{17}	2043.948	2043.890	28
I	^{18}IIRYFYNAKAGLC$_{ox}$QTFVYGGC$_{ox}$R^{39}	2637.274	2637.223	19

Figure 20. (a) Representative negative ion mass spectrum for on-target oxidation and digestion of bovine pancreatic trypsin inhibitor (BPTI). The on-target oxidation was performed for 10 min for this example at room temperature (+23˚C) followed by on-target trypsin digestion for 60 min. (b) Summary of the BPTI oxidized peptides (A-I) identified based on accurate mass measurement.

(a)

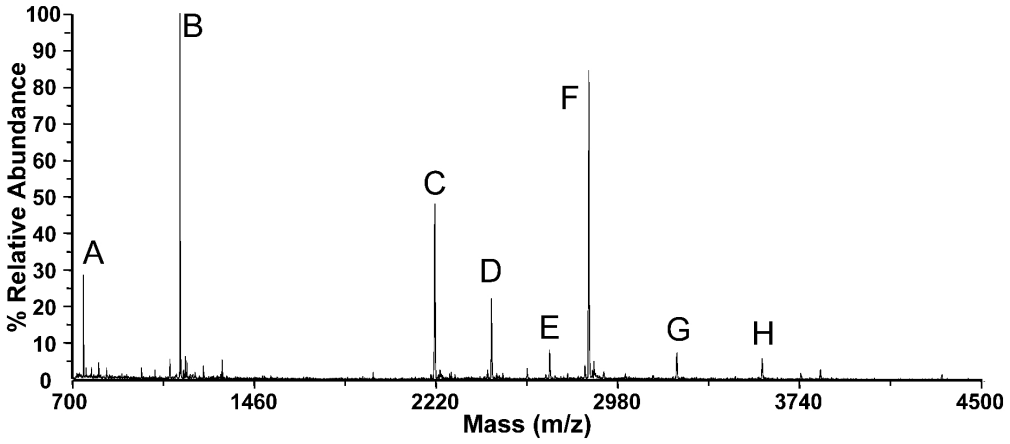

(b)

Label	Peptide Sequence	$[M-H+O_x]^-_{obs}$	$[M-H+O_x]^-_{calc}$	Mass Error
				ppm
A	^{60}NLTKDR^{65}	744.407	744.401	8
B	^{27}KETAAKFER^{36}	1148.621	1148.607	12
C	^{131}HIIVAC$_{ox}$EGNPYVPVHFDASV^{150}	2213.044	2213.034	5
D	^{37}QH***M***DSSTSAASSSNYC$_{ox}$NQ***MM***K^{57}	2449.799	2449.849	-21
E	^{37}QH***M***DSSTSAASSSNYC$_{ox}$NQ***MM***KSR^{59}	2692.920	2692.982	-23
F	^{125}TTQANKHIIVAC$_{ox}$ENPYVPVHFDASV^{150}	2856.320	2856.363	-15
G	^{60}NLTKDRC$_{ox}$KPVNTFVHESLADVQAVC$_{ox}$SQK^{87}	3224.456	3224.532	-24
H	^{34}FERQH***M***DSSTSAASSSNYC$_{ox}$NQ***MM***KSRNLTK^{63}	3581.351	3581.464	-32

Trypsin autolysis peaks at *m/z* 840.49 and 2209.09 were used for internal calibration.

Figure 21. (a) Representative negative ion mass spectrum for on-target oxidation and digestion of bovine Ribonuclease A (RNase A). The on-target oxidation was performed for 5 min for this example at room temperature (+23˚C) followed by on-target trypsin digestion for 60 min. (b) Summary of the RNase A oxidized peptides (A-H) identified based on accurate mass measurement.

Conclusion

The experimental variables associated with the on-target oxidation method were evaluated using several model cysteine and/or disulfide-containing peptides and proteins. Overall, the elevated temperature oxidation (+25˚C) does not have a detrimental effect on peptides that contain histidine, tryptophan, or tyrosine amino acid residues when CHCA is used during oxidation. Cysteine oxidation can be achieved in only 5 minutes with optimal oxidation in 15 min for small cysteine-containing peptides. Intact insulin requires increased oxidation (60 min) and an alternative MALDI matrix (2,4-DHAP) in order achieve complete oxidation of the insulin α and β-chains. An improved oxidized product yield is observed for oxidized Cys-kemptide (C_{ox}LRRASLG) when using 2,4-dihydroxyacetophenone or 3,5-dimethyl-4-hydroxycinnamic acid as the MALDI matrix during oxidation. In addition, on-target oxidation of a disulfide-containing protein followed by on-target proteolytic digestion was demonstrated for bovine pancreatic trypsin inhibitor, thus improving the digestion efficiency of a difficult-to-digest protein. Future experiments involve the investigation of the negative ion fragmentation of these cysteic acid-containing peptides.

CHAPTER V

EFFECT OF CYSTEIC ACID POSITION ON NEGATIVE ION FRAGMENTATION OF RIBONUCLEASE A PROTEOLYTIC PEPTIDES

Introduction

The vast majority of proteomics studies utilize positive ion data for single and multiple stages of mass spectrometry for protein and peptide identification. However, negative ion mass spectrometry provides a specific utility towards the detection and identification of peptide/protein post-translational modifications (*e.g.,* glycosylation, sulfation, and phosphorylation).[112, 113] The fragment ion spectra of peptide $[M - H]^-$ ions provides information not commonly afforded by positive ion tandem mass spectrometry.[112, 113] For example, tandem MS precursor ion scanning techniques have enabled the selective detection of phosphopeptides from a complex mixture owing to the diagnostic loss of m/z 79 (PO_3^-) or m/z 97 ($H_2PO_4^-$) from the parent $[M - H]^-$ ion.[114-116] Additionally, several side chain loss fragment ions (*e.g.,* Asp, Gln, Ser, Thr, and Cys) are frequently observed using either positive or negative ion tandem MS which can enable differentiation between glutamine and lysine, two near isobaric amino acid residues.[112] The backbone cleavage products of $[M - H]^-$ peptide ions are somewhat similar to positive ion fragment ions; however, the mechanism of fragment ion formation is quite different. Bowie and coworkers have developed negative ion fragmentation nomenclature to describe these processes.[112, 113, 117] For example, backbone cleavages of the peptide amide bond are called α- and β-fragmentations which are somewhat similar

to *y*-type and *b*-type fragment ions in positive ion nomenclature, respectively (See Scheme 5).

Scheme 5. Generic structures of α_n and β_n fragment ions according to nomenclature and fragmentation mechanisms described by Bowie and coworkers.[112]

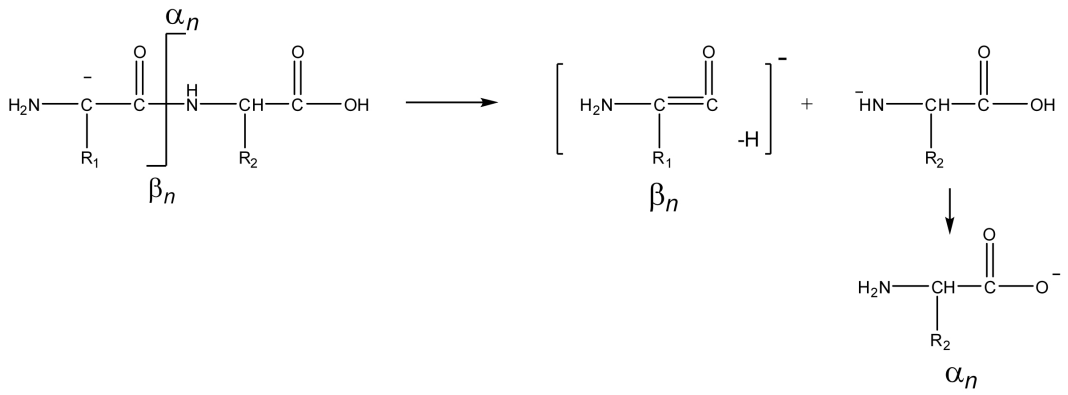

Cysteic acid-containing peptide ions are known to yield abundant fragment ions involving the loss of the cysteic acid side chain.[118, 119] For example, Gaskell and coworkers have reported *d*-type fragment ions for oxidized $RLAIFC_{ox}FR$.[119] Specifically, a d_7 (partial side-chain loss of $-SO_3H$) fragment ion is observed in the fragment ion mass spectrum of the $[M + 2H]^{2+}$ ion of the oxidized peptide. However, when the cysteic acid position changes for the oxidized peptide $RLC_{ox}IFSAFR$ a d_3 fragment ion is observed in the positive ion tandem mass spectrum. The cysteic acid is suspected to be involved in the *d*-type fragment ion formation mechanism through the interaction with the N-terminal arginine side chain. In earlier work by Gaskell *et al.* they investigated the positive ion fragmentation of a cysteic acid-containing peptide

(C_{ox}GQPLQNK) with the cysteic acid at the N-terminus.[45] The positive ion tandem mass spectrum is dominated by a *y*-type fragment ion series owing to positive charge localization at the C-terminal lysine. They conclude that the cysteic acid promotes interaction with the lysine and arginine residues at the C-terminus and allows the "mobile proton" to move freely along the peptide backbone.[118-120]

Here we investigate the effect of cysteic acid position on the negative ion fragmentation of RNase A proteolytic derived peptides. Distinct *d*-type fragment ion series are observed from peptides that contain an N-terminal cysteic acid. Our main hypothesis states as the cysteic acid position changes we suspect that the side-chain fragment ion type will change, *i.e.,* form *v*- and *w*-type fragment ions as the cysteic acid moves towards to the C-terminus. To evaluate the effect of the cysteic acid position on partial and full-side chain loss fragment ion formation we chose to study RNase A proteolytic peptides with the cysteic acid at the N-terminus, near the center of the peptide, and toward the C-terminus. Additional studies were performed on native Cys-kemptide (CLRRASLG) and oxidized Cys-kemptide (C_{ox}LRRASLG), a model peptide with cleavable side chains and an N-terminal cysteic acid after on-target performic acid oxidation.

Experimental

Chemicals

All chemicals were purchased from Sigma-Aldrich (St. Louis, MO) unless otherwise noted. Hydrogen peroxide (35% w/w) and formic acid (99% w/w) were

purchased from Acros Organics (Morris Plains, NJ). HPLC grade acetone and methanol (CH_3OH) were purchased from EMD Chemicals Inc. (Gibbstown, NJ). All experiments were performed with 18-MΩ water (ddH_2O) purified using a water purification unit (Barnstead International, Dubuque, IA).

Sample Preparation for MALDI-MS

A stock solution of Cys-kemptide (CLRRASLG) was prepared at 10 μM in 10 mM formic acid. The peptide solution was mixed 1:1 with CH_3OH and 1 μL was spotted as an overlayer to pre-spotted CHCA matrix. CHCA was prepared at 5 mg mL^{-1} in a 2:3 ddH_2O: CH_3OH solution containing 10 mM $NH_4H_2PO_4$ and 1 μL was pre-spotted as the underlayer.[90] This cysteine-containing peptide was later oxidized using the on-target oxidation procedures described below.

Ribonuclease A Proteolytic Digestion

Dual protease digestion (trypsin followed by chymotrypsin) of RNase A was performed using previously described methods.[48, 56]Briefly, RNase A was dissolved at 1 mg mL^{-1} in a 25 mM ammonium acetate buffer adjusted to pH 6.0 with 10 mM formic acid. RNase A was digested with and without chemical reduction of the disulfide bonds. For the non-reduced digest, RNase A was initially digested with trypsin (1:50 enzyme: protein ratio) for 4 hrs at 37˚C followed by chymotrypsin addition (1:50 enzyme: protein ratio) and incubation for an additional 4 hrs. For the reduced RNase A digest, the sample solution was subjected to TCEP reduction (2 μL of 50 mM TCEP prepared in ddH2O)

by incubating at 60˚C for 60 min. Following TCEP reduction, the protein was digested with trypsin followed by chymotrypsin using the same procedure as the non-reduced digest. Following proteolytic digestion, the sample was subjected to cleanup using a 10 μL C_{18} resin pipette tip. The RNase A proteolytic digest was eluted with a 60:40 CH_3CN: ddH_2O solution containing 0.1% formic acid and 1 μL was spotted as the overlayer to CHCA matrix.

On-Target Performic Acid Oxidation

On-target oxidation was performed as described previously.[48] Briefly, 40 μL of a 1:1 mixture of acetone: performic acid was placed directly on the MALDI target in a region that does not contain sample. The MALDI target was then covered in a plastic petri dish and was allowed to react at room temperature (+24˚C) for 10-60 min. Following on-target performic acid oxidation the MALDI plate is then subjected to MALDI analysis without sample cleanup.

4-Sulfophenyl Isothiocyanate Derivatization of Cys-Kemptide

Stock solutions of Cys-kemptide were prepared at 10 μM in 20 mM tetraethyl ammonium bicarbonate. The Cys-kemptide solution was first reduced with TCEP at 60˚C for 60 min. Followed by 2-iodoacetamide alkylation by incubating for 45 min at room temperature in the dark. The SPITC derivatization was performed using previously described methods with minor modifications.[121] Briefly, the SPTIC derivatization was performed in tetraethyl ammonium bicarbonate at 1000-fold molar excess of SPITC:

peptide using 55˚C reaction temperatures for 30 min. Following SPTIC derivatization, samples were subjected to cleanup using a 10 μL C_{18} resin pipette tip. The alkylated Cys-kemptide + SPITC reaction mixture was eluted with a 60:40 CH_3CN: ddH_2O solution containing 0.1% formic acid and 1 μL was spotted as the overlayer to CHCA matrix.

MALDI-MS and MALDI-MS/MS

All MALDI-MS experiments were performed using a model 4700 Proteomics Analyzer MALDI-TOF/TOF (Applied Biosystems, Framingham, MA). The MALDI-MS data were acquired using the reflectron detector in both positive and negative ion modes using 1200 laser shots with external calibration using bradykinin (2-9) (PPGFSPFR) and ACTH (18-39) (RPVKVYPNGAENESAEAFPLEF). Positive and negative ion collision-induced dissociation (CID) tandem MS spectra were acquired using 20% greater laser power than the MS spectra acquisition with atmosphere (medium pressure) as the collision gas with 1 kV of collision energy.

The peptide fragmentation nomenclature developed by Roepstorrff[122] and modified by Biemann[123] was used to describe the side-chain loss fragment ions that we observe in the negative ion tandem mass spectra. In regards to the negative ion peptide fragmentation nomenclature developed by Bowie and coworkers, several different side-chain losses are observed in the negative ion tandem mass spectra of $[M - H]^-$ peptide ions;[112] however, nomenclature to describe the site of bond cleavage and the type (partial or full) of side-chain loss has not yet been clearly defined. Hence, our rationale to use

positive ion peptide fragmentation nomenclature to describe the side-chain loss fragment ions observed within.

Results and Discussion

Positive and Negative Ion Fragmentation of Native and Oxidized Cys-Kemptide

Figure 22 contains positive and negative ion fragmentation data for Cys-kemptide (CLRRASLG) before and after on-target performic acid oxidation. The y_5 ion in the positive ion tandem mass spectrum (Figure 22a) is the most abundant fragmentation channel with several partial side-chain cleavage ions present. The peptide fragmentation nomenclature for side-chain loss fragment ions (d_n, v_n, and w_n) are illustrated in Scheme 6 for deprotonated peptide ions. Note that a d_4 fragment ion is observed at m/z 416.27 corresponding to backbone cleavage at the a_4 position with a partial arginine side chain loss (cleavage between the β and γ carbon atoms) and the overall charge is retained toward the N-terminus of the peptide. Additional *d*-type fragment ions are observed (d_6 and d_7) corresponding to the partial side chain losses of serine and leucine, respectively. It appears that the localization of the positive charge by the two arginine side chains is causing the somewhat fixed positive charge near the N-terminus to form partial side-chain cleavage fragment ions. As the positive charge carrier moves along the peptide backbone the probability of forming *w*-type fragment ions increases. In Figure 22a, abundant ion signals for w_6 and w_7 fragment ions are observed which correspond to *z*-type backbone cleavage with partial side-chain loss of arginine and leucine, respectively. However, the w_5 fragment ion formation is not favorable, owing to the lack of a positive charge carrier in the resulting fragment ion. As for the

positive ion tandem mass spectrum of oxidized Cys-kemptide (C_{ox}LRRASLG) $[M + H + O_3]^+$ ion results in several *y*-type fragment ions and the loss of 17 Da (NH_2) from the y_6 and y_7 ions which is most likely coming from the guanidino group of arginine (Figure 22b). Note that side-chain loss fragment ions (*i.e., w*- and *d*-type fragment ions) are also observed, similar to the fragment ion spectrum of native Cys-kemptide $[M + H]^+$ ion.

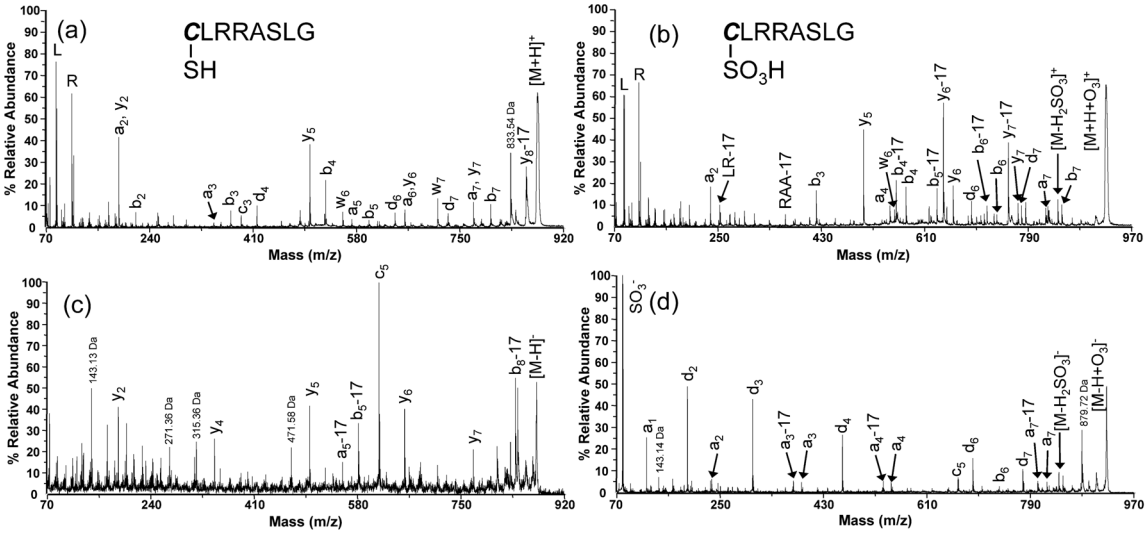

Figure 22. (a) Positive and (c) negative ion tandem mass spectra of native Cys-kemptide (CLRRASLG). (b) Positive and (d) negative ion tandem mass spectra of oxidized Cys-kemptide (C_{ox}LRRASLG).

Scheme 6. Generic peptide amino acid sequence with the γ carbon atom denoted with R_1-R_5. Structures of d_n, v_n, and w_n fragment ions are denoted below each arrow.

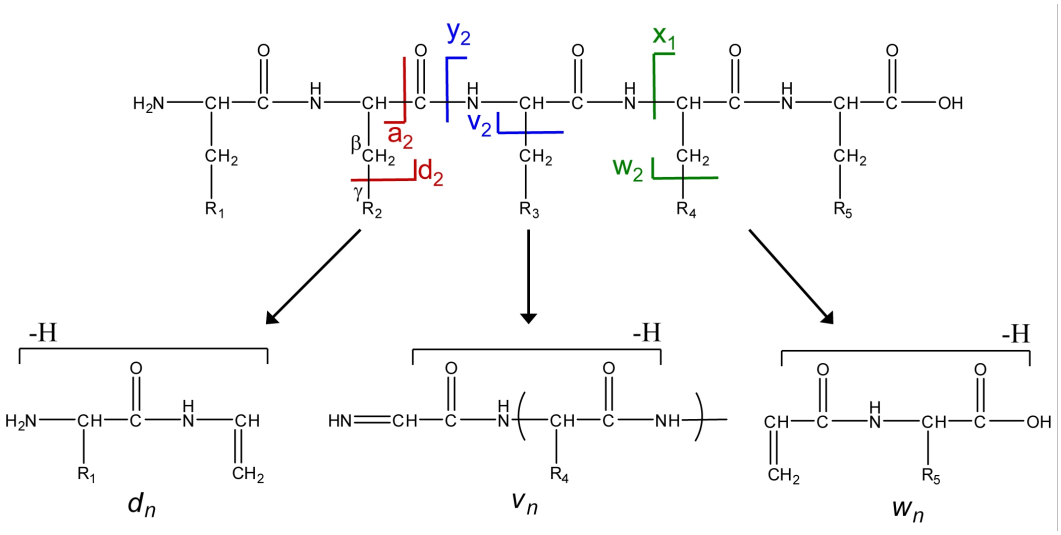

For comparison, the negative ion tandem mass spectrum for native Cys-kemptide $[M - H]^-$ ions is shown in Figure 22c. This spectrum contains a near complete series of *y*-type fragment ions. Also, note that a dominant c_5 fragment ion (m/z 615.56) is also present in Figure 22c. Conversely, the negative ion spectra of oxidized Cys-kemptide (C_{ox}LRRASLG) is composed of very different fragment ions because the cysteic acid group induces a fixed negative charge at the N-terminus of the peptide, which results in near complete *d*-type fragment ion series (Figure 22d). Note that the d_5 fragment ion is not observed because the alanine side chain does not have a cleavable β-γ carbon-carbon bond. It is important to note that side-chain loss fragment ions are not observed in the negative ion mass spectrum without CID collision gas (2.8×10^{-8} torr), thus the additional collisions at higher pressure (9.0×10^{-7} torr) are required to form the *d*-type fragment ions (See Figure 23).

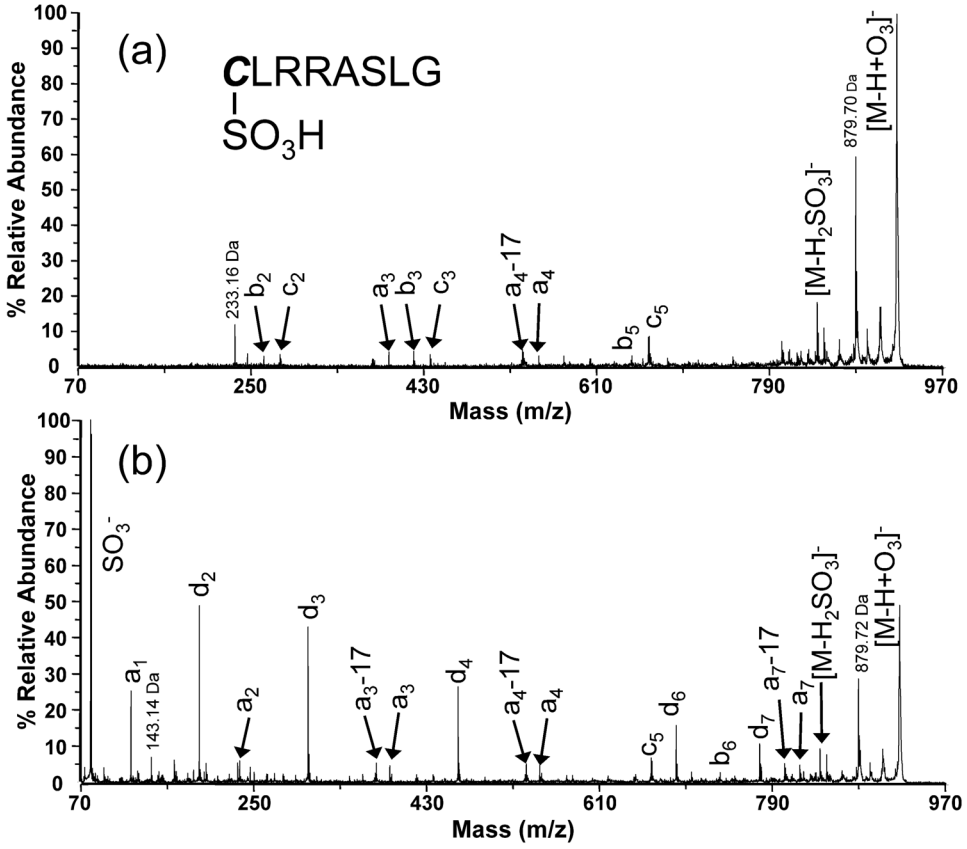

Figure 23. Negative ion tandem mass spectra of the oxidized Cys-kemptide [M – H + O_3]$^-$ ion fragmented (a) without additional collision gas (2.8E-8 torr) and (b) with collision gas set at medium pressure (9.0E-7 torr).

To further investigate the role of the fixed N-terminal negative charge in the formation of *d*-type fragment ions, we chose to perform N-terminal 4-sulfophenyl isothiocyanate (SPITC) derivatization of Cys-kemptide. SPITC is a commonly used in *de novo* peptide sequencing as a derivatization reagent to place a fixed negative charge at N-terminus of the peptide which results in primarily *y*-type fragment ion series.[121, 124] The free thiol group of Cys-kemptide was alkylated with 2-iodoactamide prior to SPITC derivatization owing to the loss of 34 Da (H_2S) during SPITC derivatization of native Cys-kemptide. Two *d*-type fragment ions are observed (d_1 and d_2) in the negative ion tandem mass spectrum of alkylated Cys-kemptide + SPITC at 1145.59 m/z (See Figure 24). There are only a few *d*-type fragment ions because the facile loss of the SPITC group during collisional activation limits the number of fragmentation channels. The cysteic acid group of oxidized Cys-kemptide stays intact after collisional activation; therefore, the near-complete series of *d*-type fragment ions are observed (Figure 22d). Therefore, we suspect that the negative charge localization at the N-terminus promotes *d*-type ion formation.

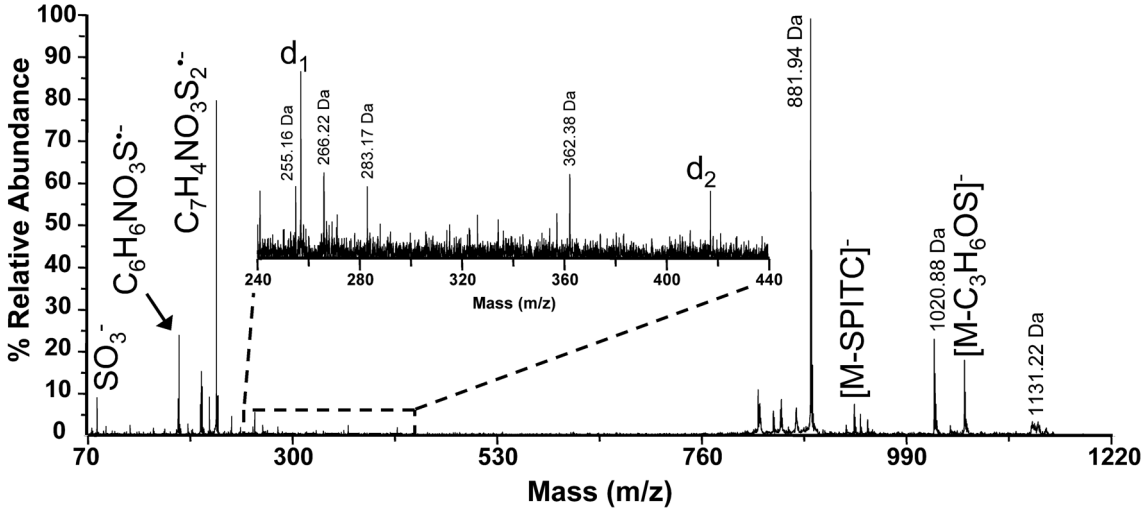

Figure 24. Negative ion tandem mass spectrum of alkylated Cys-kemptide + SPITC at m/z 1145.59. Inset: expanded view of mass range 240-440 m/z illustrating that two *d*-type fragment ions d_1 and d_2 are present.

RNase A Proteolytic Peptides: N-terminal Cysteic Acid

The results described above suggest that the cysteic acid position plays a role in *d*-type fragment ion formation; and to probe this further we investigated several RNase A proteolytic peptides that have the cysteic acid at the N-terminus, center, and toward the C-terminus of the peptide. These RNase A proteolytic peptides were produced from a dual enzyme digestion using trypsin followed by chymotrypsin. The negative ion tandem mass spectra of three oxidized RNase A proteolytic peptides that have N-terminal cysteic acid are contained in Figure 25. Several *d*-type fragment ions (d_2-d_4) are

observed for $^{52}C_{ox}$NQ***MM***^{56} in Figure 25a. The d_5 fragment ion is present at low relative abundance at m/z 598.24. Note that methionine residues are also oxidized (denoted in ***bold italics***) by using the on-target oxidation method. Similar *d*-type fragment ions are observed for $^{52}C_{ox}$NQ***MM***K^{57} which contains a C-terminal lysine residue, and a more abundant d_5 fragment ion formed by side-chain cleavage of the oxidized methionine residue is observed (Figure 25b). When the cysteic acid is adjacent to a lysine residue *d*-type fragment ions are still formed. For example, $[M - H + O_3]^-$ ions of $^{66}C_{ox}$KPVNTF^{72} form abundant d_2, d_4, and d_5 fragment ions (Figure 25c). We also observe an ion signal at 645.52 m/z which could correspond to the a_6-17 ion or the db$_6$ ion for the loss of the hydroxyl group (-OH) from the threonine residue. The d_3 ion for $^{66}C_{ox}$KPVNTF^{72} is absent because cyclic amino acids (proline) do not produce *d*-type fragment ions.[123] Collectively, the data suggests that peptides containing cysteic acid favor formation of *d*-type fragment ions under two conditions: the cysteic acid (fixed negative charge) is at the N-terminus and the amino acid side chain has a cleavable β-γ carbon-carbon bond.

For comparison, the CID spectra of model peptides containing N-terminal aspartic acid or glutamic acid were also examined. Angiotensin I (DRVYIHPFHL) which has N-terminal aspartic acid yields abundant *y*-type fragment ions (y_1, y_2, y_4, y_6, y_7, and y_9) and no *d*-type fragment ions (Figure 26). Conversely, several *d*-type fragment ions (d_3, d_5, d_{10}) are observed in the positive ion tandem mass spectrum owing to the charge-carrying arginine side chain located near the N-terminus of the peptide. The N-terminal glutamic acid-containing peptide Glu-Fibrinopeptide B (EGVNDNEEGFFSAR) fragments to form both *b*- and *y*-type fragment ions and a low abundance w_8 fragment ion (See Figure 27). Gaskell and coworkers performed similar experiments on aspartic and glutamic acid analogues of RLAIFSC_{ox}FR.[118] Specifically, they investigated RLEIFSEFR and RLDIFSDFR, where the positive ion fragmentation of RLDIFSDFR $[M + 2H]^{+2}$ ions results in d_3 and d_7 whereas for RLEIFSEFR these two *d*-type fragment ions are not observed. The aspartic acid side chain ($-CH_2COOH$) and the cysteic acid side chain ($-CH_2SO_3H$) both contain a single methylene group (*i.e., d*-type fragment ions are formed under similar pathways); whereas the glutamic acid side chain has an additional methylene spacer which prevents *d*-type ion formation.

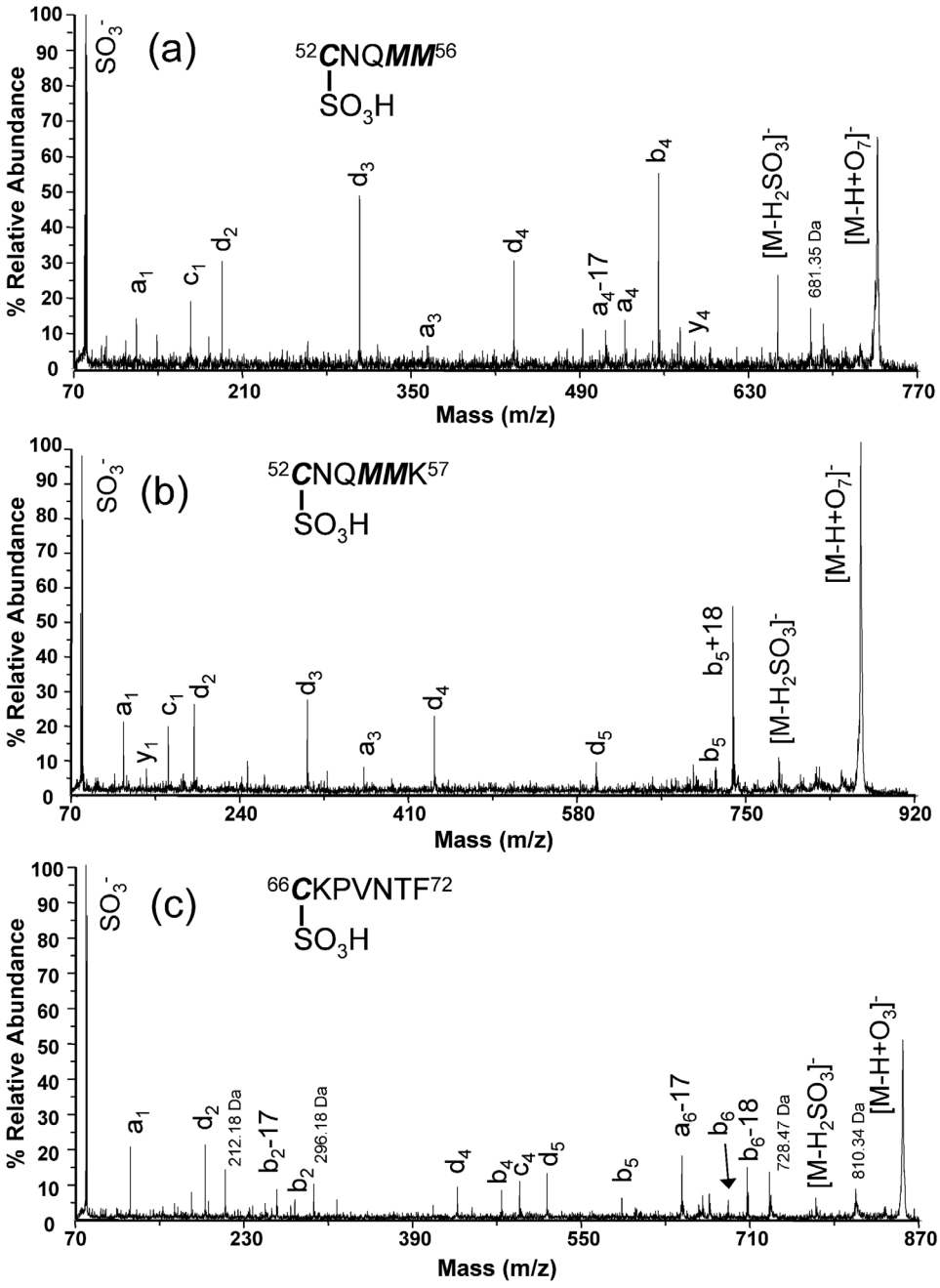

Figure 25. Typical negative ion tandem mass spectra for oxidized RNase A proteolytic peptides where the cysteic acid is at the N-terminus of the peptide. (a) $^{52}C_{ox}NQ\boldsymbol{MM}^{56}$, (b) $^{52}C_{ox}NQ\boldsymbol{MM}K^{57}$, and (c) $^{66}C_{ox}KPVNTF^{72}$.

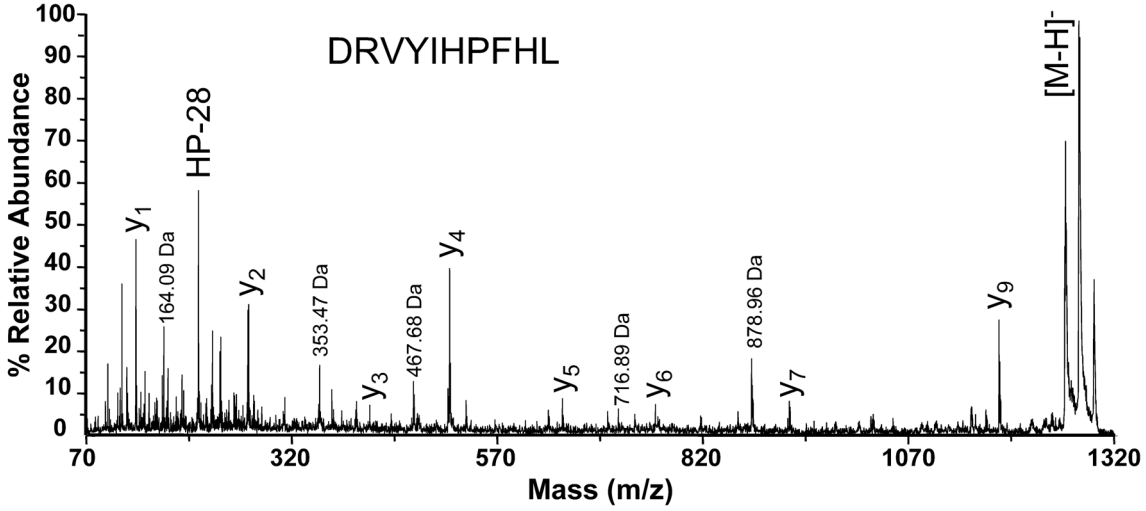

Figure 26. Negative ion tandem mass spectrum for the standard peptide Angiotensin I (DRVYIHPFHL).

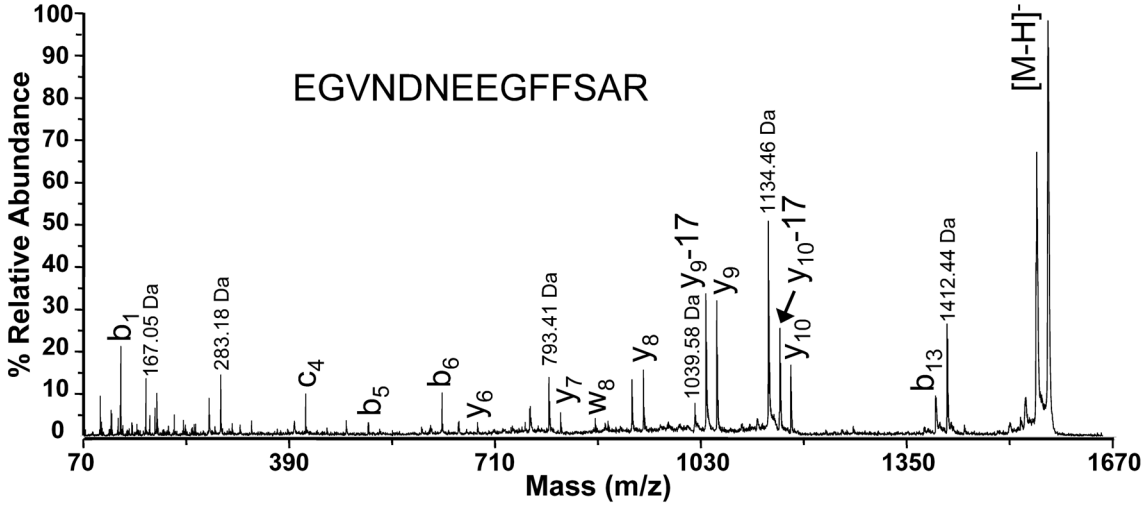

Figure 27. Negative ion tandem mass spectrum for the standard peptide Glu-Fibrinopeptide B (EGVNDNEEGFFSAR).

RNase A Proteolytic Peptides: Cysteic Acid Near the Peptide Center

RNase A proteolytic peptides with the cysteic acid towards the center of the peptide were also examined. $[M - H]^-$ ions of $^{82}AVC_{ox}SQK^{87}$ yield two *d*-type fragment ions (d_4 and d_5) by partial side chain loss of serine and glutamine, respectively (Figure 28a). For $^{118}YPNC_{ox}AY^{123}$ (Figure 28b), *d*-type fragment ions are not observed because the alanine side chain lacks a cleavable β-γ carbon-carbon bond and side chain cleavage of an aromatic side chain (tyrosine) is not favorable.[123] However, a *w*-type fragment ion is observed at the w_4 position for the side chain loss of asparagine with the negative charge retained toward the C-terminus of the peptide. It appears that *d*-type ion formation is possible for the amino acid side chains C-terminal to the cysteic acid. This is the case for $^{131}HIIVAC_{ox}EGNPY^{141}$ which yields two *d*-type fragment ions, d_7 and d_9 corresponding to side chain loss of glutamic acid and asparagine, respectively (Figure 28c). Interestingly, a w_5 ion is observed in the negative ion tandem mass spectrum for native $^{131}HIIVACEGNPY^{141}$ corresponding to the partial side chain loss of glutamic acid (See Figure 29). Similar side chain losses were previously reported for $[M - H]^-$ ions for underivatized peptides.[125] The observation of *w*-type ions is interesting; because this result supports our main hypothesis; *i.e.,* the side-chain fragment ion type will change to *v*- or *w*-type ions as the cysteic acid moves toward the C-terminus.

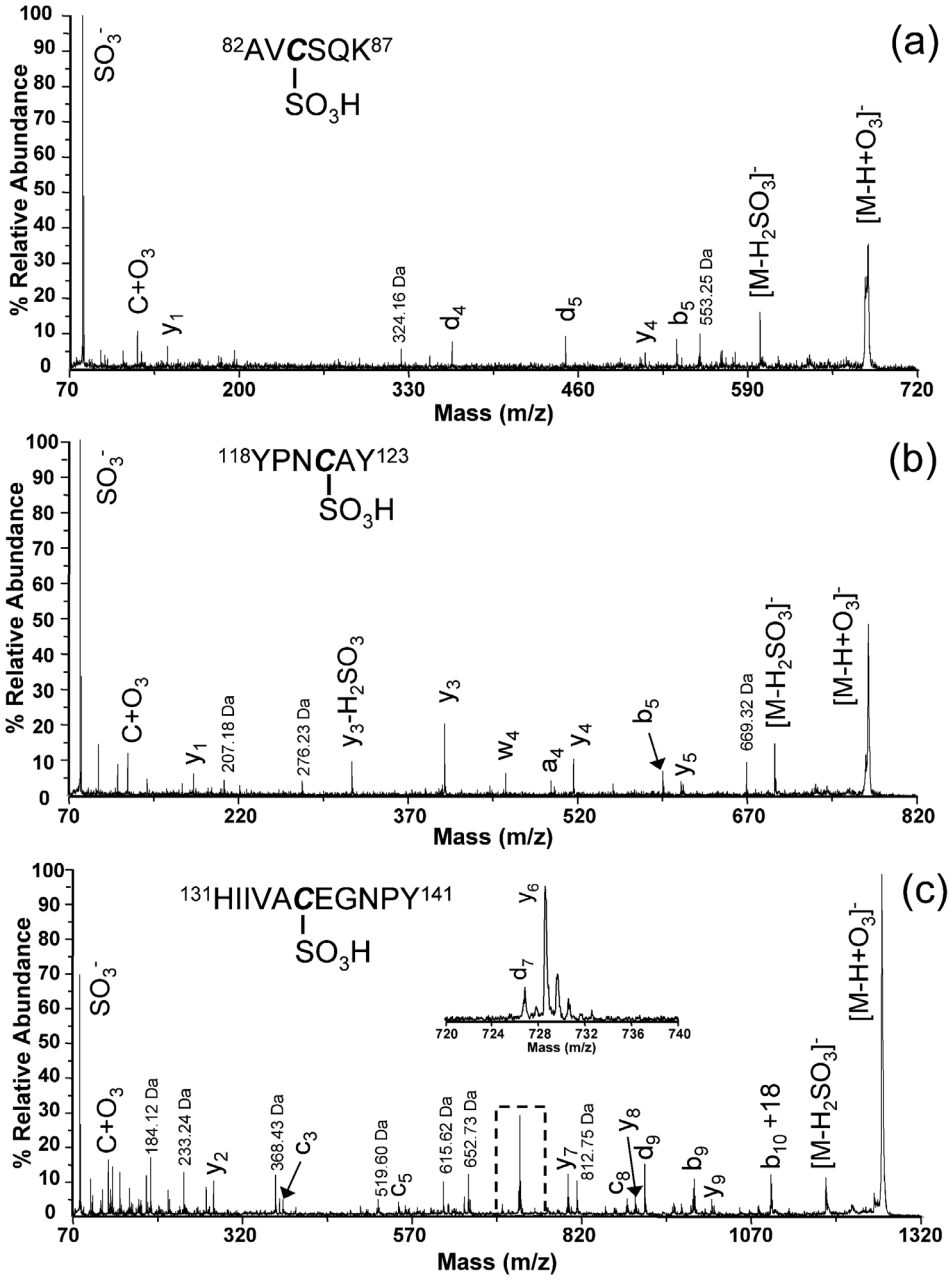

Figure 28. Typical negative ion tandem mass spectra for oxidized RNase A proteolytic peptides that have the cysteic acid side chain near the center of the peptide. (a) $^{82}AVC_{ox}SQK^{87}$, (b) $^{118}YPNC_{ox}AY^{123}$, and (c) $^{131}HIIVAC_{ox}EGNPY^{141}$. Inset figure: expanded view of mass range 720-740 m/z illustrating that two fragment ions d_7 and y_6 are present.

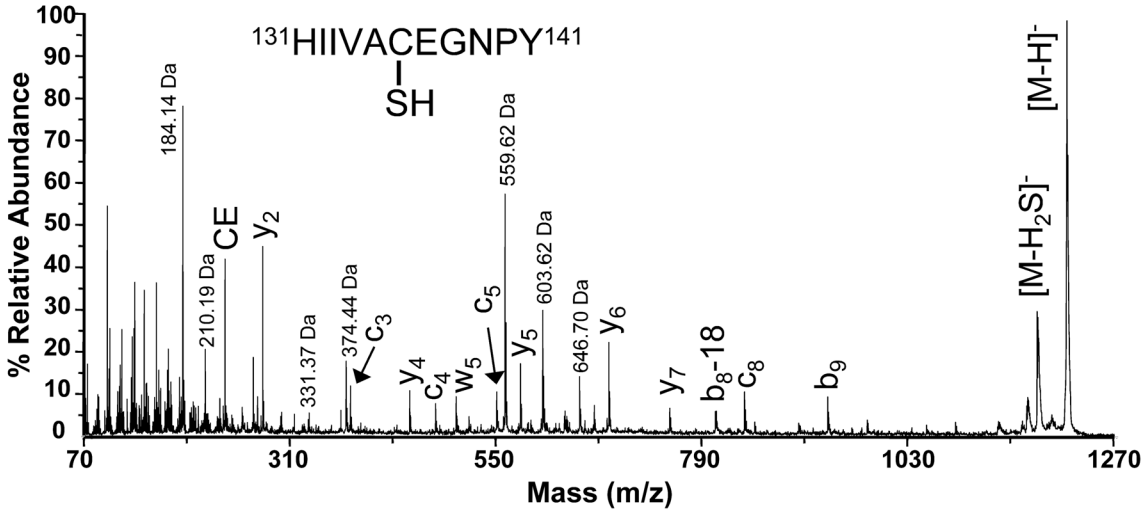

Figure 29. Negative ion tandem mass spectrum for the native RNase A peptide ^{131}HIIVACEGNPY^{141}.

RNase A Proteolytic Peptides: Cysteic Acid Toward the C-terminus

Figure 30 contains the negative ion tandem mass spectra of three RNase A proteolytic peptides that contain the cysteic acid near the C-terminus. The peptide $^{88}NVAC_{ox}K^{92}$ fragments to produce primarily *y*-type fragment ions (y_1, y_2, y_3, y_3-17, and y_4-17) with the negative charge maintained toward the C-terminus (Figure 30a). We suspect that the lysine and cysteic acid side chains are interacting with one another to prevent *v*- or *w*-type side-chain fragment ions. Similarly, the CID spectra of [M – H]- ions of $^{106}SITDC_{ox}R^{111}$ results in several *y*-type fragment ions (y_2, y_3, and y_3-17) (Figure 30b). Note the enhanced ion signal observed for y_2 fragment ions, corresponding to cleavage between the cysteic acid and aspartic acid residues, similar to fragmentation previously reported.[126-128] Side-chain loss occurs when the C-terminal amino acid is replaced with tyrosine. For example, w_3 and w_5 fragment ions are observed in the negative ion tandem mass spectrum of $^{93}NGQTNC_{ox}Y^{99}$, corresponding to the side-chain losses of asparagine and glutamine, respectively (Figure 30c). Note that these side-chain fragment ions occur without the interaction between basic side chains and cysteic acid. The v_4 ion for the full side chain loss of threonine is also observed at low relative abundance at m/z 500.37. Additionally, neither *v*- nor *w*-type side-chain cleavage fragment ions are observed in the negative ion tandem mass spectrum of native $^{93}NGQTNCY^{99}$ (See Figure 31). Further investigation of peptides with a C-terminal cysteic acid is currently underway.

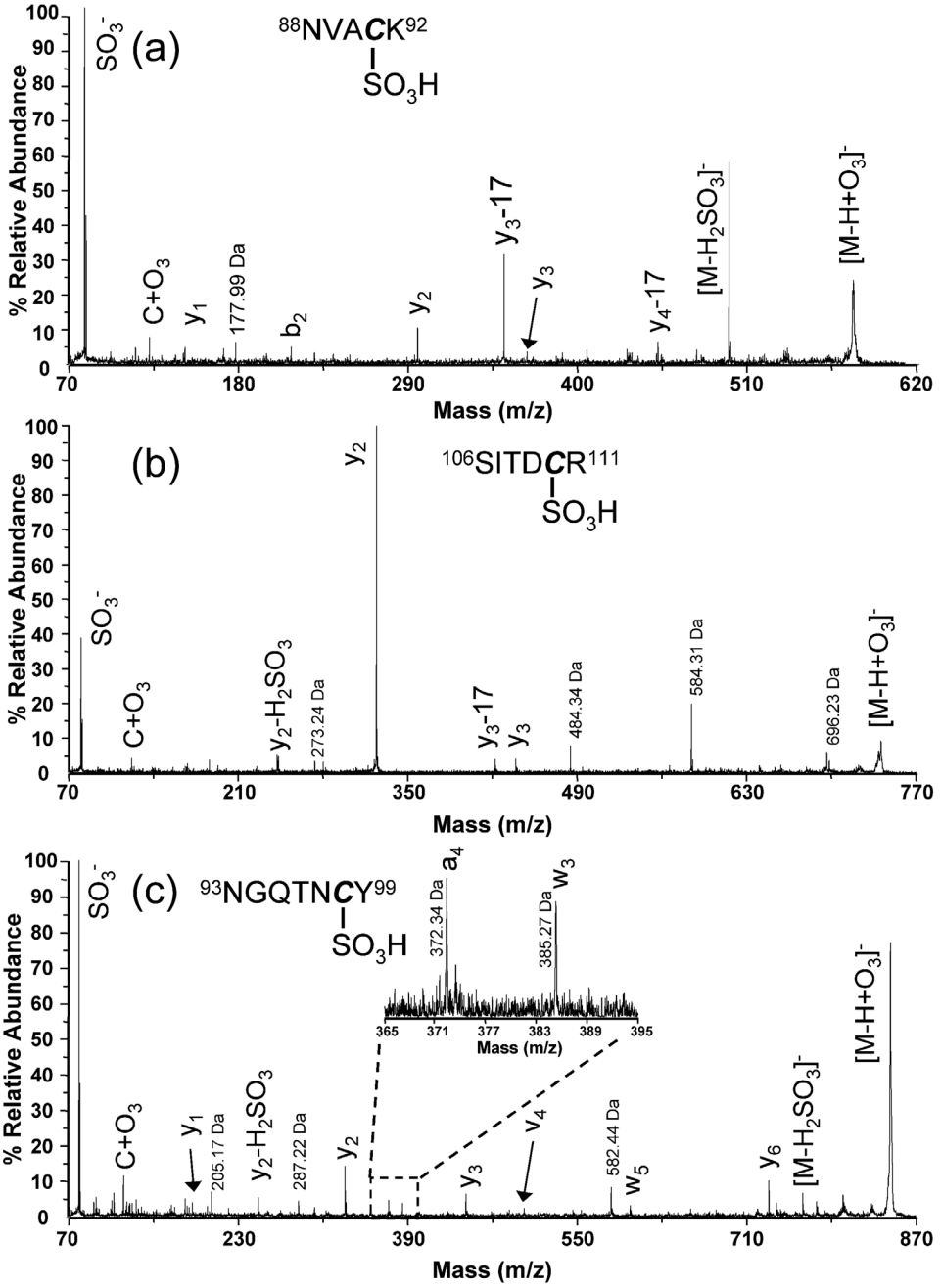

Figure 30. Typical negative ion tandem mass spectra for oxidized RNase A proteolytic peptides that contain the cysteic acid side chain near the C-terminus of the peptide. (a) $^{88}NVAC_{ox}K^{92}$, (b) $^{106}SITDC_{ox}R^{111}$, and (c) $^{93}NGQTNC_{ox}Y^{99}$. Inset figure: expanded view of mass range 365-395 m/z illustrating that two fragment ions a_4 and w_3 are present.

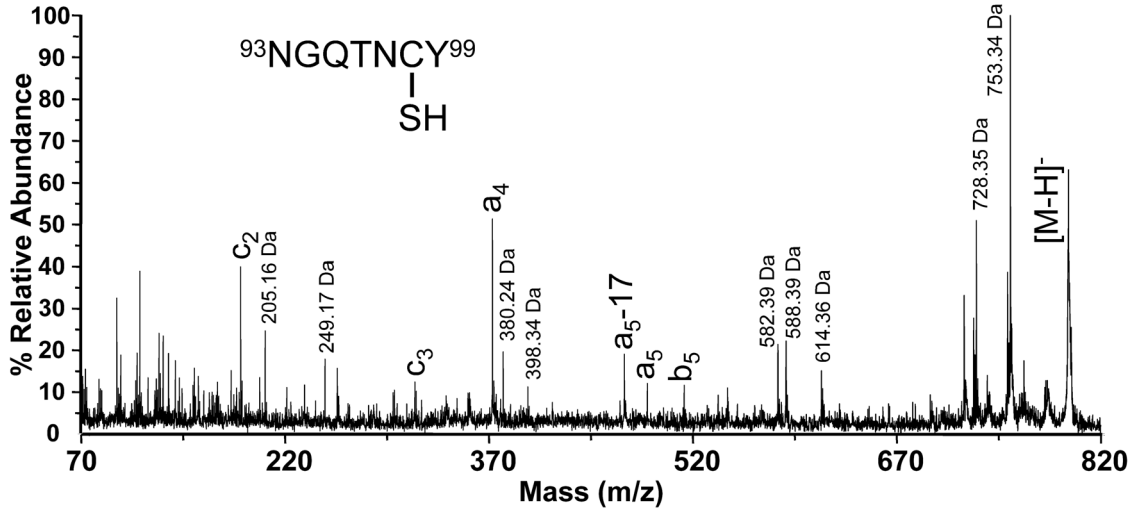

Figure 31. Negative ion tandem mass spectrum for the native RNase A peptide ^{93}NGQTNCY^{99}.

Conclusion

Near complete series of *d*-type fragment ions were observed in the negative ion tandem mass spectra for peptides containing an N-terminal cysteic acid and the side chain must require a cleavable β-γ carbon-carbon bond. The cysteic acid at the N-terminus is suspected to be interacting with the amino acid side chains to promote *d*-type ion formation. As the cysteic acid position moves toward the center of the peptide, *d*-type fragment ions are still formed, given that the amino acid side chain C-terminal to the cysteic acid contains a cleavable β-γ carbon-carbon bond. When the cysteic acid is near the C-terminus of the peptide *w*-type fragment ions are observed; however, they are in low abundance compared to the distinct *d*-type fragment ion series.

CHAPTER VI

ELUCIDATION OF DISULFIDE-LINKED PEPTIDES VIA CAPILLARY ELECTROPHORESIS – MASS SPECTROMETRY

Introduction

Disulfide bonds are among the most frequent post-translational protein modification and their primary function is to maintain and stabilize the native protein structure.[49-51] Through the proper assignment of disulfide bonds we hope to gain further understanding of protein folding and therefore biological function.[53, 54, 129] However, correctly establishing the native disulfide bond patterns in proteins still remains challenging.[51, 130] Proteolytic digestion conditions must be carefully pH and temperature controlled to prevent undesired disulfide scrambling.[51] Disulfide-containing proteins cannot undergo thermal denaturation at high temperatures (90˚C) because this results in severe disulfide scrambling which gives a false indication of the native disulfide bond pattern. Mildly acidic (pH 6) buffer solutions without thermal denaturation can minimize the disulfide bond scrambling during the digestion of bovine ribonuclease A.[56] Another challenge during proteolytic digestion is the inaccessibility of the protease to cleave the protein when buried disulfide bonds are not solvent exposed.[53, 54] Dual enzyme digestion schemes (*e.g.,* trypsin followed by chymotrypsin)[56] or alternative proteases (*e.g.,* pepsin, Endoproteinase AspN, Endoproteinase LysC, etc.) could help improve the digestion efficiency.

Several mass spectrometry (MS)-based detection schemes have been reported for disulfide bond detection/identification including: tandem MS,[57, 58] database search algorithms,[56, 59-61] chemical reduction,[55, 62, 63] chemical oxidation,[46, 47, 64] metal ion cleavage of disulfide-bonds,[65, 66] and recently gas-phase scrambling of disulfide bonds.[67] High-performance liquid chromatography (HPLC) combined with either matrix-assisted laser desorption ionization (MALDI) and electrospray ionization (ESI) have been widely used for protein identification and disulfide mapping.[47, 56, 131] For example, Xu and coworkers combine nanospray LC-MS/MS with a database search algorithm to confirm disulfide bonds from bovine Ribonuclease A (RNase A) under varied digestion conditions.[56] However, these fragmentation spectra can be complicated by gas-phase disulfide bond cleavage between inter-linked disulfide peptides, which results in a limited number of sequence-informative fragment ions from each α and β-chain peptide forming the disulfide linkage.[57] Schnaible *et al.* developed a screening method for disulfide bonds based on LC pre-fractionation combined with post-source decay of the disulfide bond to produce two peptide chains that form the inter-linked disulfide bond.[131] This approach enables disulfide bonds from bovine serum albumin and RNase A to be elucidated through working backwards to calculate the intact disulfide-linked peptide masses.

We introduced an on-target performic acid oxidation method that can rapidly oxidize disulfide-containing peptides directly on the MALDI sample deposits.[48] The possibility of disulfide-bond elucidation from a single MALDI deposit was shown for a bovine Ribonuclease A proteolytic digest. However, the extreme mass spectral

congestion resulting after on-target oxidation makes disulfide bond elucidation difficult for complex mixtures. Therefore, pre-fractionation prior to MS would drastically decrease the mass spectral complexity after on-target oxidation to allow more straightforward disulfide bond elucidation.

Capillary electrophoresis (CE) combined with MS has not been extensively used for proteomics studies when compared to LC-MS. Nonetheless, several researchers have shown that CE-MS is successful towards mapping complex proteomic mixtures.[19-24] For example, we showed that distinct charge-state trends occur in 2D plots of log (μ^{eff}) versus log (MW) (measured by MALDI-MS) for standard protein proteolytic digests and *E. coli* derived peptide fractions.[19] The charge-state trends directly correlate with the number of basic amino acid residues (Arg, Lys, His) present within the peptide, thus providing additional information to aid in the confidence of protein identification. For example, tryptic peptides along the +3 charge-state trendline have two basic amino acid residues and an N-terminal charge. Inter-linked disulfide bridged tryptic peptides would exist a high charge states (*i.e.,* +3 or +4 charge state) owing to charge contribution from each peptide forming the disulfide linkage. Therefore, these highly charged peptides are probable candidates to contain disulfide bonds. This information combined with the high-throughput on-target oxidation method will enable CE separations to be interrogated for disulfide-linked peptides. Following on-target oxidation, the highly probable candidate disulfide-linked peptides will exhibit enhanced negative ion signals for oxidized cysteine-containing peptides that are a result of oxidative cleavage of intact disulfide-linked peptides.

This report describes an alternative method for disulfide bond elucidation using on-target oxidation combined with CE-MS. On-target oxidation provides chemical selectivity towards oxidizing disulfide-linked peptides separated by CE to reduce the overall mass spectral complexity prior to MS and oxidation. The MALDI sample deposits containing enhanced negative ion signals are probable candidate disulfide-linked peptides. These oxidized cysteine-containing peptides can then be subjected to tandem MS for amino acid sequence determination. The utility of this CE-MS disulfide elucidation scheme is shown for a bovine Ribonuclease A proteolytic digest.

Experimental

Chemicals

Bradykinin (2-9) (PPGFSPFR), adrenocorticotropic hormone (ACTH) (18-39) (RPVKVYPNGAEDESAEAFPLEF), bovine ribonuclease A, α-cyano-4-hydroxycinnamic acid (CHCA), dihydrogen ammonium phosphate ($NH_4H_2PO_4$), ammonium bicarbonate (NH_4HCO_3), and mass spectrometry grade trypsin were purchased from Sigma (St. Louis, MO). HPLC grade methanol (CH_3OH), isopropanol, and acetone were purchased from EMD Chemicals Inc. (Gibbstown, NJ). Hydrogen peroxide (35% w/w) and formic acid (99% w/w) were purchased from Acros Organics (Morris Plains, NJ). All experiments were performed with 18MΩ water (ddH_2O) purified using a purification unit from Barnstead International (Dubuque, IA). All chemicals were used as received without further purification.

Standard Protein Proteolytic Digestion

Bovine ribonuclease A (RNaseA) was prepared at 1 mg mL^{-1} in 2.5 mM histidine (pH 7.1). Ribonuclease A was digested using a dual protease scheme similar to described previously.[48] Briefly, a 100 µL aliquot of the RNaseA stock solution was digested in 2.5 mM histidine buffer similar to as previously described.[132] Trypsin (0.1 µg μL^{-1}) prepared in ddH_2O was added at a 1:50 enzyme: protein ratio and incubated at 37˚C for 4 hrs. Subsequently, chymotrypsin (0.1 µg μL^{-1}) was added at a 1:50 enzyme: protein ratio and allowed to digest overnight at 37˚C. Following proteolytic digestion the RNase A digest was alkylated with 2-iodoacetamide (IAA) (100 mM prepared in ddH_2O) at a final concentration of 5 mM IAA and incubated at room temperature for 45 min in the dark.

MALDI Matrix Preparation

A layer of 5-mg mL^{-1} CHCA was applied prior to the CE separations using an x-y-z translation stage (ProBot, LC Packings, Sunnyvale, CA). CHCA was dissolved in 12:7:1 MeOH:ddH_20:IPA with 10-mM dihydrogen ammonium phosphate and doped with 50-fmol μL^{-1} bradykinin fragment 2-9 and 100-fmol μL^{-1} ACTH fragment 18-39 as internal calibrants. Dihydrogen ammonium phosphate was added according to a modified matrix preparation procedure by Smirnov and coworkers.[89] The CHCA matrix solution was infused through a fused-silica capillary at 1.0 µL min^{-1} with a 5 second spotting interval to prepare a 30 row by 30 column array (900 total spots). MALDI plates were used for CE fraction collection using the sheath liquid mentioned in the CE-MALDI section as the overlayer.[90]

CE-MALDI

CE separations were carried out on a 70-cm (50 μm i.d., 360 μm o.d.) fused-silica capillary (Polymicro Technologies, Phoenix, AZ) with 200-nm UV detection at 50 cm on a homebuilt apparatus. The cathodic end capillary tip was interfaced to a ProBot (LC Packings, Sunnyvalve, CA) as previously described.[19] The CE capillary was coated with a neutral linear polyacrylamide dynamic coating (Ultratrol LN, Target Discovery, Palo Alto, CA). The background electrolyte consisted of 250-mM FA at pH 2.20. Pressurized injections were performed at 2.0 psi for 20 seconds corresponding to a 60 nL injection volume. Separations were performed at a potential of +25 kV, using a 30-kV high-voltage power supply (Gamma High-Voltage Research, Ormond Beach, FL). UV electropherograms were collected using a homebuilt virtual instrument interface in the LabView 7.1 (National Instruments, Austin, TX) environment. CE fractions were collected using the ProBot with 10 second spotting intervals.

On-Target Performic Acid Oxidation of CE-MS Separations

Performic acid was prepared as previously described.[48] Briefly, hydrogen peroxide (35% w/w) and formic acid (99% w/w) were mixed at a 1:9 ratio respectively and allowed to age at room temperature for 2 hr. The performic acid was stored in a -20˚C freezer prior to use. On-target performic acid oxidation was performed with a 40 μL volume of a 1:1 mixture of acetone: performic acid placed directly on the MALDI target in a region that does not contain sample. The MALDI target was then placed in a

petri dish and incubated at +25˚C for 30 min. Following on-target oxidation the MALDI plate was subjected to MALDI analysis without sample cleanup.

MALDI-MS and MALDI-MS/MS

All MALDI-MS experiments were performed using a 4700 Proteomics Analyzer MALDI-TOF/TOF (Applied Biosystems, Framingham, MA). The MALDI-MS data were acquired using the reflectron detector in both positive and negative ion modes (500-4500 Da, 2100 Da focus mass) using 800 laser shots with internal calibration. Positive ion collision-induced dissociation (CID) tandem MS spectra were acquired using 10-20% greater laser power than the MS spectra acquisition with atmosphere (medium pressure) as the collision gas with 1 kV of collision energy.

Results and Discussion

The initial motivation for the on-target oxidation method was to develop methodologies to separate complex mixtures of proteolytic peptides and be able to readily distinguish disulfide-linked peptides from those that are unmodified proteolytic peptides. As illustrated in the negative ion mass spectrum of the Ribonuclease A (RNase A) proteolytic digest after on-target oxidation (Figure 12, Chapter III), there are several oxidized peptide ion signals that convolute the mass spectrum. Hence, the motivation to first pre-fractionate the proteolytic digest via capillary electrophoresis (CE) or liquid chromatography (LC) prior to MS analysis. Scheme 7 contains the overall experimental design for disulfide elucidation using CE-MS followed by on-target oxidation. First the

CE-MS separation would be acquired in positive and negative ion modes to obtain the mass spectra before oxidation. Second, the entire CE-MS separation would be subjected to on-target oxidation. For this hypothetical example, the inter-linked disulfide bridged peptide would be cleaved through oxidative cleavage to convert each α- and β-chain to their cysteic acid (SO_3H) modified form. These cysteic acid-containing peptides can be submitted to tandem MS analysis in either positive or negative ion mode for amino acid sequence determination. The disulfide-linked peptide then can be elucidated by back-calculating the mass of an inter-linked disulfide bridged peptide containing these two α- and β-chains. This experimental scheme using CE-MS combined with on-target oxidation is demonstrated for a proteolytic digest of bovine RNase A.

Scheme 7. Experimental design for disulfide elucidation using CE-MS followed by on-target oxidation.

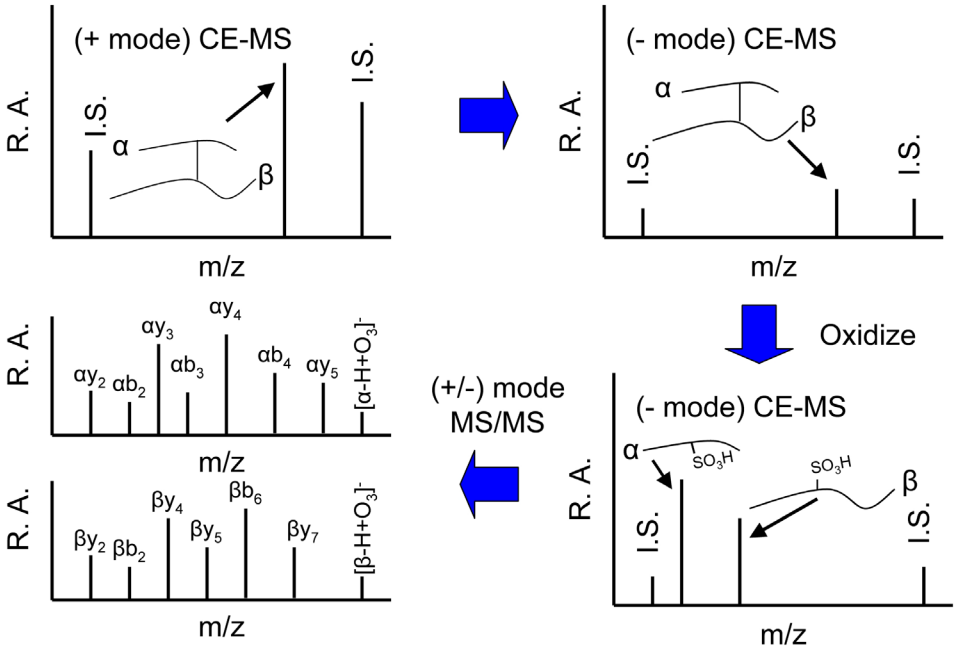

RNase A contains four native disulfide bonds, three disulfide bonds are inter-linked and the remaining disulfide bond is intra-linked.[46, 56, 69] Our experimental design for CE-MS involves performing proteolytic digestion in neutral conditions (histidine buffer, pH 7) to minimize disulfide scrambling combined with 2-iodoacetamide alkylation chemistry to protect the free-cysteine residues (*i.e.,* disulfide-linked peptides that may become reduced during digestion) from oxidation. The low conductivity of the histidine buffer was desired to perform large-volume sample stacking, similar to those previously reported.[33, 34] The low conductivity of the histidine sample plug causes the field strength (V/cm) to drastically increase which causes the positive ions to rapidly stack as a narrow band at the sample plug / background electrolyte interface.[27, 33] Once the positive ions reach the electrophoresis buffer they continue to migrate according to their size-to-charge ratio. This sample stacking technique improves the sample injection volume *ca.* 10-fold as opposed to traditional CE injection volumes (*i.e.,* $\leq$ 1% of the total capillary length).[25] Figure 32 contains a typical CE-UV electropherogram of the RNase A trypsin/chymotrypsin + 2-iodoacetamide proteolytic digest. The leading histidine peak occurs around 6.25 min (μ^{obs} = 37.3 x 10^{-5} cm^2/V s) followed by the stacked RNase A proteolytic peptides and the μ^{eo} for this particular run was 8.31 x 10^{-5} cm^2/V s.

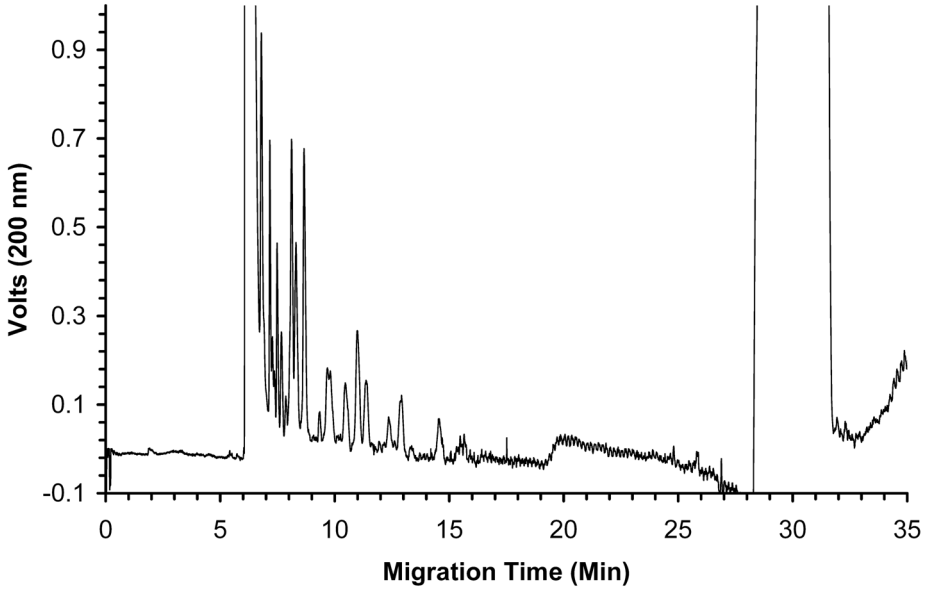

Figure 32. CE-UV electropherogram of the RNase A proteolytic digest performed in 2.5 mM histidine buffer. CE conditions: 50/70 cm x 50 μm i.d. UltraTrol LN coated capillary; +25 kV potential; 2.0 psi for 20 sec (60 nL) hydrodynamic injection; electrolyte: 250 mM formic acid (pH 2.2).

Figure 33 contains a CE-MS plot of log (μ^{eff}) versus log (MW) for the RNase A trypsin/chymotrypsin digestion mixture. The effective electrophoretic mobility for each peptide is calculated by subtracting the μ^{eo} from the observed electrophoretic mobility (μ^{obs}). The peptide molecular weights correspond to the $[M + H]^+$ value observed in the MALDI-MS data. Take notice that distinct charge-state trends are observed in these data, as we previously reported.[19] The basic amino acid residues (Arg, His, and Lys) and the N-terminus are protonated under the electrophoretic conditions (pH 2.2) of the

experiment. The highly-charged peptides either contain missed cleavages from the trypsin digestion or they could be disulfide-linked peptides. For example, a disulfide-linked peptide with an inter-linked disulfide bond would be +3 or +4 depending on the number of basic amino acid residues within each peptide chain forming the disulfide bridge. Therefore, the peptides along these high charge state trends are probable candidates to contain disulfide bonds. The charge state information is very helpful to narrow down the number of candidate disulfide-linked peptides from a complex mixture. The on-target oxidation method applied to the entire CE-MS separation should provide chemical selectivity to drastically decrease the number of candidates. The performic acid oxidation selectively cleaves the disulfide bond to create two new peptides each containing a cysteic acid which results in a 48 Da mass shift and enhanced negative ion formation. The candidate disulfide-linked peptides that have enhanced negative ion signals present in the negative ion mass spectra are denoted in Figure 33 with open diamonds (◊). Two peptides are alphabetically labeled to later illustrate the typical negative ion mass spectra before and after on-target oxidation.

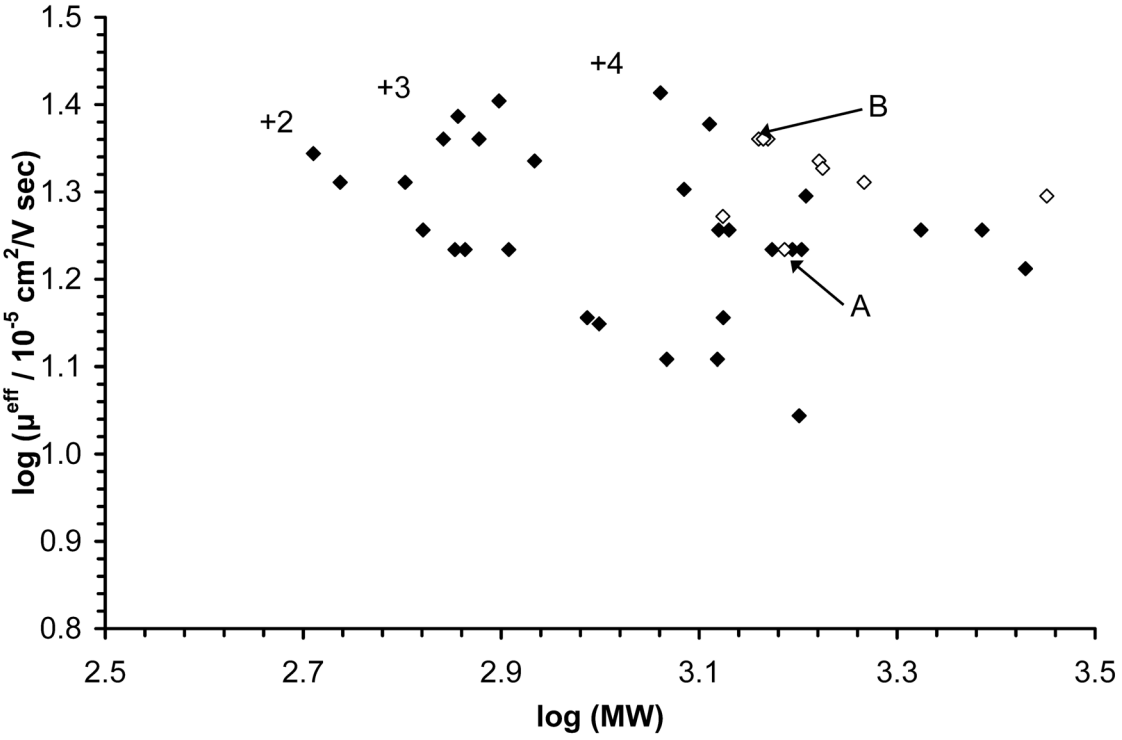

Figure 33. CE-MS plot of log (μ^{eff}) versus log (MW) for the RNase A trypsin/chymotrypsin digest + 2-iodoacetamide. The black diamonds (♦) represent proteolytic peptides derived from RNase A and the open diamonds (◊) represent candidate disulfide-linked peptides.

Figure 34 contains typical negative ion mass spectra (a) before and (b) after on-target oxidation of a single CE-MS fraction at 13.67 min (denoted as A in Figure 33). The negative ion mass spectrum prior to oxidation contains a single ion signal at m/z 1533.63 (S/N 159) and the internal calibrants bradykinin (2-9) and ACTH (18-39). Following on-target oxidation, the abundance of the m/z 1533.63 ion signal drastically decreases (S/N 23) which indicates this peptide has undergone oxidative cleavage to produce to new oxidized peptides. These oxidized peptides correspond to $^{118}YPNC_{ox}AY^{123}$ (m/z 776.26, S/N 784) and $^{66}C_{ox}KPVNTF^{72}$ (m/z 854.38, S/N 644) from RNase A. Note the enhanced negative ion signal of these two oxidized peptides compared to the abundance of the intact disulfide-linked peptide ion signal at m/z 1533.63. The increased acidity of the cysteic acid group drastically improves the ionization efficiency of the negative ions. Adding together the non-oxidized peptide masses and accounting for an inter-linked disulfide bond results in a $[M - H]^-_{calc}$ = 1533.65 Da which corresponds to a native disulfide linkage between Cys^{66} and Cys^{121} ($^{118}YPNCAY^{123}$ / $^{66}CKPVNTF^{72}$). The CE separation prior to MS analysis simplifies the mass spectrum before on-target oxidation to enable straightforward disulfide bond elucidation when compared to the on-target oxidation of the entire RNase A proteolytic digest.

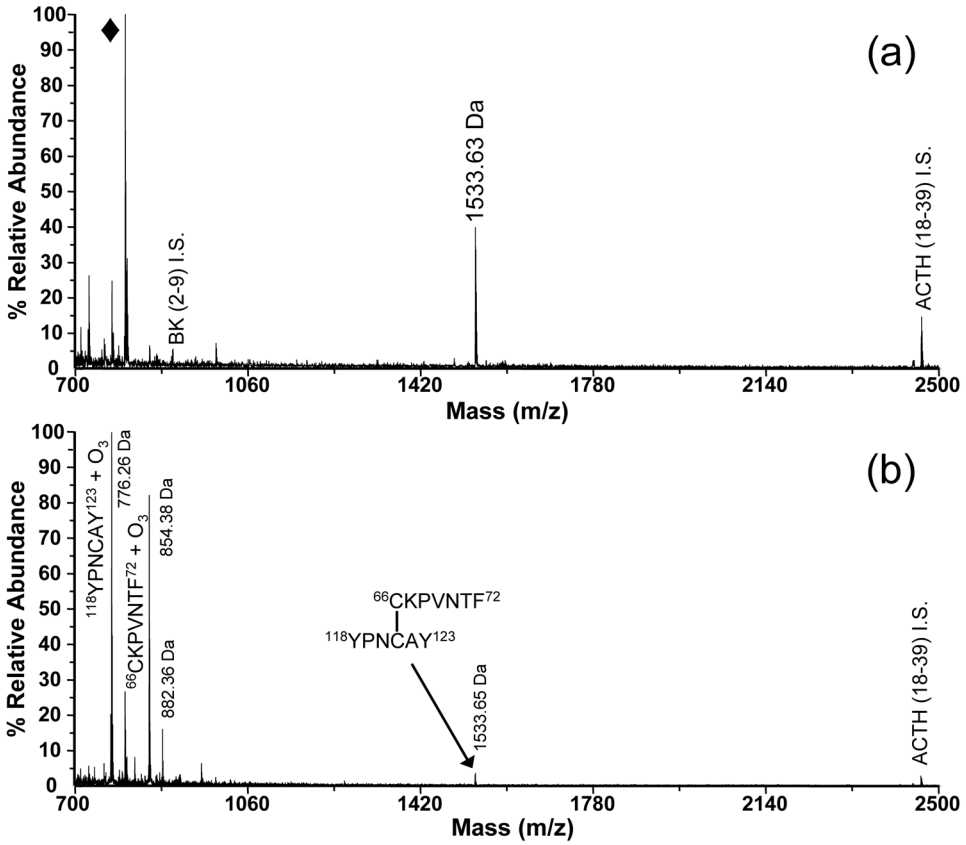

Figure 34. Typical negative ion mass spectra of a single CE-MS fraction (13.67 min) acquired (a) before and (b) after on-target oxidation. The candidate disulfide-linked peptide corresponds to ^{66}CKPVNTF^{72} / ^{118}YPNCAY^{123} ($[M-H]^-_{calc}$ = 1533.65 Da).

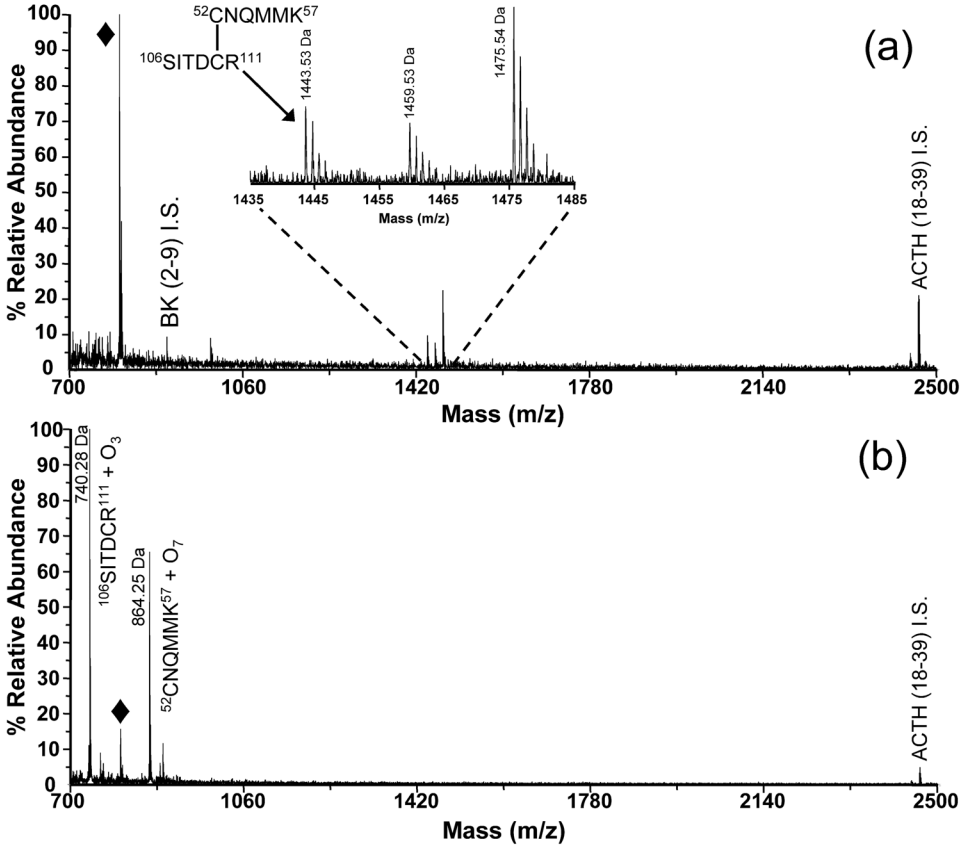

Figure 35. Typical negative ion mass spectra of a single CE-MS fraction (11.00 min) acquired (a) before and (b) after on-target oxidation. The candidate disulfide-linked peptide corresponds to ^{52}CNQMMK^{57} / ^{106}SITDCR^{111} ([M-H]$^-_{calc}$ = 1443.58 Da).

Figure 35 contains the negative ion mass spectra (a) before and (b) after on-target oxidation of a candidate disulfide-linked peptide with a migration time of 11.00 min (denoted as B in Figure 33). Note the low abundance of the $[M - H]^-$ ion (m/z 1443.53) and oxidized methionine forms of this peptide $[M - H + O]^-$ and $[M - H + O_2]^-$ at m/z 1459.53 and m/z 1475.54, respectively. These methionine residues become oxidized either in-solution during proteolytic digestion or when exposed to ambient air on the MALDI target. After on-target oxidation, these ion signals diminish to form two new oxidized peptides $^{106}SITDC_{ox}R^{111}$ (m/z 740.28, S/N 798) and $^{52}C_{ox}NQ\boldsymbol{MM}K^{57}$ (m/z 864.25, S/N 526). As we have previously shown, the methionine side chains also become fully oxidized, *i.e.,* incorporating two oxygen atoms per methionine residue (denoted in ***bold italics***).[48] Despite having several oxidized forms of the intact disulfide-linked peptide present, there are only two predominant products produced from on-target oxidation. Therefore, we are able to elucidate these peptides as the native disulfide linkage between Cys^{52} and Cys^{110} ($^{52}CNQMMK^{57}$ / $^{106}SITDCR^{111}$) with several oxidized methionine variations present.

In our previous work with on-target oxidation of RNase A proteolytic peptides we evaluated the effect of the cysteic acid position on the negative ion fragmentation of cysteic acid-containing peptides (See Chapter V). In brief, we showed that side chain loss fragment ions readily occur for peptides that contain an N-terminal cysteic acid. Similar fragment ion types are observed (*b*- and *y*-type fragment ions) in the negative ion fragmentation spectra and the peptide can be successfully sequenced; however, these side chain loss fragment ions make these fragmentation spectra not as widely accepted as the positive ion peptide fragmentation nomenclature.[122, 123] Therefore, for the CE-MS combined with on-target oxidation workflow we have decided to acquire the positive ion fragmentation spectra owing to the ease of interpretation. Figure 36 contains representative positive ion fragmentation spectra for (a) $^{52}C_{ox}NQ\boldsymbol{MM}K^{57}$ and (b) $^{106}SITDC_{ox}R^{111}$. These oxidized peptides were fragmented from the CE-MALDI sample deposit at 11.00 min. Distinct *y*-type fragment ion series are present for both oxidized peptides which enables rather straightforward peptide amino acid sequencing.

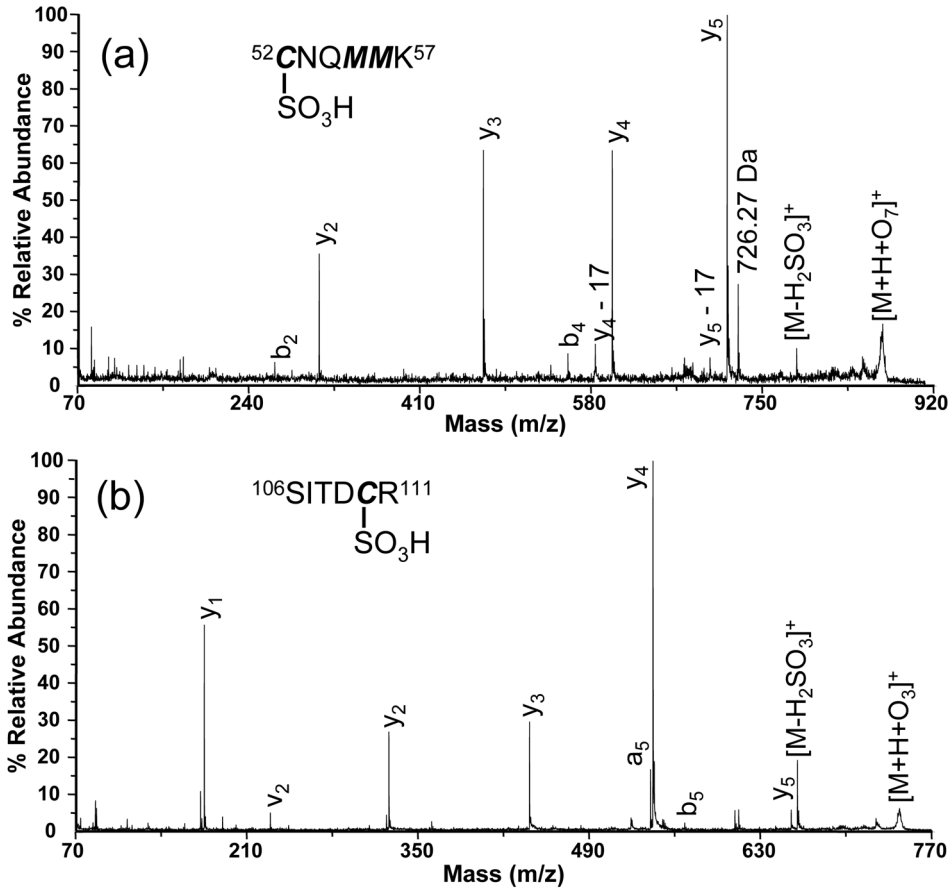

Figure 36. Positive ion fragmentation spectra of the oxidized versions of (a) $^{52}C_{ox}NQ\boldsymbol{MM}K^{57}$ and (b) $^{106}SITDC_{ox}R^{111}$ acquired from a single oxidized CE-MS fraction at 11.00 min.

Table 4 contains a summary of the confirmed cysteic acid-containing peptides detected in the negative ion mode throughout the entire RNase A proteolytic digest CE-MS separation. Note that some of the oxidized peptides are repeated because they are involved in disulfide bridging in another disulfide-linked peptides formed from a different proteolytic cleavage site. For example, the RNase A oxidized peptide $^{106}SITDC_{ox}R^{111}$ (m/z 740.27) is observed at a migration time of 11.00 and 13.17 min.

This peptide is involved in two disulfide-linked peptides: ^{52}CNQMMK^{57} / ^{106}SITDCR^{111} ($[M + H]^+_{obs}$ = 1445.59 Da) and ^{52}CNQMM^{56} / ^{106}SITDCR^{111} ($[M + H]^+_{obs}$ = 1317.49 Da) both corresponding to the native disulfide bridge from Cys^{52} – Cys^{110}. The disulfide-linked peptide at m/z 1317.49 has a longer migration time 13.17 min (μ^{eff} = 18.0 x 10^{-5} cm^2/V s) owing to the decrease in charge state from a +4 to +3 peptide. This list of oxidized RNase A proteolytic peptides can also be used to generate a list of candidate inter-linked disulfide bridged peptides, similar to the table presented in Figure 11b in Chapter III. From this list of candidate disulfide-linked peptides the calculated masses can be matched from those $[M + H]^+$ ions observed in the positive ion CE-MS data. Twelve native disulfide-linked peptides accounting for each disulfide bond in RNase A are summarized in Table 5. One major limitation of the CE-MS combined with on-target oxidation is illustrated by the disulfide-linked peptide at m/z 1161.49 (^{121}CAY^{123} / ^{66}CKPVNTF^{72}) which would result in an oxidized peptide below the typical mass range of interest for MALDI because of matrix clusters below m/z 500. Therefore, this assignment is uncertain because the oxidized peptide $^{121}C_{ox}AY^{123}$ ($[M - H + O_3]^-_{calc}$ = 402.09 Da) was not detected in the negative ion mass spectrum. Overall, the pre-fractionation step with CE provides simplified mass spectra prior to on-target oxidation to enable disulfide bond elucidation from the model protein RNase A.

Table 4. Summary of Oxidized RNase A Proteolytic Peptides Identified from the On-Target Oxidation of an Entire CE-MS Separation

Spot Label	t_m	$[M-H]^-_{obs}$	Peptide Sequence	S/N	$\log(\mu^{eff})$	log(MW)
	min				10^{-5} cm^2/V sec	
G23	10.67	854.371	(R)^{66}***C***KPVNTF^{72}(V) + O_3	41	1.378	2.932
G25	11.00	740.281	(M)^{106}SITD***C***R^{111}(E) + O_3	528	1.361	2.869
G25	11.00	864.248	(Y)^{52}***C***NQ***MM***K^{57}(S) + O_7	403	1.361	2.937
G28	11.50	904.350	(K)^{118}YPN***C***AYK^{124}(T) + O_3	33	1.335	2.956
G29	11.67	511.167	(V)^{84}***C***SQK^{87}(N) + O_3	66	1.327	2.709
G30	11.83	854.359	(R)^{66}***C***KPVNTF^{72}(V) + O_3	42	1.319	2.932
H1	12.00	681.318	(Q)^{82}AV***C***SQK^{87}(N) + O_3	271	1.311	2.833
H1	12.00	1261.585	(K)^{131}HIIVA***C***EGNPY^{141}(V) + O_3	275	1.311	3.101
H3	12.33	1659.770	(F)^{73}VHESLADVQAV***C***SQK^{87}(N) + O_3	120	1.295	3.220
H6	12.83	580.229	(K)^{88}NVA***C***K^{92}(N) + O_3	227	1.272	2.764
H6	12.83	845.267	(K)^{93}NGQTN***C***Y^{99}(Q) + O_3	121	1.272	2.927
H6	12.83	573.113	(Y)^{52}***C***NQ***M***^{55}(M) + O_5	39	1.272	2.758
H7	13.00	606.251	(R)^{66}***C***KPVN^{70}(T) + O_3	52	1.264	2.783
H8	13.17	736.158	(Y)^{52}***C***NQ***MM***^{56}(K) + O_7	52	1.256	2.867
H8	13.17	740.274	(M)^{106}SITD***C***R^{111}(E) + O_3	105	1.256	2.869
H11	13.67	776.263	(K)^{118}YPN***C***AY^{123}(K) + O_3	485	1.234	2.890
H11	13.67	854.377	(R)^{66}***C***KPVNTF^{72}(V) + O_3	403	1.234	2.932
H22	15.50	580.235	(K)^{88}NVA***C***K^{92}(N) + O_3	81	1.156	2.764

Table 5. Summary of CE-MS Confirmed RNase A Disulfide-Linked Peptides

Spot Label	t_m	$[M+H]^+_{obs}$	Peptide Sequence	$\log(\mu^{eff})$	log(MW)
	min			10^{-5} cm^2/V sec	
G25	11.00	1445.589	(Y)^{52}**C**NQMMK^{57}(S) (M)^{106}SITD**C**R^{111}(E)	1.361	3.160
G25	11.00	1477.547	(Y)^{52}**C**NQmmK^{57}(S) (M)^{106}SITD**C**R^{111}(E)	1.361	3.170
G25	11.00	1461.570	(Y)^{52}**C**NQMmK^{57}(S) (M)^{106}SITD**C**R^{111}(E)	1.361	3.165
G28	11.50	1663.746	(R)^{66}**C**KPVNTF^{72}(V) (K)^{118}YPN**C**AYK^{124}(T)	1.335	3.221
G29	11.67	1677.750	(V)^{84}**C**SQK^{87}(N) (K)^{131}HIIVA**C**EGNPY^{141}(V)	1.327	3.225
H1	12.00	1847.853	(Q)^{82}AV**C**SQK^{87}(N) (K)^{131}HIIVA**C**EGNPY^{141}(V)	1.311	3.267
H3	12.33	2826.358	(K)^{131}HIIVA**C**EGNPY^{141}(V) (F)^{73}VHESLADVQAV**C**SQK^{87}(N)	1.295	3.451
H5	12.67	1161.495	(N)^{121}**C**AY^{123}(T) (R)^{66}**C**KPVNTF^{72}(V)	1.279	3.065
H6	12.83	1330.510	(K)^{88}NVA**C**K^{92}(N) (K)^{93}NGQTN**C**Y^{99}(Q)	1.272	3.124
H8	13.17	1317.494	(Y)^{52}**C**NQMM^{56}(K) (M)^{106}SITD**C**R^{111}(E)	1.256	3.120
H8	13.17	1349.448	(Y)^{52}**C**NQmm^{56}(K) (M)^{106}SITD**C**R^{111}(E)	1.256	3.130
H11	13.67	1535.648	(R)^{66}**C**KPVNTF^{72}(V) (K)^{118}YPN**C**AY^{123}(K)	1.234	3.186

Conclusion

The on-target oxidation method was combined with CE-MS to successfully elucidate disulfide bonds from a bovine RNase A proteolytic digest. The mass spectral complexity of the CE-MS fractions was decreased when compared to an entire proteolytic digestion mixture to enable simplified disulfide elucidation. A total of twelve RNase A disulfide-linked peptides accounting for all four native disulfide bonds were detected using this CE-MS detection scheme. The oxidized cysteine-containing peptides were subjected to positive ion tandem MS analysis owing to the ease of interpretation. The low conductivity of histidine buffer digestion directly enables sample stacking injections to improve the CE sample loading capacity. In the future we plan to combine this on-target oxidation methodology with LC-MALDI-MS to locate disulfide-linked peptides within more complex proteomic mixtures.

CHAPTER VII

CONCLUSIONS

Summary

An alternative method for disulfide bond elucidation using CE-MS combined with an on-target performic acid oxidation method was developed. The charge state information (*i.e.,* number of basic amino acid residues) provided in the 2D CE-MS plots has proven useful to enhance the confidence of peptide/protein identifications in the case of limited tandem MS data. The CE-MS charge-state trends also assist in the detection of post-translationally modified peptides. Specifically, α-casein derived proteolytic peptides containing a phosphorylation are observed in a lower charge state trendline, which greatly simplifies phosphopeptide detection and enables screening.

The information provided in the charge-state trends have also been applied to disulfide-linked peptide screening using CE-MS. The highly charged interlinked disulfide-containing peptides should be located along the +3, +4, or greater charge state trends, thus creating a candidate list of disulfide-linked peptides. However, the intralinked disulfide-containing peptides will not necessarily be highly charged peptides. Therefore, an on-target performic acid oxidation method was developed to provide chemical selectivity towards locating disulfide-containing peptides. The on-target oxidation method provides significant advantages over traditional solution-phase oxidation methods because of the decreased sample handling and reaction time. The on-target oxidation method can easily be adapted to simultaneously oxidize *ca.* 900 MALDI

sample deposits in 15 minutes. From the on-target oxidation of an entire CE-MS separation, the candidate list of disulfide-linked peptides can be further narrowed down based on observing enhanced negative ion signals after oxidation. After confirming these cysteic-containing peptides via tandem MS the disulfide-linked peptides can be elucidated. Interestingly, the negative ions of these cysteic acid-containing peptides fragment to produce side chain loss fragment ions (*d*-type fragment ions) when the cysteic acid is at the N-terminus. This on-target oxidation combined with CE-MS experimental scheme was applied to a proteolytic digest of bovine RNase A. Twelve RNase A disulfide-linked peptides accounting for all four native disulfide bonds were elucidated using this CE-MS detection scheme.

The experimental variables (*e.g.,* oxidation temperature, performic acid vapor exposure time, and MALDI matrix) associated with the on-target oxidation method were extensively evaluated to improve the oxidized peptide ion yield. Overall, the elevated temperature oxidation (+25˚C) does not have a detrimental effect on peptides that contain histidine, tryptophan, or tyrosine amino acid residues when CHCA is used during oxidation. Intact insulin can be successfully oxidized to form oxidized insulin α- and β-chains when 2,4-dihydroxyacetophenone (2,4-DHAP) is used during oxidation. The alternative matrix (crystal lattice) improves the accessibility of the performic acid vapor to oxidize insulin within the crystal lattice. Improved oxidized product yield was also observed for oxidized Cys-kemptide (C_{ox}LRRASLG) when using 2,4-DHAP or 3,5-dimethyl-4-hydroxycinnamic acid as the MALDI matrix during oxidation. In addition, the on-target oxidation was adapted towards oxidizing intact proteins followed by on-

target proteolytic digestion, both performed in the presence of the MALDI matrix. For example, the disulfide bonds of bovine pancreatic trypsin inhibitor were cleaved via oxidative cleavage to expose the trypsin cleavage sites which results in improved proteolytic digestion. On-target oxidation of intact proteins followed by on-target proteolytic digestion could easily be adapted to imaging mass spectrometry to improve the digestion efficiency of highly disulfide-linked proteins found within tissue sections.

REFERENCES

(1) Anderson, L.; Anderson, N. G. *Proc. Natl. Acad. Sci. U.S.A.* **1977**, *74*, 5421-5425.

(2) Anderson, N. L.; Anderson, N. G. *Electrophoresis* **1991**, *12*, 883-906.

(3) Henzel, W. J.; Billeci, T. M.; Stults, J. T.; Wong, S. C.; Grimley, C.; Watanabe, C. *Proc. Natl. Acad. Sci. U.S.A.* **1993**, *90*, 5011-5015.

(4) Pieper, R.; Gatlin, C. L.; Makusky, A. J.; Russo, P. S.; Schatz, C. R.; Miller, S. S.; Su, Q.; McGrath, A. M.; Estock, M. A.; Parmar, P. P.; Zhao, M.; Huang, S.-T.; Zhou, J.; Wang, F.; Esquer-Blasco, R.; Anderson, N. L.; Taylor, J.; Steiner, S. *Proteomics* **2003**, *3*, 1345-1364.

(5) Pappin, D. J.; Hojrup, P.; Bleasby, A. J. *Curr. Biol.* **1993**, *3*, 327-332.

(6) Mann, M.; Hojrup, P.; Roepstorff, P. *Biol. Mass Spectrom.* **1993**, *22*, 338-345.

(7) James, P.; Quadroni, M.; Carafoli, E.; Gonnet, G. *Biochem. Biophys. Res. Commun.* **1993**, *195*, 58-64.

(8) Yates, I., John. R.; Speicher, S.; Griffen, P. R.; Hunkapiller, T. *Anal. Biochem.* **1993**, *214*, 397-408.

(9) Shen, Y.; Smith, R. D. *Electrophoresis* **2002**, *23*, 3106-3124.

(10) Cooper, J. W.; Wang, Y.; Lee, C. S. *Electrophoresis* **2004**, *25*, 3913-3926.

(11) Eriksson, J.; Fenyö, D. *J. Proteome Res.* **2005**, *4*, 387-393

(12) Washburn, M. P.; Wolters, D.; Yates, J. R. *Nat. Biotechnol.* **2001**, *19*, 242-247.

(13) Conrads, T. P.; Anderson, G. A.; Veenstra, T. D.; Paša-Tolić, L.; Smith, R. D. *Anal. Chem.* **2000**, *72*, 3349-3354.

(14) Palmblad, M.; Ramström, M.; Markides, K. E.; Håkansson, P.; Bergquist, J. *Anal. Chem.* **2002**, *74*, 5826-5830.

(15) Strittmatter, E. F.; Ferguson, P. L.; Tang, K.; Smith, R. D. *J. Am. Soc. Mass Spectrom.* **2003**, *14*, 980-991.

(16) Palmblad, M.; Ramström, M.; Bailey, C. G.; McCutchen-Maloney, S. L.; Berquist, J.; Zeller, L. C. *J. Chromatogr., B* **2004**, *803*, 131-135.

(17) Krokhin, O. V.; Ying, S.; Cortens, J. P.; Ghosh, D.; Spicer, V.; Ens, W.; Standing, K. G.; Beavis, R. C.; Wilkins, J. A. *Anal. Chem.* **2006**, *78*, 6265-6269.

(18) Jaitly, N.; Monroe, M. E.; Petyuk, V. A.; Clauss, T. R. W.; Adkins, J. N.; Smith, R. D. *Anal. Chem.* **2006**, *78*, 8374-8385.

(19) Williams, B. J.; Russell, W. K.; Russell, D. H. *Anal. Chem.* **2007**, *79*, 3850-3855.

(20) Kaiser, T.; Hermann, A.; Kielstein, J. T.; Wittke, S.; Bartel, S.; Krebs, R.; Hausadel, F.; Hillmann, M.; Golovko, I.; Koester, P.; Haller, H.; Weissinger, E. M.; Fliser, D.; Mischak, H. *J. Chromatogr., A* **2003**, *1013*, 157-171.

(21) Kaiser, T.; Wittke, S.; Just, I.; Krebs, R.; Bartel, S.; Fliser, D.; Mischak, H.; Weissinger, E. M. *Electrophoresis* **2004**, *25*, 2044-2055.

(22) Theodorescu, D.; Fliser, D.; Wittke, S.; Mischak, H.; Krebs, R.; Walden, M.; Ross, M.; Eltze, E.; Bettendorf, O.; Wulfing, C.; Semjonow, A. *Electrophoresis* **2005**, *26*, 2797-2808.

(23) Wittke, S.; Fliser, D.; Haubitz, M.; Bartel, S.; Krebs, R.; Hausadel, F.; Hillmann, M.; Golovko, I.; Koester, P.; Haller, H.; Kaiser, T.; Mischak, H.; Weissinger, E. M. *J. Chromatogr., A* **2003**, *1013*, 173-181.

(24) Wittke, S.; Mischak, H.; Walden, M.; Kolch, W.; Rädler, T.; Wiedemann, K. *Electrophoresis* **2005**, *26*, 1476-1487.

(25) Oda, R. P.; Landers, J. P. In *Handbook of Capillary Electrophoresis*; Landers, J. P., Ed.; CRC Press: Boca Raton, FL, 1994, pp 25-28.

(26) Chien, R.-L.; Burgi, D. S. *J Chromatogr A* **1991**, *559*, 141-152.

(27) Chien, R.-L.; Helmer, J. C. *Anal. Chem.* **1991**, *63*, 1354-1361.

(28) Chen, Y. R.; Tseng, M. C.; Chang, Y. Z.; Her, G. R. *Anal. Chem.* **2003**, *75*, 503-508.

(29) Chien, R.-L.; Burgi, D. S. *Anal. Chem.* **1992**, *64*, 1046-1050.

(30) Mikkers, F. E. P.; Everaerts, F. M.; Peek, J. A. F. *J Chromatogr A* **1979**, *168*, 293-315.

(31) Stutz, H.; Bordin, G.; Rodriguez, A. R. *Electrophoresis* **2004**, *25*, 1071-1089.

(32) Shihabi, Z. K. *Electrophoresis* **2000**, *21*, 2872-2878.

(33) Burgi, D. S.; Chien, R.-L. *Anal. Chem.* **1991**, *63*, 2042-2047.

(34) Shihabi, Z. K. *J. Chromatogr., A* **2000**, *902*, 107-117.

(35) Jönsson, T. J.; Tsang, A. W.; Lowther, W. T.; Furdui, C. M. *J. Biol. Chem.* **2008**, *283*, 22890-22894.

(36) Ellis, H. R.; Poole, L. B. *Biochemistry* **1997**, *36*, 15013-15018.

(37) Saurin, A. T.; Neubert, H.; Brennan, J. P.; Eaton, P. *Proc. Natl. Acad. Sci. U.S.A.* **2004**, *101*, 17982-17987.

(38) Poole, L. B.; Karplus, A. P.; Claiborne, A. *Annu. Rev. Pharmacol. Toxicol.* **2004**, *44*, 325-347.

(39) Yarnell, A. *Chemical and Engineering News*, **2009**, 87, 38-40.

(40) Reddie, K. G.; Carroll, K. S. *Curr. Opin. Chem. Biol.* **2008**, *12*, 746-754.

(41) Leonard, S. E.; Reddie, K. G.; Carroll, K. S. *ACS Chem. Biol.* **2009**, *4*, 783-799.

(42) Seo, Y. H.; Carroll, K. S. *Proc. Natl. Acad. Sci. U.S.A.* **2009**, *106*, 16163-16168.

(43) Salsbury, F. R., Jr.; Knutson, S. T.; Poole, L. B.; Fetrow, J. *Protein Sci.* **2008**, *17*, 299-312.

(44) Burlet, O.; Yang, C.-Y.; Guyton, J. R.; Gaskell, S. J. *J. Am. Soc. Mass Spectrom.* **1995**, *6*, 242-247.

(45) Burlet, O.; Yang, C.-Y.; Gaskell, S. J. *J. Am. Soc. Mass Spectrom.* **1992**, *3*, 337-344.

(46) Sun, Y.; Smith, D. L. *Anal. Biochem.* **1988**, *172*, 130-138.

(47) Dai, J.; Wang, J.; Zhang, Y.; Lu, Z.; Yang, B.; Li, X.; Cai, Y.; Qian, X. *Anal. Chem.* **2005**, *77*, 7594-7604.

(48) Williams, B. J.; Russell, W. K.; Russell, D. H. *J. Mass Spectrom.* **2010**, *45*, 157-166.

(49) Pace, C. N.; Grimsley, G. R.; Thomson, J. A.; Barnett, B. J. *J. Biol. Chem.* **1988**, *263*, 11820-11825.

(50) Thornton, J. M. *J. Mol. Biol.* **1981**, *151*, 261-287.

(51) Gorman, J. J.; Wallis, T. P.; Pitt, J. J. *Mass Spectrom. Rev.* **2002**, *21*, 183-216.

(52) Yu, X.; Wu, Z.; Fenselau, C. *Biochemistry* **1995**, *34*, 3377-3385.

(53) Apuy, J. L.; Park, Z.-Y.; Swartz, P. D.; Dangott, L. J.; Russell, D. H.; Baldwin, T. O. *Biochemistry* **2001**, *40*, 15153-15163.

(54) Apuy, J. L.; Chen, X.; Russell, D. H.; Baldwin, T. O.; Giedroc, D. P. *Biochemistry* **2001**, *40*, 15164-15175.

(55) Morris, H. R.; Pucci, P. *Biochem. Biophys. Res. Commun.* **1985**, *126*, 1122-1128.

(56) Xu, H.; Zhang, L.; Freitas, M. A. *J. Proteome Res.* **2008**, *7*, 138-144.

(57) Bean, M. F.; Carr, S. A. *Anal. Biochem.* **1992**, *201*, 216-226.

(58) Patterson, S. D.; Katta, V. *Anal. Chem.* **1994**, *66*, 3727-2732.

(59) Craig, R.; Krokhin, O.; Wilkins, J.; Beavis, R. C. *J. Proteome Res.* **2003**, *2*, 657-661.

(60) Caporale, C.; Bertini, L.; Pucci, P.; Buonocore, V.; Caruso, C. *FEBS Lett.* **2005**, *579*, 3048-3054.

(61) Wefing, S.; Schnaible, V.; Hoffmann, D. *Anal. Chem.* **2006**, *78*, 1235-1241.

(62) Fukuyama, Y.; Iwamoto, S.; Tanaka, K. *J. Mass Spectrom.* **2006**, *41*, 191-201.

(63) Quinton, L.; Demeure, K.; Dobson, R.; Gilles, N.; Gabelica, V.; Pauw, E. D. *J. Proteome Res.* **2007**, *6*, 3216-3223.

(64) Thakur, S. S.; Balaram, P. *J. Am. Soc. Mass Spectrom.* **2008**, *19*, 358-366.

(65) Gunawardena, H. P.; O'Hair, R. A. J.; McLuckey, S. A. *J. Proteome Res.* **2006**, *5*, 2087-2092.

(66) Lioe, H.; Duan, M.; O'Hair, R. A. J. *Rapid Commun. Mass Spectrom.* **2007**, *21*, 2727-2733.

(67) Zhao, L.; Almaraz, R. T.; Xiang, F.; Hedrick, J. L.; Franz, A. H. *J. Am. Soc. Mass Spectrom.* **2009**, *20*, 1603-1616.

(68) Johnson, R. S.; Martin, S. A.; Biemann, K.; Stults, J. T.; Watson, J. T. *Anal. Chem.* **1987**, *59*, 2621-2625.

(69) Hirs, C. H. W. *Methods of Enzymology* **1967**, *11*, 197-199.

(70) Pesavento, J. J.; Garcia, B. A.; Streeky, J. A.; Kelleher, N. L.; Mizzen, C. A. *Mol. Cell. Proteomics* **2007**, *6*, 1510-1526.

(71) Lucas, J. E., Chemical Oxidation of Tryptic Digests to Improve Sequence Coverage in Peptide Mass Fingerprint Protein Identification, M.S. thesis, Texas A&M University, College Station, TX, 2003.

(72) Matthiesen, R.; Bauw, G.; Welinder, K. G. *Anal. Chem.* **2004**, *76*, 6848-6852.

(73) Gygi, S. P.; Rist, B.; Gerber, S. A.; Turecek, F.; Gelb, M. H.; Aebersold, R. *Nat. Biotechnol.* **1999**, *17*, 994-999.

(74) Fridriksson, E. K.; Beavil, A.; Holowka, D.; Gould, H. J.; Baird, B.; McLafferty, F. W. *Biochemistry* **2000**, *39*, 3369-3376.

(75) Florens, L.; Washburn, M. P.; Raine, J. D.; Anthony, R. M.; Grainger, M.; Haynes, J. D.; Moch, J. K.; Muster, N.; Sacci, J. B.; Tabb, D. L.; Witney, A. A.; Wolters, D.; Wu, Y.; Gardner, M. J.; Holder, A. A.; Sinden, R. E.; Yates, J. R.; Carucci, D. J. *Nature (London, U. K.)* **2002**, *419*, 520-526.

(76) Champion, M. M.; Campbell, C. S.; Siegele, D. A.; Russell, D. H.; Hu, J. C. *Mol. Microbiol.* **2003**, *47*, 383-396.

(77) Braunagel, S. C.; Russell, W. K.; Rosas-Acosta, G.; Russell, D. H.; Summers, M. D. *Proc. Natl. Acad. Sci. U.S.A.* **2003**, *100*, 9797-9802.

(78) Wolters, D.; Washburn, M. P.; Yates, J. R., III *Anal. Chem.* **2001**, *73*, 5683-5690.

(79) Dongré, A. R.; Eng, J. K.; Yates, J. R., III *Trends Biotechnol.* **1997**, *15*, 418-425.

(80) Shen, Y.; Smith, R. D.; Unger, K. K.; Kumar, D.; Lubda, D. *Anal. Chem.* **2005**, *77*, 6692-6701.

(81) Walker, K. L.; Chiu, R. W.; Monnig, C. A.; Wilkins, C. L. *Anal. Chem.* **1995**, *67*, 4197-4204.

(82) Nagra, D. S.; Li, L. *J. Chromatogr., A* **1995**, *711*, 235-245.

(83) Johnson, T.; Bergquist, J.; Ekman, R.; Nordhoff, E.; Schürenberg, M.; Klöppel, K.-D.; Müller, M.; Lehrach, H.; Gobom, J. *Anal. Chem.* **2001**, *73*, 1670-1675.

(84) Wall, D. B.; Berger, S. J.; Finch, J. W.; Cohen, S. A.; Richardson, K.; Chapman, R.; Drabble, D.; Brown, J.; Gostick, D. *Electrophoresis* **2002**, *23*, 3193-3204.

(85) Rosas-Acosta, G.; Russell, W. K.; Deyrieux, A.; Russell, D. H.; Wilson, V. G. *Mol. Cell. Proteomics* **2005**, *4*, 56-72.

(86) Williams, B. J.; Russell, W. K.; Russell, D. H. *Proceedings of the 54th American Society for Mass Spectrometry Conference on Mass Spectrometry an Allied Topics* **2006**, Seattle, WA, (June 2006).

(87) Offord, R. E. *Nature* **1966**, *211*, 591-593.

(88) Park, Z.-Y.; Russell, D. H. *Anal. Chem.* **2000**, *72*, 2667-2670.

(89) Smirnov, I. P.; Zhu, X.; Taylor, T.; Huang, Y.; Ross, P.; Papayanopoulos, I. A.; Martin, S. A.; Pappin, D. J. *Anal. Chem.* **2004**, *76*, 2958-2965.

(90) Edmondson, R. D.; Russell, D. H. *J. Am. Soc. Mass Spectrom.* **1996**, *7*, 995-1001.

(91) Koomen, J. M.; Russell, W. K.; Hettick, J. M.; Russell, D. H. *Anal. Chem.* **2000**, *72*, 3860-3866.

(92) Perkins, D. N.; Pappin, D. J.; Creasy, D. M.; Cottrell, J. S. *Electrophoresis* **1999**, *18*, 3551-3567.

(93) Adamson, N. J.; Reynolds, E. C. *J. Chromatogr., B: Anal. Technol. Biomed. Life Sci.* **1997**, *699*, 133-147.

(94) Cifuentes, A.; Poppe, H. *Electrophoresis* **1997**, *18*, 2362-2376.

(95) Castagnola, M.; Rossetti, D. V.; Corda, M.; Pellegrini, M.; Misiti, F.; Olianas, A.; Giardina, B.; Messana, I. *Electrophoresis* **1998**, *19*, 2273-2277.

(96) Janini, G. M.; Metral, C. J.; Issaq, H. J.; Muschik, G. M. *J. Chromatogr., A* **1999**, *848*, 417-433.

(97) Kim, J.; Zand, R.; Lubman, D. M. *Electrophoresis* **2002**, *23*, 782-793.

(98) Jalali-Heravi, M.; Shen, Y.; Hassanisadi, M.; Khaledi, M. G. *Electrophoresis* **2005**, *26*, 1874-1885.

(99) http://www.innovagen.se/custom-peptide-synthesis/peptide-property-calculator/peptide-property-calculator.asp., Accessed on 12/09/09.

(100) Zimmer, J. S. D.; Monroe, M. E.; Qian, W.-J.; Smith, R. D. *Mass Spectrom. Rev.* **2006**, *25*, 450-482.

(101) Brown, J. R.; Hartley, B. S. *Biochem. J.* **1966**, *101*, 214-228.

(102) Beavis, R. C.; Bridson, J. N. *J. Phys. D: Appl. Phys.* **1993**, *26*, 442-447.

(103) Williams, B. J.; Russell, W. K.; Russell, D. H. **2010**, *Manuscript in preparation*.

(104) Hamann, M.; Zhang, T.; Hendrich, S.; Thomas, J. A. *Methods Enzymol.* **2002**, *348*, 146-156.

(105) Horneffer, V.; Reichelt, R.; Strupat, K. *Int. J. Mass Spectrom.* **2003**, *226*, 117-131.

(106) Horneffer, V.; Forsmann, A.; Strupat, K.; Hillenkamp, F.; Kubitscheck, U. *Anal. Chem.* **2001**, *73*, 1016-1022.

(107) Horneffer, V.; Dreiswerd, K.; Lüdemann, H.-C.; Hillenkamp, F.; Läge, M.; Strupat, K. *Int. J. Mass Spectrom.* **1999**, *185-187*, 859-870.

(108) Groseclose, M. R.; Andersson, M.; Hardesty, W. M.; Caprioli, R. M. *J. Mass Spectrom.* **2007**, *42*, 254-262.

(109) Koomen, J. M.; Russell, D. H. *J. Mass Spectrom.* **2000**, *35*, 1025-1034.

(110) Qiao, L.; Roussel, C.; Wan, J.; Kong, J.; Yang, P.; Girault, H. H.; Liu, B. *Angew. Chem., Int. Ed. Engl.* **2008**, *47*, 2646-2648.

(111) Zimmerman, T. A.; Monroe, E. B.; Sweedler, J. V. *Proteomics* **2008**, *8*, 3809-3815.

(112) Bowie, J. H.; Brinkworth, C. S.; Dua, S. *Mass Spectrom. Rev.* **2002**, *21*, 87-107.

(113) Bilusich, D.; Bowie, J. H. *Mass Spectrom. Rev.* **2009**, *28*, 20-34.

(114) Huddleston, M. J.; Annan, R. S.; Bean, M. F.; Carr, S. A. *J. Am. Soc. Mass Spectrom.* **1993**, *4*, 710-717.

(115) Steen, H.; Küster, B.; Mann, M. *J. Mass Spectrom.* **2001**, *36*, 782-790.

(116) Edelson-Averbukh, M.; Pipkorn, R.; Lehmann, W. D. *Anal. Chem.* **2006**, *78*, 1249-1256.

(117) Bradford, A. M.; Waugh, R. J.; Bowie, J. H. *Rapid Commun. Mass Spectrom.* **1995**, *9*, 677-685.

(118) Summerfield, S. G.; Whiting, A.; Gaskell, S. J. *Int. J. Mass Spectrom. Ion Processes* **1997**, *162*, 149-161.

(119) Summerfield, S. G.; Cox, K. A.; Gaskell, S. J. *J. Am. Soc. Mass Spectrom.* **1997**, *8*, 25-31.

(120) Dongré, A. R.; Jones, J. L.; Somogyi, Á.; Wysocki, V. H. *J. Am. Chem. Soc.* **1996**, *118*, 8365-8374.

(121) Wang, D.; Kalb, S. R.; Cotter, R. J. *Rapid Commun. Mass Spectrom.* **2004**, *18*, 96-102.

(122) Roepstorff, P.; Fohlman, J. *Biol. Mass Spectrom.* **1984**, *11*, 601.

(123) Johnson, R. S.; Martin, S. A.; Biemann, K. *Int. J. Mass Spectrom. Ion Processes* **1988**, *86*, 137-154.

(124) Gevaert, K.; Demol, H.; Martens, L.; Hoorelbeke, B.; Puype, M.; Goethals, M.; Van Damme, J.; De Boeck, S.; Vandekerckhove, J. *Electrophoresis* **2001**, *22*, 1645-1651.

(125) Brinkworth, C. S.; Dua, S.; Bowie, J. H. *Rapid Commun. Mass Spectrom.* **2002** *16*, 713-721.

(126) Yu, W.; Vath, J. E.; Huberty, M. C.; Martin, S. A. *Anal. Chem.* **1993**, *65*, 3015-3023.

(127) Tsaprailis, G.; Nair, H.; Somogyi, Á.; Wysocki, V. H.; Zhong, W.; Futrell, J. H.; Summerfield, S. G.; Gaskell, S. J. *J. Am. Chem. Soc.* **1999**, *121*, 5142-5154.

(128) Gu, C.; Tsaprailis, G.; Breci, L. A.; Wysocki, V. H. *Anal. Chem.* **2000**, *72*, 5804-5813.

(129) Pitt, J. J.; Da Silva, E.; Gorman, J. J. *J. Biol. Chem.* **2000**, *275*, 6469-6478.

(130) Wallis, T. P.; Huang, C.-Y.; Nimkar, S. B.; Young, P. R.; Gorman, J. J. *J. Biol. Chem.* **2004**, *279*, 20729-20741.

(131) Schnaible, V.; Wefing, S.; Resemann, A.; Suckau, D.; Bücker, A.; Wolf-Kümmeth, S.; Hoffmann, D. *Anal. Chem.* **2002**, *74*, 4980-4988.

(132) Cologna, S. M.; Williams, B. J.; Russell, W. K.; Vigh, G.; Russell, D. H. *Electrophoresis* **2010**, *Manuscript in preparation*.

APPENDIX A

AMERICAN CHEMICAL SOCIETY LICENSE
TERMS AND CONDITIONS

Dec 14, 2009

This is a License Agreement between Brad J Williams ("You") and American Chemical Society ("American Chemical Society") provided by Copyright Clearance Center ("CCC"). The license consists of your order details, the terms and conditions provided by American Chemical Society, and the payment terms and conditions.

All payments must be made in full to CCC. For payment instructions, please see information listed at the bottom of this form.

License Number	2327710492167
License Date	Dec 14, 2009
Licensed content publisher	American Chemical Society
Licensed content publication	Analytical Chemistry
Licensed content title	Utility of CE−MS Data in Protein Identification
Licensed content author	Brad J. Williams et al.
Licensed content date	May 1, 2007
Volume number	79
Issue number	10
Type of Use	Thesis/Dissertation
Requestor type	Not specified
Format	Print

Portion	Full article
Author of this ACS article	Yes
Order reference number	BJW_dissertation
Title of the thesis / dissertation	An On-Target Performic Acid Oxidation Method Suitable for Disulfide Bond Elucidation using Capillary Electrophoresis - Mass Spectrometry
Expected completion date	Jan 2010
Estimated size(pages)	175
Billing Type	Invoice
Billing Address	Texas A&M University Chemistry Dept. MS3255 College Station, TX 77843 United States
Customer reference info	
Total	0.00 USD

Terms and Conditions

Thesis/Dissertation

ACS / RIGHTSLINK TERMS & CONDITIONS
THESIS/DISSERTATION

INTRODUCTION
The publisher for this copyrighted material is the American Chemical Society. By clicking "accept" in connection with completing this licensing transaction, you agree that the following terms and conditions apply to this transaction (along with the Billing and Payment terms and conditions established by Copyright Clearance Center, Inc. ("CCC"), at the time that you opened your Rightslink account and that are available at any time at <http://myaccount.copyright.com>).

ACS journal may affect publication in that journal. Whether Web posting is considered prior publication may be evaluated on a case-by-case basis by the journal's editor. If an ACS journal editor considers Web posting to be "prior publication", the paper will not be accepted for publication in that journal. If you intend to submit your unpublished paper to ACS for publication, check with the appropriate editor prior to posting your manuscript electronically.

If your paper has already been published by ACS and you want to include the text or portions of the text in your thesis/dissertation in **print or microfilm formats**, please print the ACS copyright credit line on the first page of your article: "Reproduced (or 'Reproduced in part') with permission from [FULL REFERENCE CITATION.] Copyright [YEAR] American Chemical Society." Include appropriate information.

Submission to a Dissertation Distributor: If you plan to submit your thesis to UMI or to another dissertation distributor, you should not include the unpublished ACS paper in your thesis if the thesis will be disseminated electronically, until ACS has published your paper. After publication of the paper by ACS, you may release the entire thesis (**not the individual ACS article by itself**) for electronic dissemination through the distributor; ACS's copyright credit line should be printed on the first page of the ACS paper.

Use on an Intranet: The inclusion of your ACS unpublished or published manuscript is permitted in your thesis in print and microfilm formats. If ACS has published your paper you may include the manuscript in your thesis on an intranet that is not publicly available. Your ACS article cannot be posted electronically on a publicly available medium (i.e. one that is not password protected), such as but not limited to, electronic archives, Internet, library server, etc. The only material from your paper that can be posted on a public electronic medium is the article abstract, figures, and tables, and you may link to the article's DOI or post the article's author-directed URL link provided by ACS. This paragraph does not pertain to the dissertation distributor paragraph above.

APPENDIX B

JOHN WILEY AND SONS LICENSE
TERMS AND CONDITIONS

Dec 14, 2009

This is a License Agreement between Brad J Williams ("You") and John Wiley and Sons ("John Wiley and Sons") provided by Copyright Clearance Center ("CCC"). The license consists of your order details, the terms and conditions provided by John Wiley and Sons, and the payment terms and conditions.

All payments must be made in full to CCC. For payment instructions, please see information listed at the bottom of this form.

License Number	2327720749379
License date	Dec 14, 2009
Licensed content publisher	John Wiley and Sons
Licensed content publication	Journal of Mass Spectrometry
Licensed content title	High-throughput method for on-target performic acid oxidation of MALDI-deposited samples
Licensed content author	Williams, Brad J., Russell, William K., Russell, David H.
Licensed content date	Nov 24, 2009
Start page	157
End page	166
Type of Use	Dissertation/Thesis
Requestor type	University/Academic
Format	Print and electronic

Portion	Full article
Will you be translating?	No
Order reference number	BJW_oxidation
Total	0.00 USD

Terms and Conditions

TERMS AND CONDITIONS

This copyrighted material is owned by or exclusively licensed to John Wiley & Sons, Inc. or one if its group companies (each a “Wiley Company”) or a society for whom a Wiley Company has exclusive publishing rights in relation to a particular journal (collectively “WILEY”). By clicking “accept” in connection with completing this licensing transaction, you agree that the following terms and conditions apply to this transaction (along with the billing and payment terms and conditions established by the Copyright Clearance Center Inc., (“CCC’s Billing and Payment terms and conditions”), at the time that you opened your Rightslink account (these are available at any time at http://myaccount.copyright.com).

Terms and Conditions

1. The materials you have requested permission to reproduce (the "Materials") are protected by copyright.

2. You are hereby granted a personal, non-exclusive, non-sublicensable, non-transferable, worldwide, limited license to reproduce the Materials for the purpose specified in the licensing process. This license is for a one-time use only with a maximum distribution equal to the number that you identified in the licensing process. Any form of republication granted by this licence must be completed within two years of the date of the grant of this licence (although copies prepared before may be distributed thereafter). Any electronic posting of the Materials is limited to one year from the date permission is granted and is on the condition that a link is placed to the journal homepage on Wiley’s online journals publication platform at www.interscience.wiley.com. The Materials shall not be used in any other manner or for any other purpose. Permission is granted subject to an appropriate acknowledgement given to the author, title of the material/book/journal and the publisher and on the understanding that nowhere in the text is a previously published source acknowledged for all or part of this Material. Any third party material is expressly excluded from this permission.

3. With respect to the Materials, all rights are reserved. No part of the Materials may be

copied, modified, adapted, translated, reproduced, transferred or distributed, in any form or by any means, and no derivative works may be made based on the Materials without the prior permission of the respective copyright owner. You may not alter, remove or suppress in any manner any copyright, trademark or other notices displayed by the Materials. You may not license, rent, sell, loan, lease, pledge, offer as security, transfer or assign the Materials, or any of the rights granted to you hereunder to any other person.

4. The Materials and all of the intellectual property rights therein shall at all times remain the exclusive property of John Wiley & Sons Inc or one of its related companies (WILEY) or their respective licensors, and your interest therein is only that of having possession of and the right to reproduce the Materials pursuant to Section 2 herein during the continuance of this Agreement. You agree that you own no right, title or interest in or to the Materials or any of the intellectual property rights therein. You shall have no rights hereunder other than the license as provided for above in Section 2. No right, license or interest to any trademark, trade name, service mark or other branding ("Marks") of WILEY or its licensors is granted hereunder, and you agree that you shall not assert any such right, license or interest with respect thereto.

5. WILEY DOES NOT MAKE ANY WARRANTY OR REPRESENTATION OF ANY KIND TO YOU OR ANY THIRD PARTY, EXPRESS, IMPLIED OR STATUTORY, WITH RESPECT TO THE MATERIALS OR THE ACCURACY OF ANY INFORMATION CONTAINED IN THE MATERIALS, INCLUDING, WITHOUT LIMITATION, ANY IMPLIED WARRANTY OF MERCHANTABILITY, ACCURACY, SATISFACTORY QUALITY, FITNESS FOR A PARTICULAR PURPOSE, USABILITY, INTEGRATION OR NON-INFRINGEMENT AND ALL SUCH WARRANTIES ARE HEREBY EXCLUDED BY WILEY AND WAIVED BY YOU.

6. WILEY shall have the right to terminate this Agreement immediately upon breach of this Agreement by you.

7. You shall indemnify, defend and hold harmless WILEY, its directors, officers, agents and employees, from and against any actual or threatened claims, demands, causes of action or proceedings arising from any breach of this Agreement by you.

8. IN NO EVENT SHALL WILEY BE LIABLE TO YOU OR ANY OTHER PARTY OR ANY OTHER PERSON OR ENTITY FOR ANY SPECIAL, CONSEQUENTIAL, INCIDENTAL, INDIRECT, EXEMPLARY OR PUNITIVE DAMAGES, HOWEVER CAUSED, ARISING OUT OF OR IN CONNECTION WITH THE DOWNLOADING, PROVISIONING, VIEWING OR USE OF THE MATERIALS REGARDLESS OF THE FORM OF ACTION, WHETHER FOR BREACH OF CONTRACT, BREACH OF WARRANTY, TORT, NEGLIGENCE, INFRINGEMENT OR OTHERWISE (INCLUDING, WITHOUT LIMITATION, DAMAGES BASED ON LOSS OF PROFITS, DATA, FILES, USE, BUSINESS OPPORTUNITY OR CLAIMS OF

THIRD PARTIES), AND WHETHER OR NOT THE PARTY HAS BEEN ADVISED OF THE POSSIBILITY OF SUCH DAMAGES. THIS LIMITATION SHALL APPLY NOTWITHSTANDING ANY FAILURE OF ESSENTIAL PURPOSE OF ANY LIMITED REMEDY PROVIDED HEREIN.

9. Should any provision of this Agreement be held by a court of competent jurisdiction to be illegal, invalid, or unenforceable, that provision shall be deemed amended to achieve as nearly as possible the same economic effect as the original provision, and the legality, validity and enforceability of the remaining provisions of this Agreement shall not be affected or impaired thereby.

10. The failure of either party to enforce any term or condition of this Agreement shall not constitute a waiver of either party's right to enforce each and every term and condition of this Agreement. No breach under this agreement shall be deemed waived or excused by either party unless such waiver or consent is in writing signed by the party granting such waiver or consent. The waiver by or consent of a party to a breach of any provision of this Agreement shall not operate or be construed as a waiver of or consent to any other or subsequent breach by such other party.

11. This Agreement may not be assigned (including by operation of law or otherwise) by you without WILEY's prior written consent.

12. These terms and conditions together with CCC’s Billing and Payment terms and conditions (which are incorporated herein) form the entire agreement between you and WILEY concerning this licensing transaction and (in the absence of fraud) supersedes all prior agreements and representations of the parties, oral or written. This Agreement may not be amended except in a writing signed by both parties. This Agreement shall be binding upon and inure to the benefit of the parties' successors, legal representatives, and authorized assigns.

13. In the event of any conflict between your obligations established by these terms and conditions and those established by CCC’s Billing and Payment terms and conditions, these terms and conditions shall prevail.

14. WILEY expressly reserves all rights not specifically granted in the combination of (i) the license details provided by you and accepted in the course of this licensing transaction, (ii) these terms and conditions and (iii) CCC’s Billing and Payment terms and conditions.

15. This Agreement shall be governed by and construed in accordance with the laws of England and you agree to submit to the exclusive jurisdiction of the English courts.

BY CLICKING ON THE "I ACCEPT" BUTTON, YOU ACKNOWLEDGE THAT YOU HAVE READ AND FULLY UNDERSTAND EACH OF THE SECTIONS OF

AND PROVISIONS SET FORTH IN THIS AGREEMENT AND THAT YOU ARE IN AGREEMENT WITH AND ARE WILLING TO ACCEPT ALL OF YOUR OBLIGATIONS AS SET FORTH IN THIS AGREEMENT.

VITA

Brad Jay Williams

Department of Chemistry
Texas A&M University, MS3255
College Station, TX 77843

Email: bwilliams@mail.chem.tamu.edu Phone: 903-815-9283

EDUCATION

May 2010 Ph.D. / Analytical Chemistry
Texas A&M University, College Station, TX
Thesis: An On-Target Performic Acid Oxidation Method Suitable for Disulfide Bond Elucidation Using Capillary Electrophoresis – Mass Spectrometry (Prof. David H. Russell)

May 2003 B.S. / Chemistry
Southeastern Oklahoma State University, Durant, OK

Aug. 2001 A.S. / Mathematics
Grayson County College, Denison, TX

HONORS

May 2003 Magna Cum Laude, Southeastern Oklahoma State University

MEMBERSHIPS

Phi Theta Kappa, National Honor Society, Grayson County College
Alpha Chi, National Honor Society, Southeastern Oklahoma State University
Phi Lambda Upsilon, National Honorary Chemical Society, Texas A&M University

SELECTED PUBLICATIONS

1. Williams, B.J.; Russell, W.K.; Russell, D.H. High-throughput On-Target Performic Acid Oxidation Method for MALDI Deposited Samples, *J. Mass Spectrom.* **2010**, 45, 157-166.

2. Williams, B.J.; Russell, W.K.; Russell, D.H. Utility of CE-MS Data in Protein Identification, *Analytical Chemistry* **2007**, 79, 3850-3855